2019

Characterizing the Role of Neurogenic Atrophy-Induced Protein Phosphatases in Skeletal Muscle

Sydney Ann Labuzan
University of North Florida, slabuzan14@gmail.com

CHARACTERIZING THE ROLE OF NEUROGENIC ATROPHY-INDUCED PROTEIN PHOSPHATASES IN SKELETAL MUSCLE

By Sydney Ann Labuzan

A thesis submitted to the Department of Biology

in partial fulfillment of the requirements for the degree of

Master of Science in Biology

UNIVERSITY OF NORTH FLORIDA

COLLEGE OF ARTS AND SCIENCES

April 2019

CERTIFICATE OF APPROVAL

The thesis "Characterizing the Role of Neurogenic Atrophy-Induced Protein Phosphatases in Skeletal Muscle" submitted by Sydney Ann Labuzan

Approved by the thesis committee: Date

_____ _____
Dr. David Waddell, Ph.D.
Committee Chair Person

_____ _____
Dr. Judith Ochrietor, Ph.D.

_____ _____
Dr. Michael Lentz, Ph.D.

Accepted for the Department:

_____ _____
Dr. Cliff Ross, Ph.D.
Chairperson

Accepted for the College:

_____ _____
Dr. George Rainbolt, Ph.D.
Dean

Accepted for the University:

_____ _____
Dr. John Kantner, Ph.D.
Dean of the Graduate School

Table of Contents

List of Figures

List of Tables

Abstract

Dusp4 and Ppme1 have been identified as novel genes in skeletal muscle that are upregulated in response to neurogenic atrophy in a mouse model. Overexpression (OE) of Dusp4 wild-type (Dusp4-WT), as well as a Dusp4 Dominant Negative (Dusp4-DN) in C_2C_{12} cells inhibits proper muscle differentiation potentially through its attenuation of ERK-MAPK signaling. Co-immunoprecipitation analysis shows Dusp4-DN associating with ERK1/2 but not p38, suggesting Dusp4 is specific for ERK1/2 but not p38. Quantitative PCR as well as Western blot analysis confirm that Ppme1 is expressed uniformly during muscle cell proliferation and differentiation. Interestingly, Ppme1 mRNA levels appear to decrease as differentiation proceeds whereas the protein levels remain constant throughout proliferation and differentiation. Transcriptional regulation of Ppme1 was observed by cloning proximal promoter fragments of the gene. The Ppme1 promoter is highly active on its own but when myogenic regulatory factors are ectopically expressed they repress promoter activity. Furthermore, mutation of a conserved E-box sequence inhibits full induction of the Ppme1 reporter gene , suggesting this E-box element is necessary for full Ppme1 expression. Additionally, inhibition of Ppme1 using a pharmacologic inhibitor results in delayed muscle cell differentiation and significant attenuation of AP-1 reporter activity. However, Ppme1 inhibition does not result in significant effects on phosphorylation of ERK1/2, c-Jun, or AKT. Additionally, C_2C_{12} cells were treated with ERK1/2 and MEK1/2 inhibitors to compare results to that of Ppme1 inhibition and Dusp4 OE. While all of these conditions exhibit attenuation of AP-1 reporter activity, western blotting showed Dusp4 OE and Ppme1 inhibition do not mimic the results of ERK1/2 and MEK1/2 inhibition. Thus, Dusp4 and Ppme1 likely do not just block phosphorylation but act through more complex protein-protein interactions.

Chapter 1: Background on Skeletal Muscle Atrophy, MuRF1, and MAPK Signaling in Skeletal Muscle , and Materials and Methods

Skeletal Muscle and Skeletal Muscle Atrophy

Skeletal muscle constitutes a significant portion of an individual's tissue, comprising 40% of total body weight and 50-75% of the body's total proteins (Trovato et al.,2016; Crist, 2017). Unlike the other two major muscle types, smooth and cardiac, skeletal muscle is required for voluntary movement, maintains posture and breathing, and serves as an essential thermogenic organ in vertebrates (Crist, 2017). Skeletal muscle mass is regulated by a coordination between protein synthesis (hypertrophy) and protein degradation (atrophy) based upon an individual's physiological needs. Skeletal muscle atrophy occurs when protein degradation outpaces protein synthesis, leading to the partial or complete wasting away of skeletal muscle (McKinnell and Rudnicki, 2004; Bodine and Baehr, 2014). The process of muscle wasting occurs for a number of reasons, including aging (sarcopenia), cancer, disuse, corticosteroid treatments, and denervation (Bodine et al., 2001; Waddell et al., 2008). Increasing our understanding of this condition by studying the molecular mechanisms of skeletal muscle atrophy may provide new insights into alleviating the damaging effects of pathological muscle wasting.

The Ubiquitin Proteasome System and E3 Ubiquitin Ligases

Skeletal muscle atrophy is mediated in part by increased protein degradation carried out via the ubiquitin proteasome system. Specific proteins are targeted for degradation by the 26S proteasome through the polyubiquitination of target proteins (McNaught et al, 2001; Bodine et al., 2001; Ardley and Robinson, 2005). This occurs through covalent modification of a lysine residue on the target protein mediated by the reactions of three enzymes (E1, E2, and E3) within

this pathway (Figure 1). The first step involves the E1 ubiquitin-activating enzyme hydrolyzing ATP and then adenylating a molecule of ubiquitin, which will be transferred to a cysteine residue in the active site of the E1 (McNaught et al, 2001; Bodine et al., 2001; Ardley and Robinson, 2005). The adenylated ubiquitin is then transferred to a cysteine on the E2 ubiquitin conjugating enzyme. The last step of this process involves an E3 ubiquitin ligase, which catalyzes the transfer of ubiquitin from the E2 enzyme to the target protein. The ubiquitin ligase provides the specificity of this pathway in that each E3 enzyme only recognizes certain substrates as targets for degradation (Bodine and Baehr, 2014; Ardley and Robinson, 2005). The substrate will continue to be polyubiquitinated, and must have at least four ubiquitin molecules to be recognized by the 26S proteasome (Bodine and Baehr, 2014; Ardley and Robinson, 2005). The number of different E1, E2, and E3 enzymes present in each organism varies and the different E1/E2/E3 combinations and their importance in substrate recognition remain poorly understood.

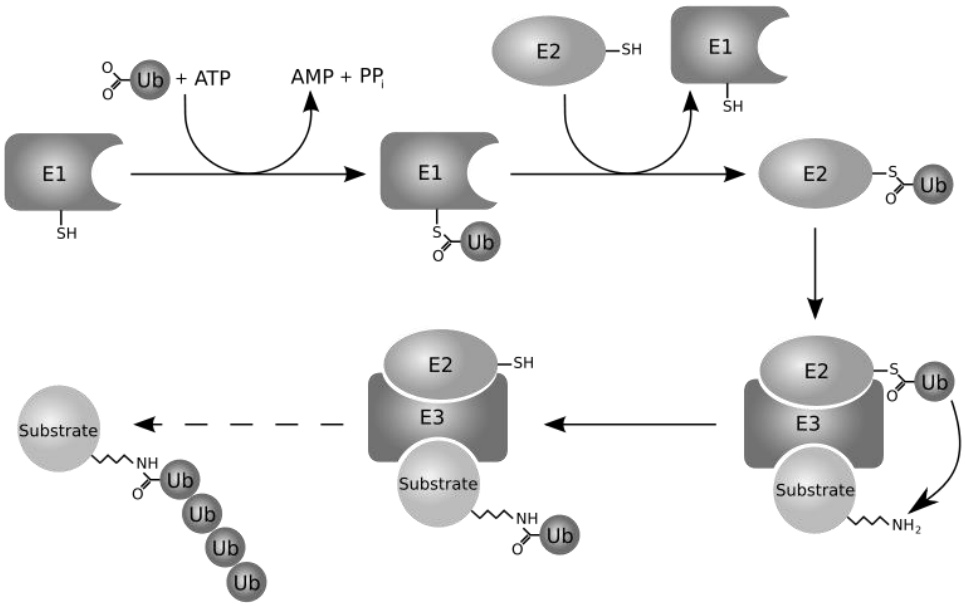

Figure 1. Schematic of the Ubiquitin Proteasome System. The ubiquitin activating enzyme (E1), the ubiquitin conjugating enzyme (E2), and the ubiquitin ligase (E3) work together in order to ubiquitinate proteins for degradation via the 26S proteasome (Dodd, 2011).

MuRF1 and MAFbx

Because the specificity of protein degradation is dictated by E3 ubiquitin ligases, identification of E3s and their potential targets is paramount for better understanding of the muscle atrophy pathway. Muscle RING Finger 1 (MuRF1) and Muscle Atrophy F-box (MAFbx) are two E3 ubiquitin ligases that have been characterized as being upregulated in virtually all atrophy-inducing conditions (Bodine et al., 2001). In a study conducted in 2001 by Bodine et al., muscle tissue isolated from rats subjected to immobilization, denervation, and hindlimb suspension was analyzed to identify genes differentially expressed during these atrophy-inducing conditions. Of the 74 genes analyzed, most were only expressed under immobilization and denervation conditions, but not hindlimb suspension. Only MuRF1 and MAFbx were upregulated during all three conditions, with highest expression being 3 days post-treatment (Figure 2) (Bodine et al., 2001). Further, when compared to wild-type mice, MuRF1 and MAFbx knockout (KO) mice both displayed atrophy resistance, with the MuRF1 KO mice maintaining greater muscle integrity than the MAFbx KO mice (Bodine et al., 2001). While it is clear that MuRF1 and MAFbx act as important regulators in the skeletal muscle atrophy cascade, the exact molecular mechanisms are not well understood and very few potential targets have been identified (Bodine and Baehr, 2014). The lack of clear protein targets for ubiquitination by the ubiquitin ligases MuRF1 and MAFbx leads to questions about their respective roles in the atrophy cascade.

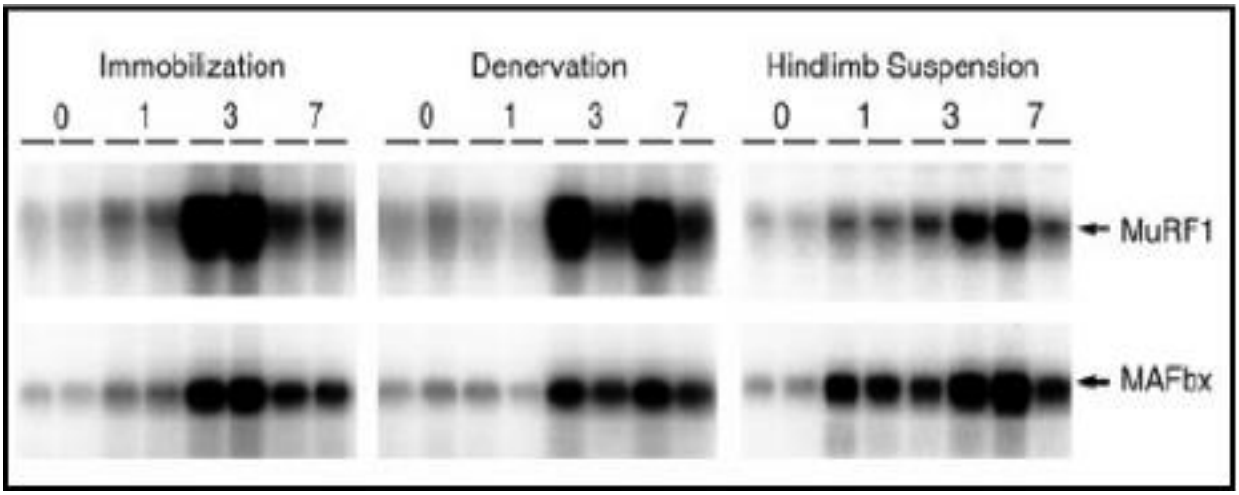

Figure 2. Northern blot displaying the mRNA expression profiles of MuRF1 and MAFbx during three atrophy-inducing conditions: immobilization, denervation, and hindlimb suspension. Increased expression of both genes is observed at day 1 and reaches maximum expression at day 3. (Bodine, et al., 2001).

MuRF1 as a transcriptional regulator

In 2013, a study published by Furlow et al. suggested that the role of MuRF1 in the atrophy pathway might be more complex than previously thought. Two populations of 4 to 6 month old female mice, consisting of wild-type (WT) and MuRF1 knockout (KO) littermates, were compared under control and atrophy-induced conditions (Furlow et al., 2013). The KO mice were designed by inserting a β-galactosidase-encoding LacZ cassette into the MuRF1 gene (Furlow et al., 2013). If the MuRF1 promoter is active, rather than producing functional MuRF1, functional β-galactosidase is produced. This system allowed the researchers to produce KO mice while still being able to quantify MuRF1 endogenous promoter activity. Following denervation, the gastrocnemius muscle was isolated and a genome-wide microarray was performed to identify differential gene expression between WT and MuRF1 KO mice at 3 and 14 days post-denervation (Furlow et al., 2013). In the WT mice, MuRF1 expression increased at day 3 but returned to baseline by day 14. However, in the MuRF1 KO mice, β-galactosidase levels were

elevated at day 3 and remained elevated at day 14 as well (Figure 3) (Furlow et al., 2013). These data suggests that MuRF1 may negatively regulate its own expression.

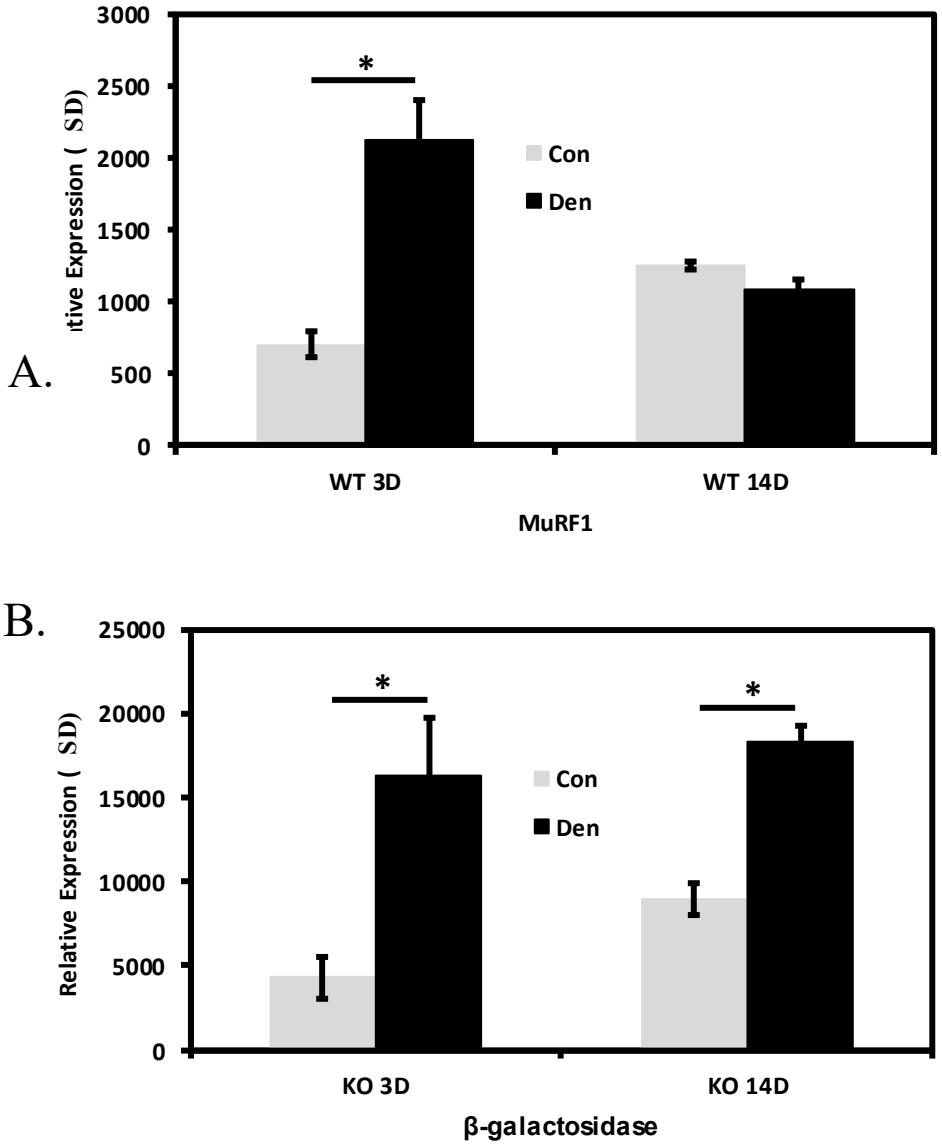

Figure 3. Transcriptional activity of MuRF1 in WT and MuRF1 KO mice post-denervation. A) Denervated WT mice showed increased MuRF1 gene expression at day 3 (3D) but returned to baseline levels by day 14 (14D) post-denervation. B) Denervated KO mice showed an increase in β-galactosidase expression under the control of the MuRF1 promoter at 3D, while expression remaining elevated at 14D (Furlow et al, 2013).

Additionally, MAFbx expression was compared in WT versus MuRF1 KO mice, and was also shown to be affected by levels of MuRF1 gene expression. In WT mice, MAFbx expression was elevated at day 3 but returned to baseline by day 14, whereas in MuRF1 KO mice, MAFbx expression remained elevated at both time points post-denervation (Figure 4) (Furlow et al., 2013). This data suggests that MuRF1 may also negatively regulate MAFbx expression.

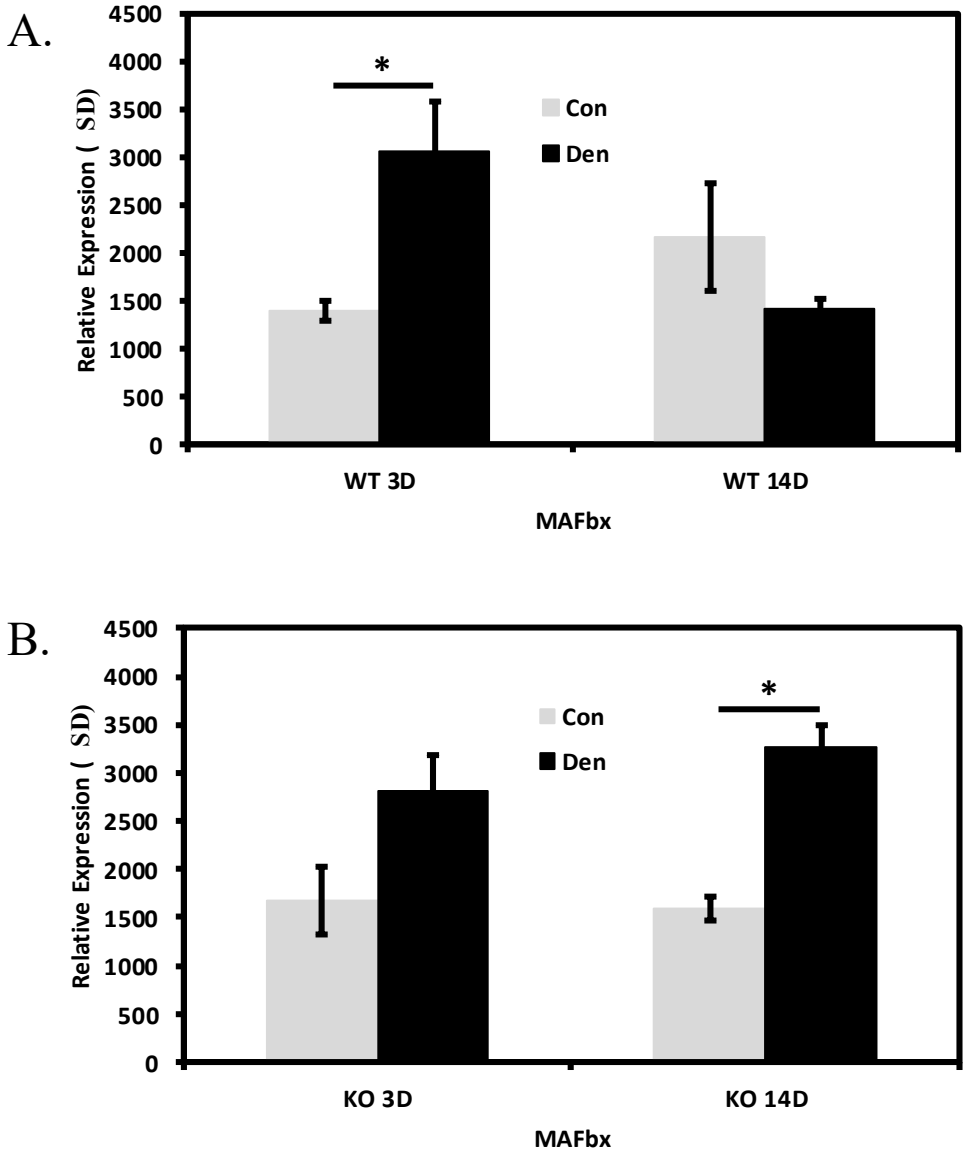

Figure 4. Transcriptional activity of MAFbx in WT and MuRF1 KO mice post-denervation. A) Denervated WT mice showed an increase in MAFbx gene expression at day 3 (3D) but a return to baseline levels by day 14 (14D) post-denervation. B) Denervated MuRF1 KO mice showed increased expression of MAFbx at 3D that remained elevated by 14D (Furlow et al, 2013).

The microarray revealed an even greater amount of differential transcriptional activity, demonstrated by a whole suite of genes that were found to be differentially expressed in mice experiencing neurogenic atrophy regardless of MuRF1 expression levels. Many of these differentially expressed genes have been shown to possess a range of potential functions, such as roles in muscle structure and function, metabolic pathways, and signal transduction cascades. Of note, several of these identified genes have been previously linked to regulation of Mitogen-Activated Protein Kinase (MAPK) and AKT signaling in various tissue types. Since MAPK and AKT signaling play a role in proper muscle development, genes relating to this pathway are of particular interest for investigation in skeletal muscle.

The role of the AKT signaling pathway in the regulation of muscle growth

Muscle cells undergo development based upon extracellular cues that they receive that activate signaling cascades within the cell, with one pathway being the IGF1/PI3K/AKT pathway. Binding of insulin-like growth factor (IGF1) to its receptor activates intrinsic tyrosine kinase and autophosphorylation, thus creating docking sites for insulin receptor substrate (IRS), which is phosphorylated by the IGF1 receptor (Schiaffino and Mammucari, 2011; Stitt et al., 2004) (Figure 5). Phosphorylated IRS recruits and activates phosphatidylinositol-3-kinase (PI3K) which then phosphorylates phosphoinositide-4,5-biphosphate (PIP2) to create phosphoinositide-3,4,5-triphosphatse (PIP3). PIP3 is then able to act as a docking site for phosphoinositide-dependent kinase 1 (PDK1) and AKT (Schiaffino and Mammucari, 2011) (Figure 5). AKT is phosphorylated at serine 308 by PDK1 which then activates AKT (Figure 5). AKT is essential in regulating both protein synthesis as well as protein degradation pathways, which work in tandem to regulate muscle mass (Otto and Patel, 2010; Egerman and Glass, 2014). AKT stimulates protein synthesis via the mammalian target of rapamycin (mTOR) and glycogen synthase kinase

3β (GSK3β) (Egerman and Glass, 2014; Schiaffino and Mammucari, 2011) (Figure 5). AKT also inhibits protein degradation by phosphorylating and repressing transcription factors of the FoxO family, which are required for transcriptional regulation of the E3 ubiquitin ligases MuRF1 and MAFbx (Schiaffino and Mammucari, 2011; Stitt et al., 2004) (Figure 5). Thus, MuRF1 and MAFbx are no longer transcriptionally activated and are unavailable to function within the atrophy cascade. Due to the role of AKT in regulating identified mediators of skeletal muscle cell function, genes that potentially regulate the activation of AKT are of interest for elucidating the mechanisms by which the atrophy cascade occurs.

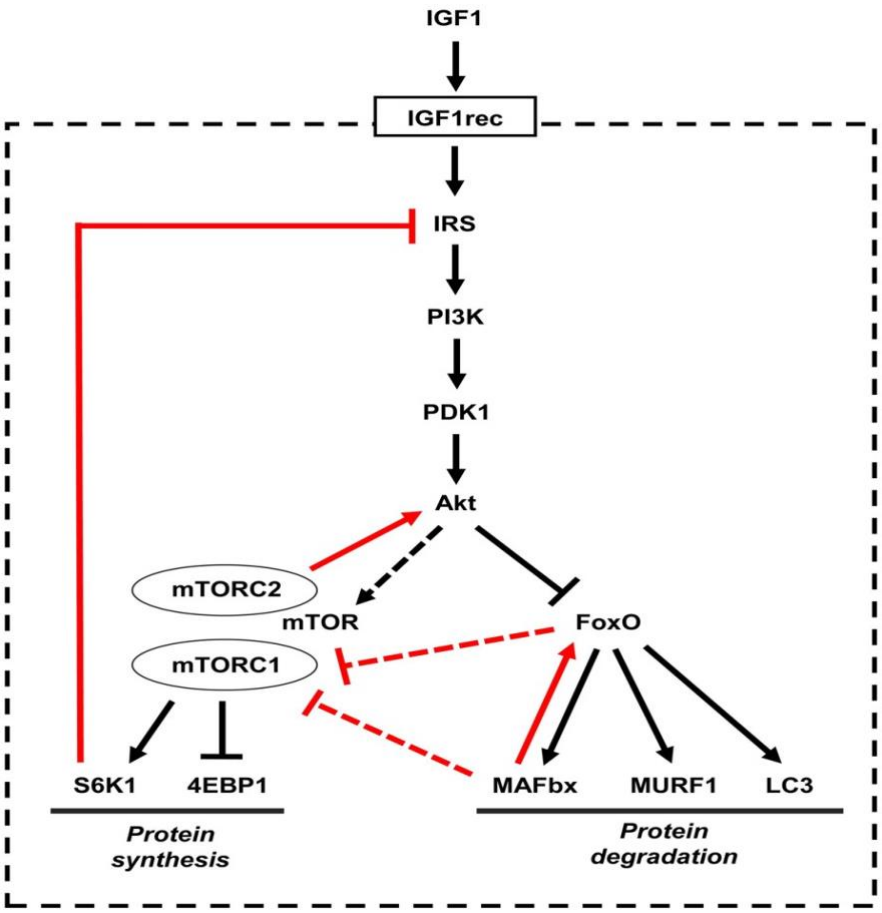

Figure 5. The IGF1-AKT pathway controls muscle growth via mammalian target of rapamycin (mTOR) and FoxO family members. The internal feedback loops that control the IGF1-Akt pathway are indicated in red. The dotted line indicates that the effect of Akt on mTOR is indirect, being mediated by the tuberous sclerosis complex (TSC) proteins 1 and 2 and by Rheb (Ras homolog enriched in brain). (Adapted from Schiaffino and Mammucari, 2011).

The role of the MAPK Signaling Pathway in Myogenesis and Atrophy

Another pathway that regulates proper myogenesis is the Mitogen Activated Protein Kinase (MAPK) signaling pathway. MAPK signaling regulates important cellular processes such as embryogenesis, proliferation, differentiation, and even apoptosis (Raman et al., 2007; Morrison 2012). There are several different branches within MAPK signaling, with the four most common branches being the extracellular signal-regulated kinases1/2 (ERK1/2), c-Jun N-terminal kinase (JNK), p38 family, and ERK5, which all possess distinct functions. Despite being composed of

differing kinases, each of these signaling cascades share a homologous three tiered system of kinases (MAP3Ks, MAP2Ks, and MAPKs) that properly regulate each of these branches (Figure 6) (Raman et al., 2007; Garrington and Johnson 1999; Morrison 2012; Plotnikov et al., 2010). Within these systems, MAP kinase kinase kinases (MAP3Ks) phosphorylate MAP2Ks to activate them, which then in turn activate MAPKs by phosphorylation as well. When activated, MAPKs can translocate to the nucleus where they phosphorylate designated target proteins, including transcription factors, that then modulate gene expression. Likewise, MAPK members can be dephosphorylated and thus inactivated in order to properly regulate when these signaling pathways are activated throughout the cell cycle (Raman et al., 2007; Morrison 2012).

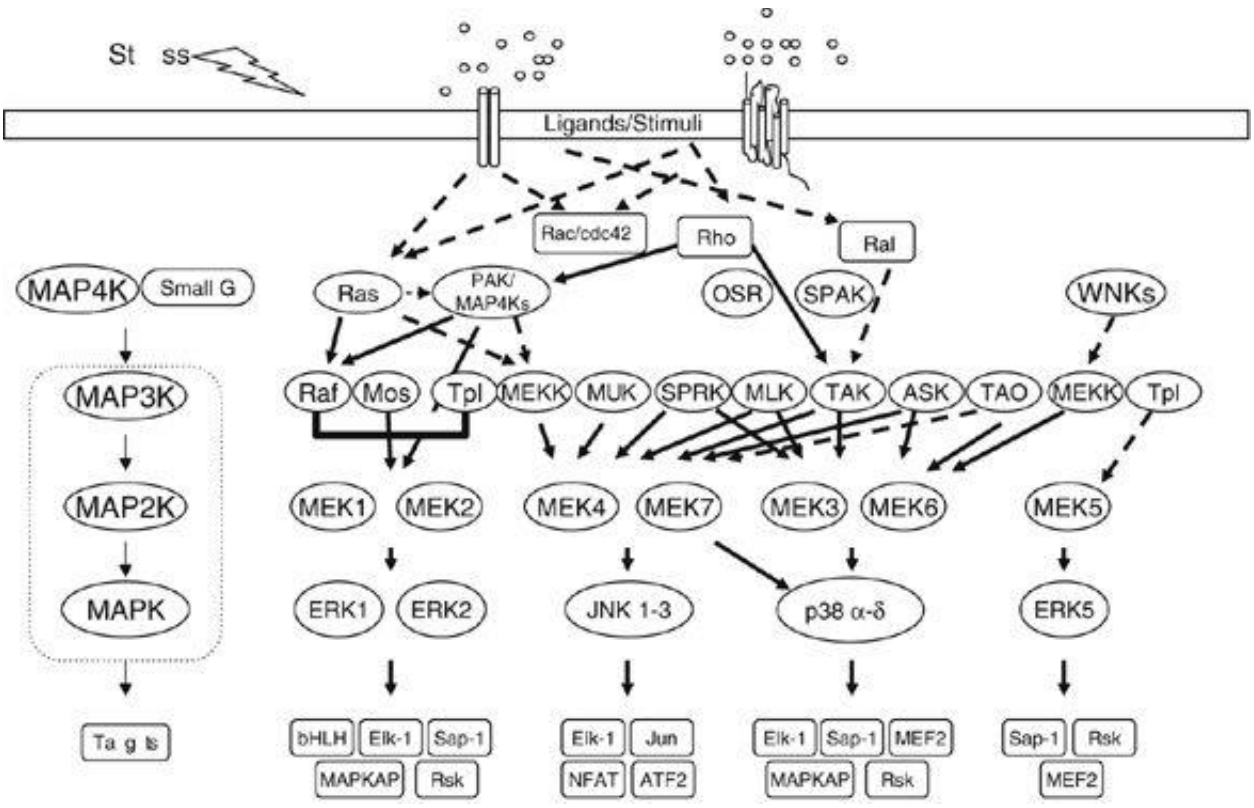

Figure 6. Illustration of MAPK cascades for ERK1/2, JNK, p38, and ERK5. (Adapted from Raman et al., 2007).

ERK1/2 activity within myoblast development occurs in biphasic peaks that are crucial for proper proliferation and differentiation. ERK1/2 is critical for positively regulating cellular proliferation, as well as, preventing cell cycle exit during G_1 to prevent premature differentiation, although the mechanisms by which this role is achieved has yet to be fully elucidated (Knight and Kothary, 2011). ERK activity decreases in early differentiation to allow myoblasts to start the differentiation process, however ERK activity again is critical during terminal differentiation to promote proper myocyte fusion (Knight and Kothary, 2011; Adi et al, 2002; Sarbassov et al., 1997). Inhibition of ERK1/2 signaling has been shown to induce muscle atrophy and was reflected by decreased size of myotubes and reduced protein content in a study that compared the use of MEK, p38α/β, and JNK inhibitors. In corroboration with this finding, MAFbx and MuRF1 expression levels were found to be transcriptionally upregulated in cells treated with the MEK1/2 inhibitor, whereas no significant changes were found in the levels of MuRF1 and MAFbx in cells treated with the other inhibitors (Shi et al., 2009). Thus, ERK1/2 signaling is crucial for maintaining proper skeletal muscle mass and dysregulation of this pathway results in significant atrophy of both slow and fast twitch muscles.

The role of p38 in muscle cell differentiation is less well characterized, but appears to be correlated strongly to p38's interaction with the MyoD family. The activity of p38 α, β, and γ isoforms have been found to be induced during myoblast differentiation. (Keren et al., 2006). It appears the activation of p38 is critical for promoting the differentiation process, while its sustained activation does not seem to affect differentiation as it proceeds. Research has suggested that there may be coordination between the ERK and p38 pathways to properly carry out differentiation, as inhibition of ERK activity appears to enhance p38 and inhibition of p38 enhances ERK activity (Keren et al., 2006; Khurana and Dey 2002). Thus, it is hypothesized that

the reduction in ERK activity allowing for withdrawal from the cell cycle works in tandem with the increased activity of p38, which together initiate proper muscle cell differentiation (Keren et al., 2006). Additionally, while the JNK pathway is most commonly associated with cell stress, it also plays a regulatory role in proliferation and survival. JNK levels appear to be upregulated during muscle cell differentiation and are required for muscle cell viability throughout the differentiation process (Khurana and Dey, 2004). Inhibition of JNK during differentiation leads to apoptosis and subsequently delays muscle cell differentiation, which is thought to be coordinated by activation of ERK and p38 as well as the c-Jun transcription factor (Khurana and Dey, 2004). This previous research taken together suggests that these three major MAPK pathways crucially interplay to coordinate proper muscle cell differentiation, and that no one pathway is sufficient to initiate and maintain proper differentiation.

As previously mentioned, members of these MAPK cascades can be negatively controlled by dephosphorylation, carried out by phosphatases possessing specificity for substrates within this pathway. Phosphoprotein phosphatases are classified based upon whether they preferentially dephosphorylate tyrosine, serine/threonine or both types of phosphoresidues. Dual-specificity phosphatases (DUSPs) dephosphorylate both tyrosine as well as serine/threonine residues, and exhibit substrate specificity for different MAPKs (Raman et al., 2007; Kondoh and Nishida, 2006). DUSPs that act upon MAPK members are known as MAPK phosphatases (MKPs). Another phosphatase that plays an important role in regulating MAPK signaling is protein phosphatase 2A, which has been linked previously as an important regulator of the ERK1/2 MAPK cascade (Raman et al., 2007; Junttila et al., 2008; Shanley et al., 2001). Thus, due to the roles of these enzymes, phosphatases that are upregulated under atrophy conditions are of

particular interest and studying their function in the context of skeletal muscle differentiation and atrophy is likely to be of significant importance.

Chapter 2: Characterization of the Role of Dusp4 in the MAPK Signaling Pathway in Muscle Cells

Dusp4 Background

Overview of Dusp4

The family of dual-specificity phosphatases (DUSPs) contains approximately 25 members that have the ability to dephosphorylate nuclear localized MAP kinases (Type 1), cytoplasmic localized MAP kinases (Type 2), or can function in both the nucleus and the cytoplasm (Type 3) (Huang and Tan, 2012). Dual specificity phosphatase 4 (Dusp4) is a type 1 dual specificity phosphatase that can dually act to dephosphorylate serine/threonine residues as well as tyrosine residues on nuclear MAP kinases. Dusp4 contains a number of functional domains, including an N-terminal MAP kinase binding domain, a C-terminal catalytic phosphatase domain, and a nuclear localization signal (NLS). (Farooq and Zhou, 2004; Lawan et al., 2012). Previous literature suggests that Dusp4's substrate specificity for MAP kinases may differ depending on tissue type. Some findings suggest Dusp4 can act to negatively regulate ERK, JNK, and/or p38 MAP kinases, whereas other studies suggest it acts with more specificity for either ERK or p38 MAP kinase (Auger-Messier et al., 2013; Huang and Tan, 2012; Peng et al., 2010). Despite other DUSP members having been studied in muscle, very little has been done to investigate the role of Dusp4 in skeletal muscle.

Dusp4 is induced during skeletal muscle atrophy and is differentially expressed in MuRF1-null mice.

In the microarray conducted by Furlow et al. (2013), RNA was isolated from triceps surae (TS) muscle from mice undergoing denervation-induced skeletal muscle atrophy. Numerous genes previously not described in skeletal muscle were identified as exhibiting differential expression

patterns in response to neurogenic atrophy. Two probes (ID:2690044 and ID: 100630110) were utilized for evaluating Dusp4 expression, and both showed low baseline expression levels in the control mice, but significant induction at both 3 and 14 days post-denervation (Figure 7A and 7B). Due to this upregulation of Dusp4 under neurogenic atrophy conditions, Dusp4 became a prime candidate for investigation into its probable function within the atrophy pathway.

A.

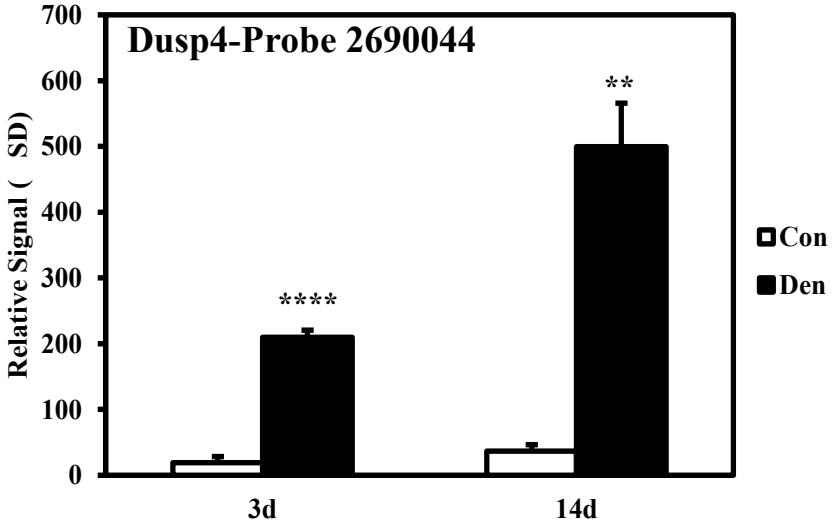

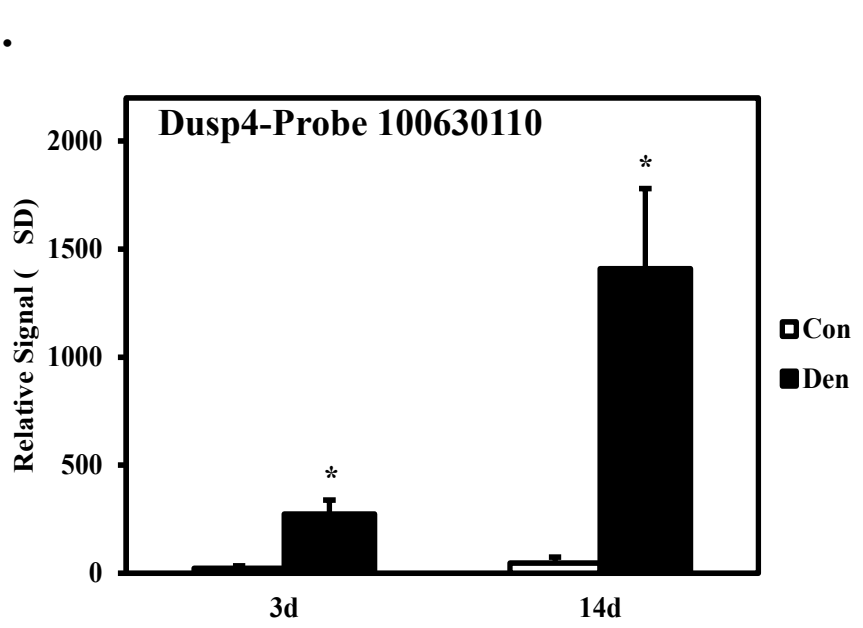

Figure 7. Dusp4 is induced during neurogenic skeletal muscle atrophy. Whole genome expression analysis was conducted on triceps surae muscle from wild-type control (Con) mice after 3 days (3d) and 14 days (14d) of denervation (Den). Dusp4 expression (A) probe identification number 2690044 and (B) probe identification number 100630110 increased significantly at both 3 and 14 days post-denervation. Each condition represents the average expression from three animals (n=3) and error bars represent ± SD. White bars, controls; black bars, denervation. Significant difference between denervated mice and control mice in the same group, (*: $P \leq 0.05$, **: $P \leq 0.01$, ****: $P \leq 0.0001$).

Dusp4 is expressed during proliferation but decreases as muscle cells differentiate.

As Dusp4 expression had never been characterized previously in skeletal muscle, our lab sought to examine the expression profile at the transcriptional as well as the translational level. To assess the endogenous Dusp4 transcriptional profile, RT-qPCR was performed using RNA isolated from proliferating myoblasts and early and late stage myofibers. The results demonstrate that Dusp4 is expressed highest in proliferating myoblasts (PD2) and rapidly drops off in expression once differentiation begins (DD2) and remains low into late differentiation (DD7) (Figure 8A) (Haddock, 2016). To determine if the protein expression was consistent with the transcriptional expression of Dusp4, C_2C_{12} cells were cultured and harvested over a 10 day

time course and cell lysates were analyzed by Western blotting for endogenous Dusp4. Dusp4 protein level was detectable through proliferation but not detectable at any differentiation time point (Figure 8B). Myosin heavy chain, a marker of muscle cell differentiation, was used to determine that the C_2C_{12} cells properly differentiated, while α-tubulin was probed to confirm even loading (Figure 8B) (Haddock, 2016).

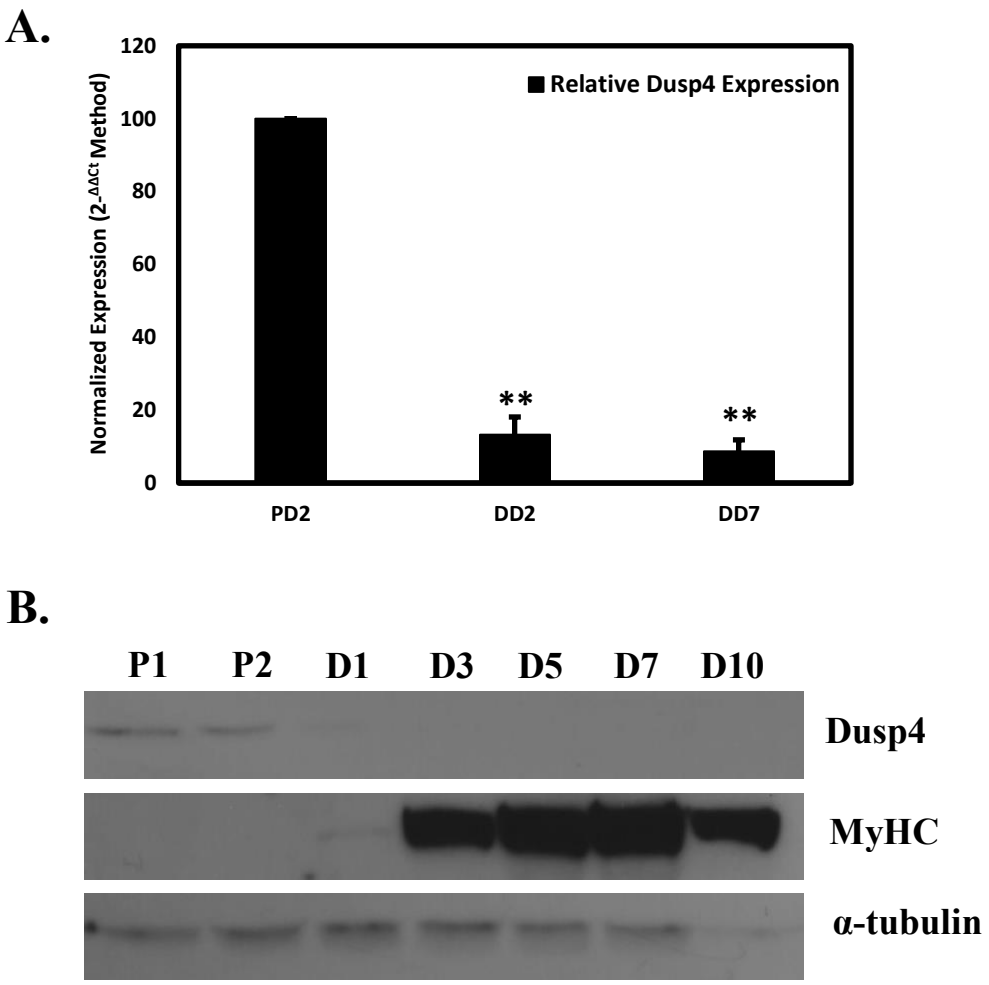

Figure 8. Dusp4 is down regulated during muscle cell differentiation. (A) qPCR analysis of Dusp4 expression in proliferating (PD2) C_2C_{12} myoblasts and myofibers at early (DD2) and late (DD7) stages of differentiation. RNA was isolated from three biological replicates (n=3) for each time point and the experiment was repeated three times. Significant difference observed between proliferation and differentiation time points (**: $P \leq 0.01$). (B) Western blot analysis was performed using protein homogenates from proliferating (P) and differentiated (D) C_2C_{12} cells harvested over a 10 day differentiation time course. Cells were maintained in proliferation media (10% serum) and harvested 1 and 2 days post-plating (P1 and P2) and the remaining cells were switched to differentiation media (2% serum) and harvested at 1, 3, 5, 7, and 10 days post-media change. Myosin Heavy Chain (MyHC) was analyzed as a marker for differentiation and α-tubulin was analyzed to confirm equal protein loading. Western blots were repeated at least three times and the blots are representative of the results obtained (Haddock et al., 2019).

Dusp4 negatively modulates the ERK1/2 branch of MAPK signaling in skeletal muscle

Murine Dusp4 is 398 amino acids in length, with two major putative functional domains identified as an N-terminal MAP kinase binding domain and a C-terminal phosphatase domain (Figure 9A). The Dusp4 amino acid sequence is also highly conserved, with human Dusp4 sharing approximately 96% sequence similarity to mouse and rat Dusp4. Previously, our lab wanted to see if Dusp4 alters MAP kinase signaling when it is overexpressed during proliferation, and thus developed an AP-1 reporter plasmid system by fusing a canonical AP-1 response element with a minimal SV40 promoter to create the pSEAP-Pro-AP-1 reporter plasmid. Ectopic overexpression of wild-type Dusp4 significantly repressed the AP-1 reporter in a dose-dependent manner (Figure 9B). Mutation of cysteine 284, within the phosphatase domain, (Figure 9A) resulted in significantly less repression of the AP-1 reporter compared to wild-type Dusp4 (Figure 9B). Additionally, a Dusp4 dominant negative construct was created by mutating cysteine 284 to glycine as well as mutating alanine 93 to serine within the MAP kinase binding domain (Figure 9A). This Dusp4-C284G/A93S double mutant showed significant repression of the AP-1 reporter in a similar manner to wild-type Dusp4 (Figure 9B) (Haddock, 2016).

After seeing effects on the AP-1 reporter, we next wanted to determine if Dusp4 possessed any effect on ERK phosphorylation. To that end, C_2C_{12} cells were transfected with wild-type Dusp4, Dusp4-C284G, or Dusp4-C284G/A93S expression plasmids and treated with epidermal growth factor (EGF) for 15 or 30 minutes. EGF acts by binding to the epidermal growth factor receptor (EGFR) on the cell surface, which then initiates a signal transduction cascade resulting in phosphorylation and activation of ERK (Lee et al., 2016; Oda et al., 2005). Cells were harvested and the phosphorylation status of ERK was evaluated by Western blot. Overexpression of wild-type Dusp4 resulted in nearly complete loss of phosphorylated ERK (p-ERK) (Figure 9C and

9D) (Haddock, 2016). By comparison, the Dusp4-C284G phosphatase dead mutant exhibited some dephosphorylation of ERK compared to control cells, but significantly less than the cells overexpressing wild-type Dusp4. This suggests there is impaired phosphatase activity in the catalytic mutant and that catalytic activity is necessary for ERK dephosphorylation by Dusp4 (Figure 9C and 9D) (Haddock, 2016). Interestingly, despite seeing dramatic reduction in AP-1 reporter levels, ectopic expression of the Dusp4-A93S/C284G double mutant resulted in significant loss of Dusp4's ability to dephosphorylate ERK (Figure 9C and 9D) (Haddock, 2016).

After having observed the effects of overexpression of the Dusp4 constructs on ERK MAPK signaling, we next wanted to observe potential effects on muscle cell differentiation. Additionally, we wanted to observe Dusp4 effects on ERK phosphorylation as muscle cells proceed through differentiation. Based upon previous results, we hypothesized that the Dusp4-A93S/C284G double mutant (Dusp4-DN) may be acting in a dominant-negative fashion by preferentially binding to and not releasing phosphorylated ERK, thus we used co-immunoprecipitation analysis to investigate this possibility. Furthermore, we wanted to compare the effects of Dusp4 overexpression with the effects of treating muscle cells with small-molecule inhibitors for ERK1/2 and MEK1/2.

A.

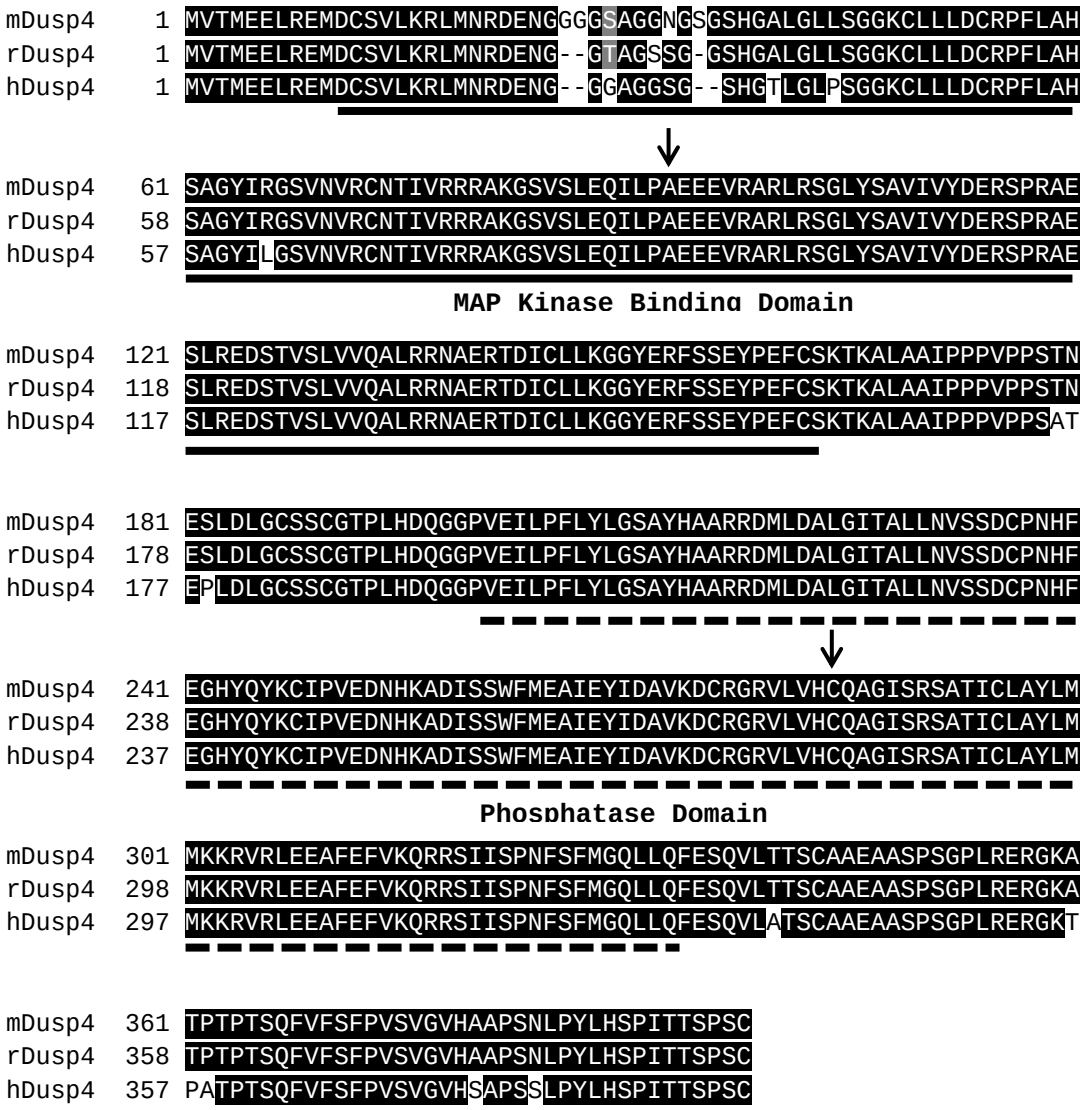
mDusp4 1 MVTMEELREMDCSVLKRLMNRDENGGGGSAGGNGSGSHGALGLLSGGKCLLLDCRPFLAH
rDusp4 1 MVTMEELREMDCSVLKRLMNRDENG--GTAGSSG-GSHGALGLLSGGKCLLLDCRPFLAH
hDusp4 1 MVTMEELREMDCSVLKRLMNRDENG--GGAGGSG--SHGTLGLPSGGKCLLLDCRPFLAH
mDusp4 61 SAGYIRGSVNVRCNTIVRRRAKGSVSLEQILPAEEEVRARLRSGLYSAVIVYDERSPRAE
rDusp4 58 SAGYIRGSVNVRCNTIVRRRAKGSVSLEQILPAEEEVRARLRSGLYSAVIVYDERSPRAE
hDusp4 57 SAGYILGSVNVRCNTIVRRRAKGSVSLEQILPAEEEVRARLRSGLYSAVIVYDERSPRAE
MAP Kinase Binding Domain
mDusp4 121 SLREDSTVSLVVQALRRNAERTDICLLKGGYERFSSEYPEFCSKTKALAAIPPPVPPSTN
rDusp4 118 SLREDSTVSLVVQALRRNAERTDICLLKGGYERFSSEYPEFCSKTKALAAIPPPVPPSTN
hDusp4 117 SLREDSTVSLVVQALRRNAERTDICLLKGGYERFSSEYPEFCSKTKALAAIPPPVPPSAT
mDusp4 181 ESLDLGCSSCGTPLHDQGGPVEILPFLYLGSAYHAARRDMLDALGITALLNVSSDCPNHF
rDusp4 178 ESLDLGCSSCGTPLHDQGGPVEILPFLYLGSAYHAARRDMLDALGITALLNVSSDCPNHF
hDusp4 177 EPLDLGCSSCGTPLHDQGGPVEILPFLYLGSAYHAARRDMLDALGITALLNVSSDCPNHF
mDusp4 241 EGHYQYKCIPVEDNHKADISSWFMEAIEYIDAVKDCRGRVLVHCQAGISRSATICLAYLM
rDusp4 238 EGHYQYKCIPVEDNHKADISSWFMEAIEYIDAVKDCRGRVLVHCQAGISRSATICLAYLM
hDusp4 237 EGHYQYKCIPVEDNHKADISSWFMEAIEYIDAVKDCRGRVLVHCQAGISRSATICLAYLM
Phosphatase Domain
mDusp4 301 MKKRVRLEEAFEFVKQRRSIISPNFSFMGQLLQFESQVLTTSCAAEAASPSGPLRERGKA
rDusp4 298 MKKRVRLEEAFEFVKQRRSIISPNFSFMGQLLQFESQVLTTSCAAEAASPSGPLRERGKA
hDusp4 297 MKKRVRLEEAFEFVKQRRSIISPNFSFMGQLLQFESQVLATSCAAEAASPSGPLRERGKT
mDusp4 361 TPTPTSQFVFSFPVSVGVHAAPSNLPYLHSPITTSPSC
rDusp4 358 TPTPTSQFVFSFPVSVGVHAAPSNLPYLHSPITTSPSC
hDusp4 357 PATPTSQFVFSFPVSVGVHSAPSSLPYLHSPITTSPSC

B.

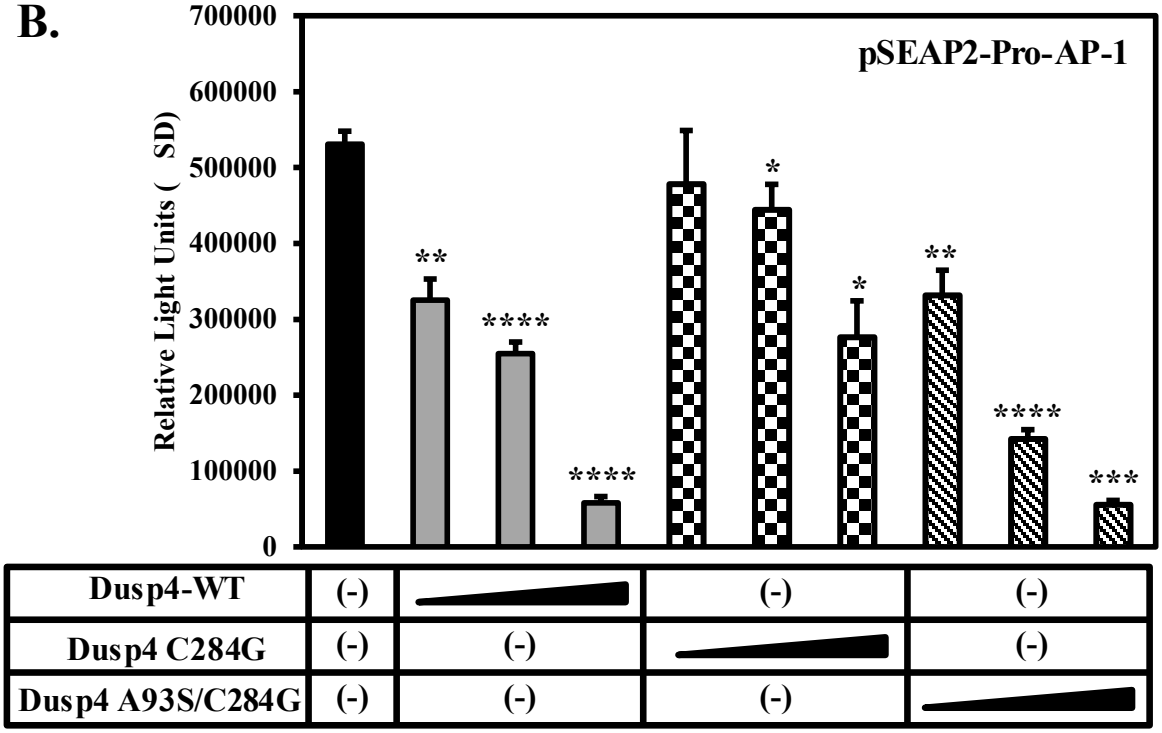
pSEAP2-Pro-AP-1
Relative Light Units (SD)
700000
600000
500000
400000
300000
200000
100000
0
**
****
****
*
*
**
****
***
Dusp4-WT
Dusp4 C284G
Dusp4 A93S/C284G
(-)

C.

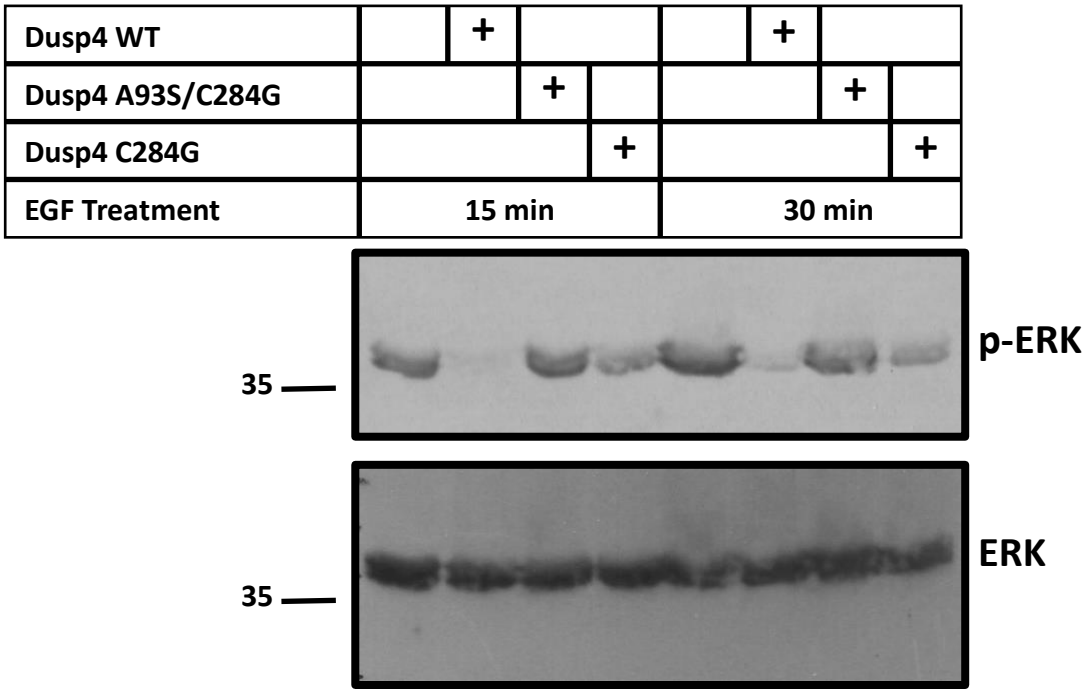
Dusp4 WT
Dusp4 A93S/C284G
Dusp4 C284G
EGF Treatment
15 min
30 min
+
35
p-ERK
ERK

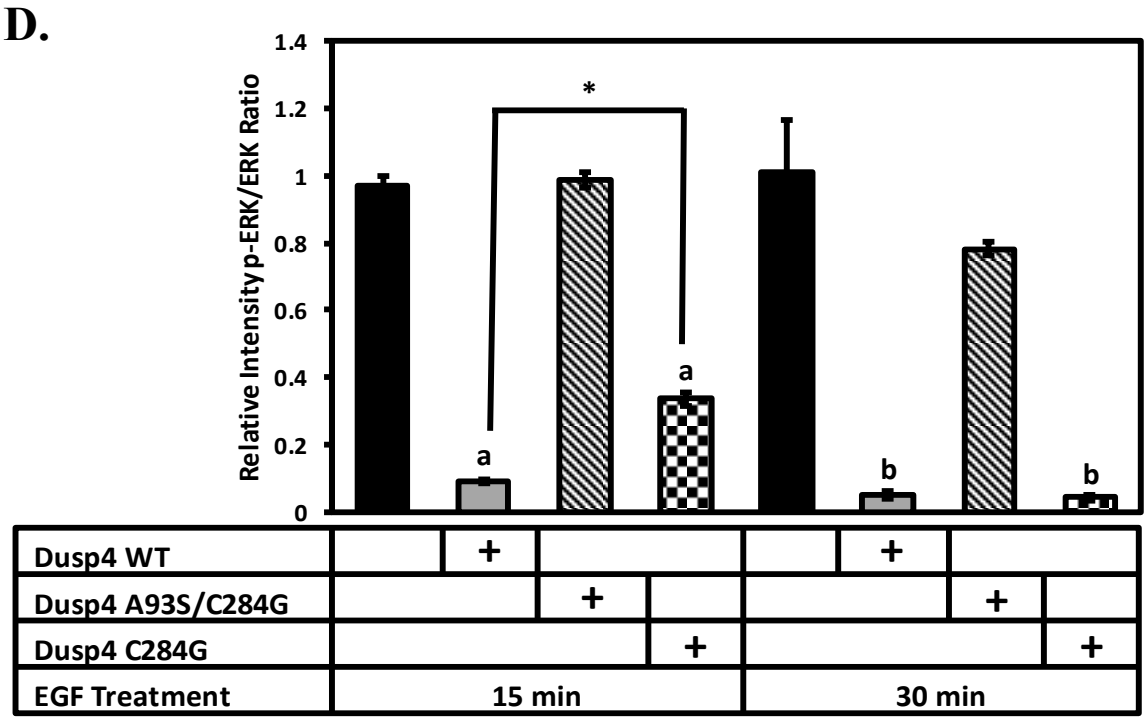

Figure 9. Dusp4 represses MAP kinase signaling by dephosphorylation of ERK1/2. (A) Schematic of putative functional domains of Dusp4. Dusp4 is predicted to contain a MAP kinase binding domain, a nuclear localization signal, and a phosphatase domain. (B) C_2C_{12} myoblasts were transfected with an AP-1 reporter plasmid (pSEAP2-Pro-AP-1) and increasing concentrations of expression plasmids containing cDNA of Dusp4 wild-type (WT) (gray bars), Dusp4-C284G phosphatase dead (PD) mutant (checkered bars), or the Dusp4-A93S/C248G dominant negative (DN) mutant (striped bars). Each condition was performed in triplicate and each experiment (n=3) was repeated at least three times. The graphs are representative of these experiments and values correlate to the mean relative light unit (RLU) values ± SD. Significant differences between control (black bar) and wild-type Dusp4, phosphatase dead Dusp4, or dominant negative Dusp4 ectopic expression, (*: $P \leq 0.05$, **: $P \leq 0.01$, ***: $P \leq 0.001$, ****: $P \leq 0.0001$). Dusp4 inhibits MAP kinase signaling by dephosphorylation of ERK in C_2C_{12} cells. Western blot analysis of phosphorylated ERK (p-ERK) and whole ERK (ERK) levels in C_2C_{12} cells overexpressing Dusp4-WT, Dusp4-PD, and Dusp4-DN. (D) Quantification of p-ERK levels relative to whole ERK levels in response to Dusp4-WT, Dusp4-PD, or Dusp4-DN ectopic expression. Western blots were repeated at least three times (n=3) and the blots shown are representative of the results obtained. Significant differences between controls (black bars) and Dusp4 ectopic expression (a= 15 minutes, b=30 minutes EGF treatment and a,b: *$P \leq 0.05$) (Haddock et al., 2019).

Materials and Methods

Cell Culture

The C_2C_{12} immortalized mouse myoblast cell line (CRL-1772) obtained from the American Type Culture Collection (Manassas, VA) was maintained in DMEM (Life Technologies, Grand Island,

NY) with 10% Fetal Bovine Serum (FBS), non-essential amino acids (both from GE Healthcare HyClone Laboratories, Logan, UT), 1X Penicillin/Streptomycin and Gentamicin (both from Life Technologies, Grand Island, NY) and grown at 37℃ in a 5% CO_2 humidified incubator. To induce myoblasts to differentiate cells were switched to DMEM supplemented with 2% serum, non-essential amino acids, Penicillin/Streptomycin, and Gentamicin.

Transfections

C_2C_{12} myoblast cells were plated into 12 well plates at a density of 75,000 cells/well and cultured overnight. All conditions assessed were conducted in triplicate. Transfections were performed utilizing Turbofect Transfection Reagent (Thermo Scientific, Rockford, IL) following manufacturer protocol. Media was changed approximately 1 hour prior to transfection and 1 μg of total DNA (250 ng/well of reporter plasmid, 125 ng/well of β-galactosidase (β-gal) as the internal control plasmid, and empty pBluescript vector as filler DNA to 1 μg DNA/well) was allowed to complex with Turbofect for 20 minutes prior to overlaying the cells. Cells were incubated overnight with these complexes, then switched to differentiation media (DMEM + 2% FBS) 24 hours post-transfection and incubated for an additional 24-72 hours until reporter assays were performed.

For transfections that required treatment with an inhibitor, C_2C_{12} cells were transfected approximately 24 hours post-plating according to the protocol described above, then the media was refreshed (DMEM + 10% FBS) 24 hours post-transfection and the small-molecule inhibitor was applied at the appropriate concentrations or cells were mock-treated with DMSO. Cells were then switched to differentiation media (DMEM + 2% FBS) approximately 24-hours later, treated

again with inhibitor or DMSO, and incubated for an additional 24 hours until a reporter assay was performed.

Reporter gene assays

Culture media was sampled 24-72 hours post 2% FBS media change and analyzed for secreted alkaline phosphatase (SEAP) activity levels using the Phospha-Light SEAP Reporter Gene Assay System following manufacturer protocol (Life Technologies, Grand Island, NY). Glow luminescence levels were detected utilizing a Synergy 2 microplate reader set for an endpoint read with a 2 second integration time. Once all desired time points were assayed, cells were lysed with 1X Passive Lysis Buffer (Promega, Madison, WI), homogenates were centrifuged and analyzed for β-gal levels to determine transfection efficiency. SEAP activity values were divided by β-gal activity values to correct for variations in transfection efficiency between replicates and conditions.

Protein purification and Western blot analysis

C_2C_{12} cells were differentiated over a 10 day time course by plating cells into 10cm culture dishes and maintaining them in proliferation media (DMEM + 10% serum) for 2 days followed by a switch to differentiation media (DMEM + 2% serum) at 2 days post-plating. The time course consisted of harvesting cells grown in proliferation media for 1 and 2 days, as well as, cells grown for 2 days in proliferation media followed by continued culturing for 1, 3, 5, 7, 9, and 10 days in differentiation media. Harvested cells were spun down and stored at -80℃ until cell lysis and protein purification was performed.

Harvested cells were lysed on ice for 30 minutes in $ULB^{(+)}$ (50 mM Tris, pH 7.5, 150mM NaCl, 50mM NaF, 0.5% IGEPAL, 1mM PMSF, 1mM DTT, 10mM β-glycerophosphate, 2mM sodium

molbydate, 0.5mM sodium orthovanadate, and a protease inhibitor cocktail). Cell lysates were cleared by centrifugation and protein concentrations were determined using the Quick Start Bradford 1X Dye Reagent (Bio-Rad, Hercules, CA) following manufacturer protocol.

Western blot analysis was performed by separating 75-150μg total protein on a SDS-PAGE gel and then transferring the separated proteins overnight to Immobilon-P PVDF membrane (EMD Millipore, Billerica, MA). The membrane was Ponceau S stained to confirm equal protein loading and then blocked in blocking solution (5% w/v dry milk dissolved in Tris-buffered Saline with 0.05% Tween-20 (TTBS)). Blots were probed with anti-MKP2 (S-18, Santa Cruz Biotechnology), anti-Myosin Heavy Chain (MYH1/2/4/6) (F59, Santa Cruz Biotechnology, Dallas, TX), anti- myogenin (F5D, Santa Cruz Biotechnology, Dallas, TX), anti-p-ERK (E-4, Santa Cruz Biotechnology, Dallas, TX), anti-ERK (K-23, Santa Cruz Biotechnology, Dallas, TX), anti-p38α/β (A-12, Santa Cruz Biotechnology, Dallas, TX)or anti-α-tubulin (DM1A, Santa Cruz Biotechnology, Dallas, TX) primary antibodies followed by incubation with either Mouse anti-Rabbit IgG-HRP (Santa Cruz Biotechnology, Dallas, TX) or Rabbit anti-Mouse IgG (H+L) (Thermo Scientific, Rockford, IL) HRP-conjugated secondary as appropriate for the primary antibody species. Then blots were imaged using ECL Western Blotting Substrate (Pierce/Thermo Scientific, Rockford, IL). Blots were stripped by incubating at 50°C for 15-20 minutes in Stripping Buffer (10% SDS, 0.5M Tris-HCl pH 6.8, β-mercaptoethanol), washed, and then blocked, re-probed, and imaged as described above.

Dusp4 overexpression and Co-Immunoprecipitation

Dusp4 WT was exogenously expressed in C_2C_{12} cells that were plated into 10cm culture dishes and transfected with the pcDNA-zeo-Dusp4 WT expression plasmid 24 hours post-plating. The

transfected cells were differentiated over a 5 day time course by maintaining them in proliferation media (DMEM + 10% serum) for 2 days followed by a switch to differentiation media (DMEM + 2% serum) 2 days post-plating. The time course consisted of harvesting cells grown in proliferation media for 2 days and cells grown for 2 days in proliferation media followed by continued culturing for 1, 2, 3, and 4 days in differentiation media. Harvested cells were spun down and stored at -80℃ until cell lysis and protein purification was performed. The same protocol was followed for exogenously expressing Dusp4 DN.

Co-immunoprecipitation (Co-IP) was conducted by transfecting C_2C_{12} cells 24 hours post-plating with pcDNA3-Dusp4-WT or pcDNA-Dusp4-DN plasmids or mock transfected and harvested after an additional 24 hours in proliferation media. The protein isolation was conducted as described above for Western blots. Experiments were carried out by preclearing 500μg protein using Protein A/G-agarose beads (GenDEPOT, Barker, TX). Lysates were mixed with anti-Dusp4 primary antibody (S-18, Santa Cruz Biotechnology) and incubated for 4 hours at 4°C. Agarose beads were then added and incubated overnight at 4°C. Finally, the beads were washed three times and immunoprecipitated samples were run on an SDS-PAGE gel and analyzed by Western blot.

Inhibitor Treatments

Pharmacologic inhibitors SCH772984 (2 μM) (Apexbio Technology, Houston, TX), GSK1120212 (5 μM) (SYNkinase, San Diego, CA), or AMZ-30 (20 μM) (EMD Millipore Corp., Billerica, MA) were applied to C_2C_{12} cells 24 hours post-plating. Cells were maintained in proliferation media (DMEM + 10% FBS) for 2 days followed by a switch to differentiation media (DMEM + 2% FBS) 2 days post-plating. Inhibitor treatments were applied every 24 hours

until cells were harvested at 48 hours post-plating (PD2), as well as 24, 48, and 72 hours after those cells were switched to differentiation media (DD1, DD2, and DD3). Harvested cells were spun down and stored at -80℃ until the cells were lysed and the protein was isolated and purified.

Statistics

Data are presented as the mean ± standard deviation (SD). Statistical analysis was conducted using a two-tailed t-test and a difference was considered statistically significant at a P value < 0.05.

Results

Ectopic expression of Dusp4 inhibits muscle cell differentiation.

The pcDNA3-Dusp4 WT expression plasmid was transfected into C_2C_{12} mouse myoblasts and cells were harvested at 24 hours post-transfection (PD2), while the remaining cells were switched to differentiation media (2% serum) and harvested at 24, 48, 72, and 96 hours post-media switch. Western blots were then performed to analyze the effect of Dusp4 on markers of muscle cell differentiation over time. Mouse monoclonal antibodies against Myosin Heavy Chain (MyHC) and myogenin were used to analyze the expression of these canonical markers of muscle cell differentiation in control muscle cells and cells ectopically expressing Dusp4. Overexpression of Dusp4 resulted in decreased expression of MyHC in early differentiation (DD1) (Figure 10A and 10B) as well as myogenin at the onset of differentiation (DD1-DD3) (Figure 10A and 10C). It did not prevent muscle cells from eventually differentiating as MyHC and myogenin levels are approximately equal by later differentiation (DD2 and DD4,

respectively) (Figure 10A, 10B, and 10C). Dusp4 overexpression, analyzed using a rabbit polyclonal antibody against MKP2/Dusp4 , decreased significantly as cells begin to differentiate, which correlates with increased expression of muscle cell differentiation markers, and suggests that Dusp4 is likely post-transcriptionally and/or post-translationally regulated during muscle cell differentiation (Figure 10A and 10D). α-tubulin protein levels were analyzed to confirm equal protein loading and demonstrated that α-tubulin levels remained constant from proliferation through differentiation (Figure 10A).

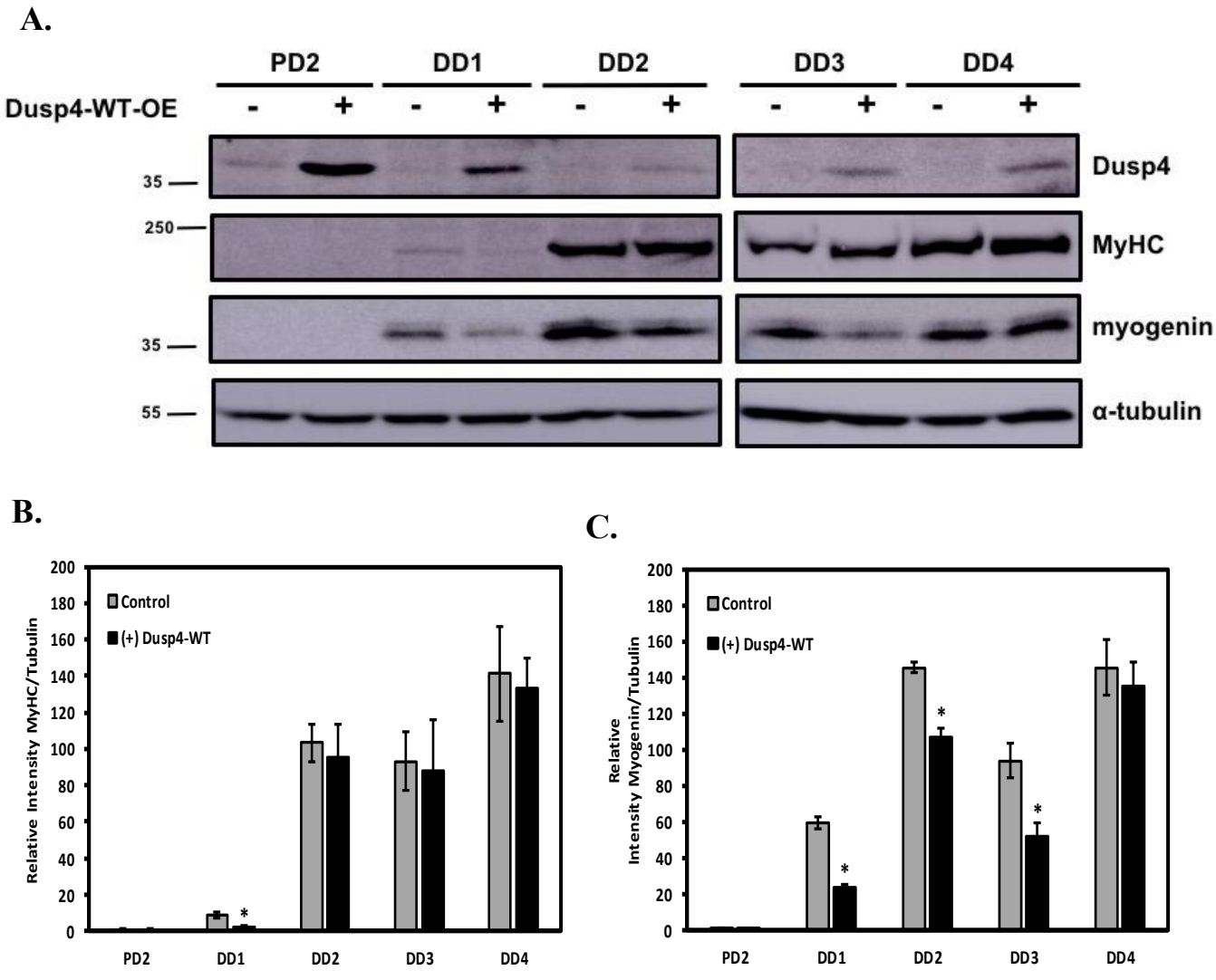

D.

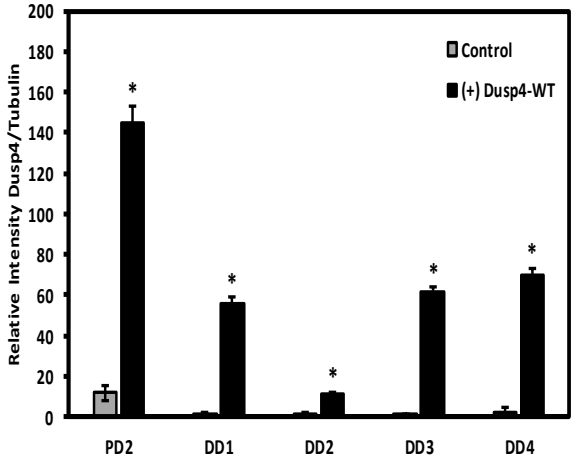

Figure 10. Ectopic expression of Dusp4 in C_2C_{12} muscle cells inhibits muscle cell differentiation. C_2C_{12} cells were transfected with the pcDNA3-Dusp4-WT expression plasmid or mock transfected followed by Western blot analysis. Proliferating (PD) and differentiated (DD) control C_2C_{12} cells and cells overexpressing Dusp4-WT were harvested over a 4 day differentiation time course. Cells were maintained in proliferation media (10% serum) and harvested 2 days post-plating and the remaining cells were switched to differentiation media (2% serum) and harvested at 1, 2, 3 and 4 days post-media change. (A) Western blot analysis of Dusp4, Myosin Heavy Chain (MyHC), and myogenin. Quantification of (B) MyHC (C) myogenin and (D) Dusp4 from blots after normalization to α-tubulin. Western blots were repeated and the blots shown are representative of results. Significant difference between control cells and cells overexpressing Dusp4-WT (*: $P \leq 0.05$).

Ectopic expression of Dusp4 attenuates MAP Kinase signaling in muscle cells.

Dusp4 was overexpressed in C_2C_{12} myoblasts and cells were harvested at 24 hours post-transfection (PD2), while the remaining cells were switched to differentiation media (2% serum) and harvested at 24, 48, 72, and 96 hours post-media switch. Western blots were then performed to evaluate markers of the MAP Kinase signaling pathway over the time course. A mouse monoclonal antibody against phosphorylated ERK (p-ERK) was used to analyze the level of p-ERK in muscle cells ectopically expressing Dusp4 compared to control cells. Overexpression of Dusp4 resulted in significantly lower levels of p-ERK in cells overexpressing Dusp4 (Figure 11A and 11B). ERK protein levels were evaluated using a rabbit polyclonal antibody showed

ERK expression levels remained equal between control cells and cells overexpressing Dusp4 overexpressed at all time points (PD2-DD4) (Figure 11A and 11B).

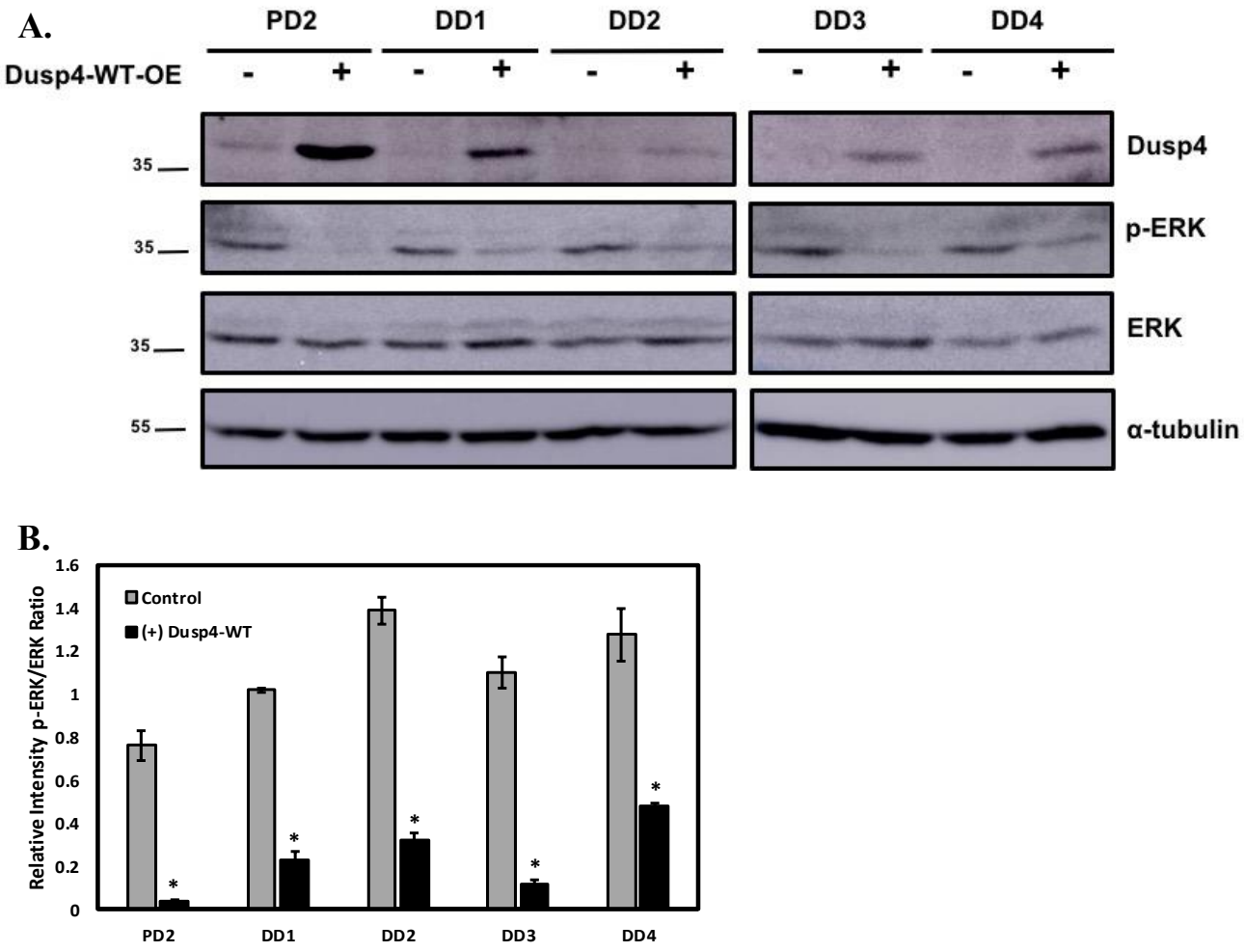

Figure 11. Ectopic expression of Dusp4 attenuates ERK1/2 MAPK signaling. Proliferating (PD) and differentiated (DD) control C_2C_{12} cells and cells overexpressing Dusp4 were harvested over a 4 day differentiation time course. Cells were maintained in proliferation media (10% serum) and harvested 2 days post-plating and the remaining cells were switched to differentiation media (2% serum) and harvested at 1, 2, 3 and 4 days post-media change. (A) Western blot analysis of phosphorylated-ERK (p-ERK) and whole ERK (ERK) using protein lysates from proliferating (PD) and differentiating (DD) C_2C_{12} overexpressing Dusp4 harvested over a 4 day differentiation time course. (B) Quantification of p-ERK levels relative to whole-ERK levels in response to overexpression of Dusp4. Western blots were repeated and the blots are representative of the results obtained. Significant difference between control cells and cells overexpressing Dusp4 (*:$P \leq 0.05$).

Ectopic expression of a Dusp4 Dominant Negative (DN) significantly inhibits muscle cell differentiation.

The pcDNA3-Dusp4-DN expression plasmid was transfected into C_2C_{12} mouse myoblasts and cells were harvested at 24 hours post-transfection (PD2), while the remaining cells were switched to differentiation media (2% serum) and harvested at 24, 48, 72, and 96 hours post-media switch. Western blots were then performed to analyze markers of muscle cell differentiation over the time course. Mouse monoclonal antibodies against Myosin Heavy Chain (MyHC) and myogenin were used to analyze the expression of these canonical markers of muscle cell differentiation in control cells and cells ectopically expressing Dusp4-DN. Overexpression of Dusp4-DN resulted in dramatically reduced expression of MyHC and myogenin through late differentiation (DD1-DD4) and ultimately prevented cells from terminally differentiating (Figure 12A, 12B, and 12C). Dusp4-DN overexpression, analyzed using a rabbit polyclonal antibody against MKP2/Dusp4, decreased significantly as cells begin to differentiate (Figure 12A and 12D). α-tubulin protein levels were analyzed to confirm equal protein loading and demonstrated that α-tubulin levels remained constant from proliferation through differentiation (Figure 12A).

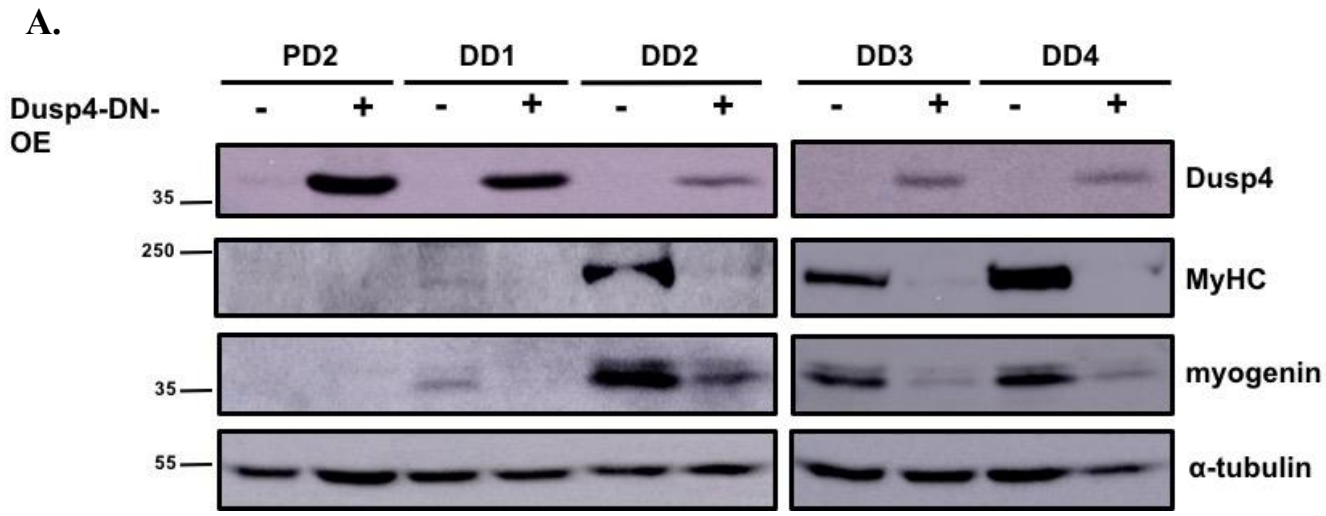

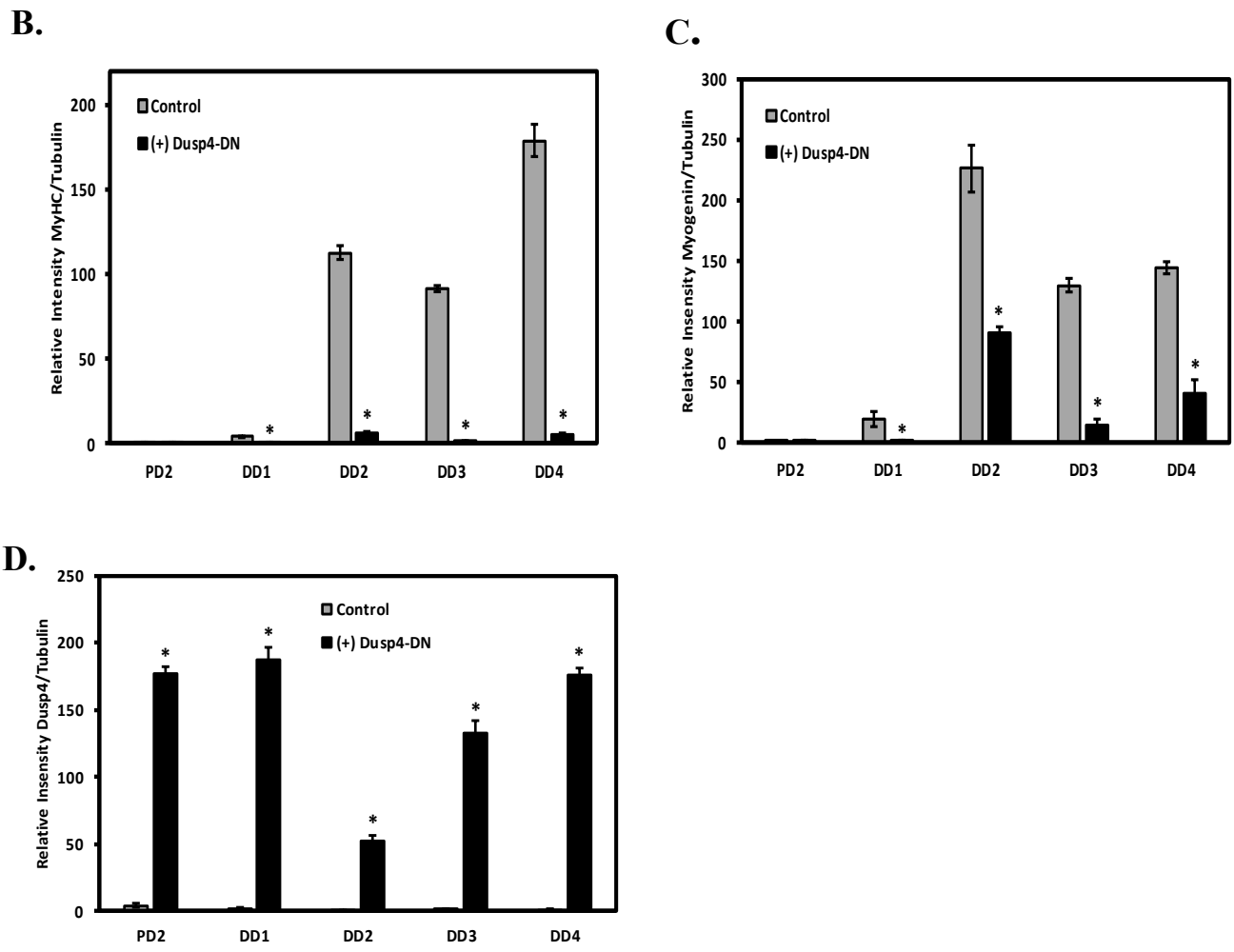

Figure 12. Ectopic expression of Dusp4-DN in C_2C_{12} muscle cells inhibits muscle cell differentiation. C_2C_{12} cells were transfected with the pcDNA3-Dusp4-DN expression plasmid or mock transfected followed by Western blot analysis. Proliferating (PD) and differentiated (DD) control C_2C_{12} cells and cells overexpressing Dusp4-DN were harvested over a 4 day differentiation time course. Cells were maintained in proliferation media (10% serum) and harvested 2 days post-plating and the remaining cells were switched to differentiation media (2% serum) and harvested at 1, 2, 3 and 4 days post-media change. (A) Western blot analysis of Dusp4-DN, Myosin Heavy Chain (MyHC), and myogenin. Quantification of (B) MyHC (C) myogenin and (D) Dusp4 from blots after normalization to α-tubulin. Western blots were repeated and the blots shown are representative of results. Significant difference between control cells and cells overexpressing Dusp4-DN (*: $P \leq 0.05$).

Ectopic expression of Dusp4-DN attenuates MAP kinase signaling in muscle cells.

Dusp4-DN was overexpressed in C_2C_{12} myoblasts and cells were harvested at 24 hours post-transfection (PD2), while the remaining cells were switched to differentiation media (2% serum)

and harvested at 24, 48, 72, and 96 hours post-media switch. Western blots were then performed to evaluate markers of the MAP kinase signaling pathway over the time course. A mouse monoclonal antibody against phosphorylated ERK (p-ERK) was used to analyze the level of p-ERK in muscle cells ectopically expressing Dusp4-DN compared to control cells. Overexpression of Dusp4-DN resulted in significantly higher levels of p-ERK during proliferation and early differentiation (PD2 and DD1) with a decrease in p-ERK seen during later differentiation (DD3 and DD4) (Figure 13A and 13B). Interestingly, overall ERK protein levels evaluated using a rabbit polyclonal antibody also showed an overall increase during early time points (PD2, DD1, and DD2) but returned to control levels by later differentiation (Figure 13A).

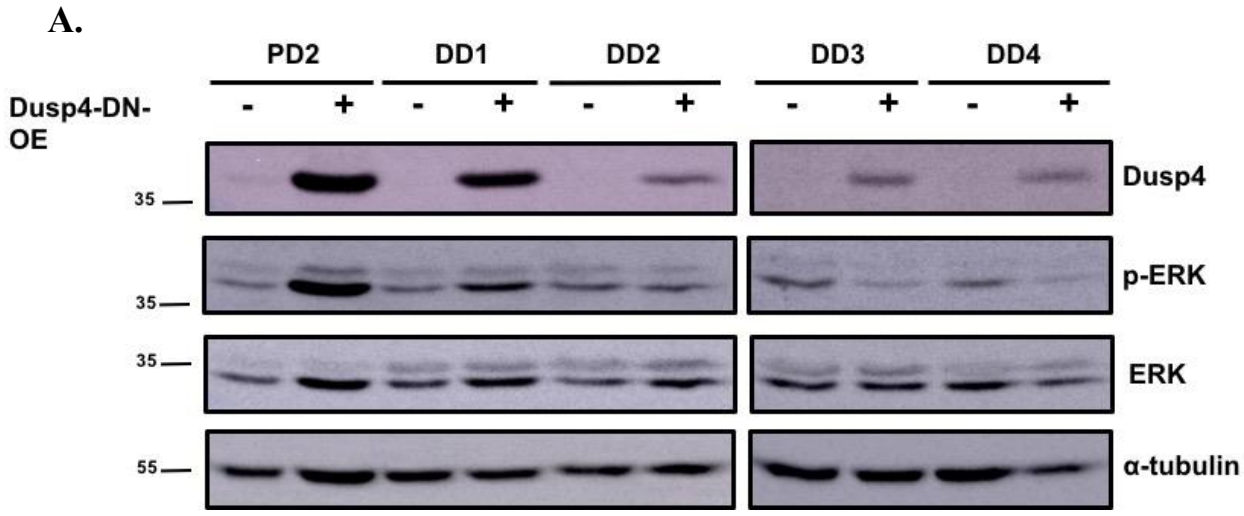

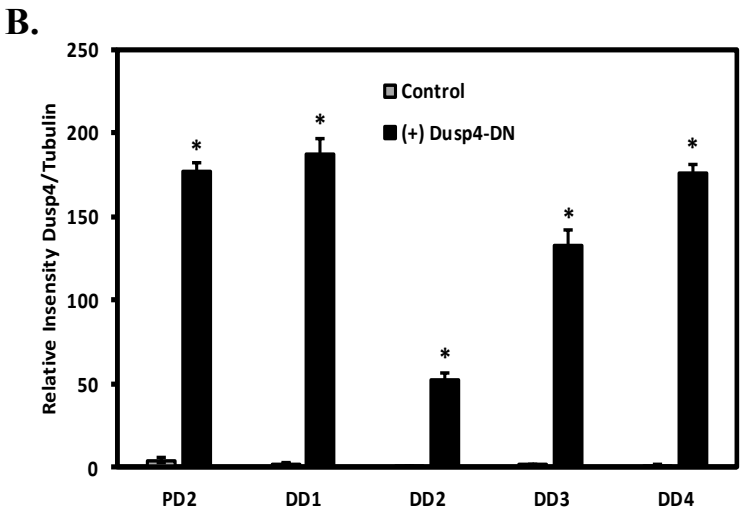

Figure 13. Ectopic expression of Dusp4-DN inhibits ERK1/2 MAPK signaling. Proliferating (PD) and differentiated (DD) control C_2C_{12} cells and cells overexpressing Dusp4-DN were harvested over a 4 day differentiation time course. Cells were maintained in proliferation media (10% serum) and harvested 2 days post-plating and the remaining cells were switched to differentiation media (2% serum) and harvested at 1, 2, 3 and 4 days post-media change. (A) Western blot analysis of phosphorylated-ERK (p-ERK) and whole ERK (ERK) using protein lysates from proliferating (PD) and differentiating (DD) C_2C_{12} overexpressing Dusp4-DN harvested over a 4 day differentiation time course. (B) Quantification of p-ERK levels relative to whole-ERK levels in response to overexpression of Dusp4-DN. Western blots were repeated and the blots are representative of the results obtained. Significant difference between control cells and cells overexpressing Dusp4-DN (*:$P \leq 0.05$).

Dusp4 is ERK1/2 specific and does not interact with p38 in skeletal muscle cells.

Based upon the Dusp4-DN overexpression impact on p-ERK and whole ERK levels, we hypothesized that the Dusp4-A93S/C284G double mutant (Dusp4-DN) acts in a dominant negative fashion by specifically and irreversibly binding to phosphorylated ERK. Thus, we performed a co-immunoprecipitation (co-IP) analysis followed by Western blot to determine if Dusp4 was interacting directly with ERK and/or with p38, another MAPK member. Dusp4-WT and Dusp4-DN were overexpressed in C_2C_{12} myoblasts and cells were harvested at 24 hours post-transfection (PD2). Co-IP was then performed using a rabbit polyclonal antibody against Dusp4 to pulldown any proteins associating directly with Dusp4 in the control, Dusp4-WT, and Dusp4-DN overexpressing cells. Western blot was then performed using anti-Dusp4, anti-

ERK1/2, and anti-p38 antibodies. We observed that Dusp4-DN binds significantly with ERK1/2 but not with p38, whereas we did not see any pulldown with the Dusp4-WT as the interaction between Dusp4 and ERK1/2 is likely a transient event (Figure 14).

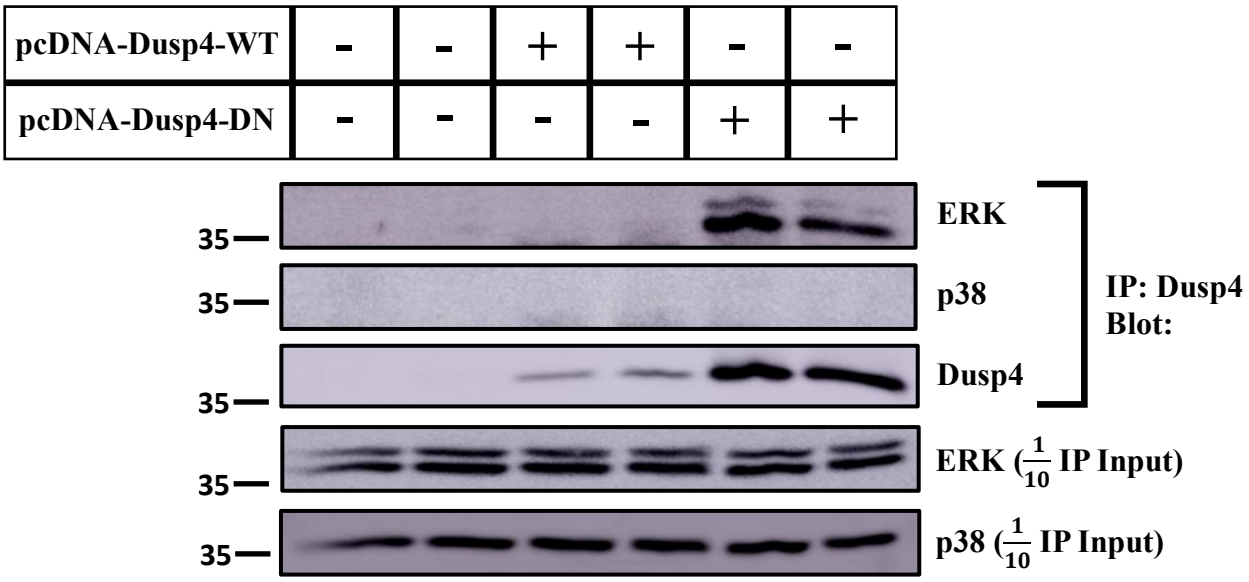

Figure 14. Dusp4 directly interacts with ERK1/2 but not p38 MAP kinase. Co-immunoprecipitation was conducted for Dusp4 from control C_2C_{12} cells and cells overexpressing Dusp4-WT or Dusp4-DN followed by Western blotting for ERK1/2, p38, and Dusp4 (top three panels). Western blot analysis confirmed equal ERK1/2 and p38 protein levels in homogenates from the control C_2C_{12} cells as well as the cells overexpressing Dusp4-WT or Dusp4-DN (bottom two panels).

Inhibition of MEK1/2 and ERK1/2 attenuates AP-1 reporter activity in a dose-dependent manner.

To confirm that muscle cells treated with SCH772984 or GSK1120212 exhibit decreased downstream MAPK signaling similar to ectopic Dusp4 expression, the AP-1 reporter was transfected into C_2C_{12} cells. Cells were then treated with either inhibitor or mock-treated with DMSO 24 hours post-transfection and again 48 hours post-transfection when the cells were switched to differentiation media (2% serum). Reporter gene activity was measured by sampling the media 24 hours post-media change (DD1) and analyzing secreted alkaline phosphatase

(SEAP) activity. Muscle cells treated with SCH772984 or GSK1120212 exhibited significantly lower AP-1 reporter activity in a dose dependent manner compared to control cells treated with DMSO (Figures 15 and 16).

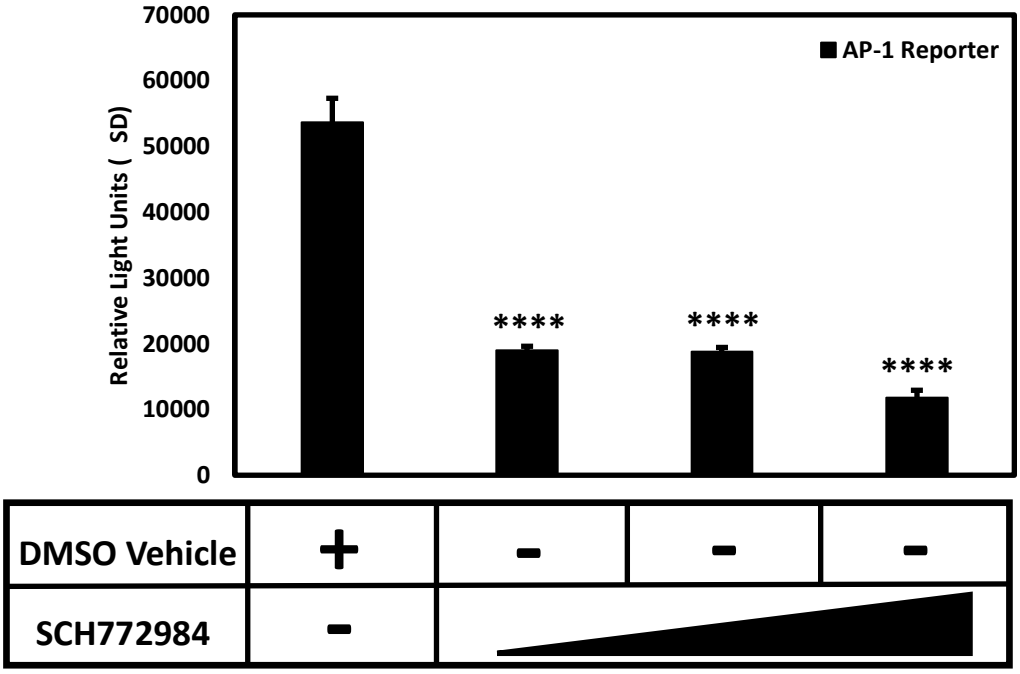

Figure 15. Treatment with an ERK1/2 inhibitor attenuates AP-1 reporter activity in C_2C_{12} myoblasts in a dose-dependent manner. C_2C_{12} cells were transfected with an AP-1 reporter plasmid approximately 24 hours post-plating, the media was refreshed (DMEM + 10% FBS) 24 hours post-transfection and the inhibitor SCH772984 (1μM, 2μM, or 4μM) was applied or cells were mock-treated with DMSO. Cells were then switched to differentiation media (DMEM + 2% FBS) approximately 24-hours later, treated again with inhibitor or DMSO, and incubated for an additional 24 hours until the reporter assay was performed (****: $P \leq 0.0001$).

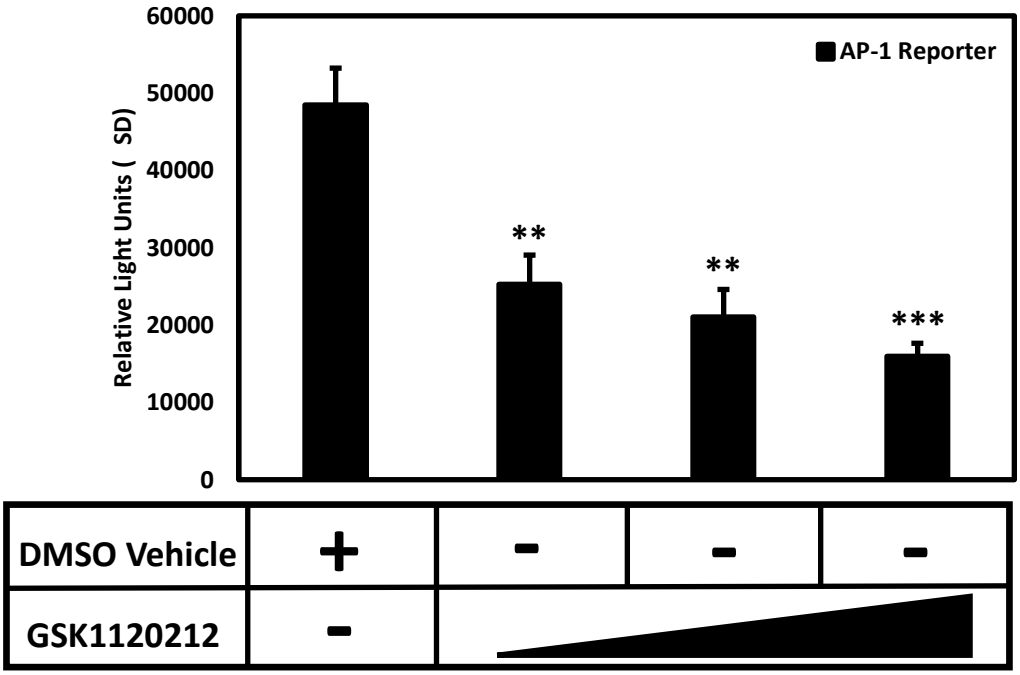

Figure 16. Treatment with a MEK1/2 inhibitor attenuates AP-1 reporter activity in C_2C_{12} myoblasts in a dose-dependent manner. C_2C_{12} cells were transfected with an AP-1 reporter plasmid approximately 24 hours post-plating, the media was refreshed (DMEM + 10% FBS) 24 hours post-transfection and the inhibitor GSK1120212 (2.5μM, 5μM, or 10μM) was applied or cells were mock-treated with DMSO. Cells were then switched to differentiation media (DMEM + 2% FBS) approximately 24-hours later, treated again with inhibitor or DMSO, and incubated for an additional 24 hours until the reporter assay was performed (**: $P \leq 0.01$, ***: $P \leq 0.001$).

Inhibition of ERK1/2 inhibits proper muscle cell differentiation.

C_2C_{12} cells were treated with either 2 μM ERK inhibitor (SCH772984) or treated with the vehicle DMSO 24 hours post-plating and then harvested 24 hours post-treatment (PD2), while the remaining cells were switched to differentiation media (2% serum) and treated every 24 hours until being harvested at 24, 48, and 72 hours post-media switch. Western blots were conducted to analyze markers of skeletal muscle differentiation across this time course. Mouse monoclonal antibodies against MyHC and myogenin were used to analyze expression of markers of muscle cell differentiation in control muscle cells compared to cells that had been

treated with SCH772984. Inhibition of ERK results in a significant increase in MyHC expression at the start of differentiation (DD1) and an increase in myogenin is also observed during proliferation (PD2) (Figure 17). MyHC levels are similar to control cells as differentiation proceeds (DD2-DD3), while myogenin levels remain reduced during differentiation (DD1-DD3) (Figure 17).

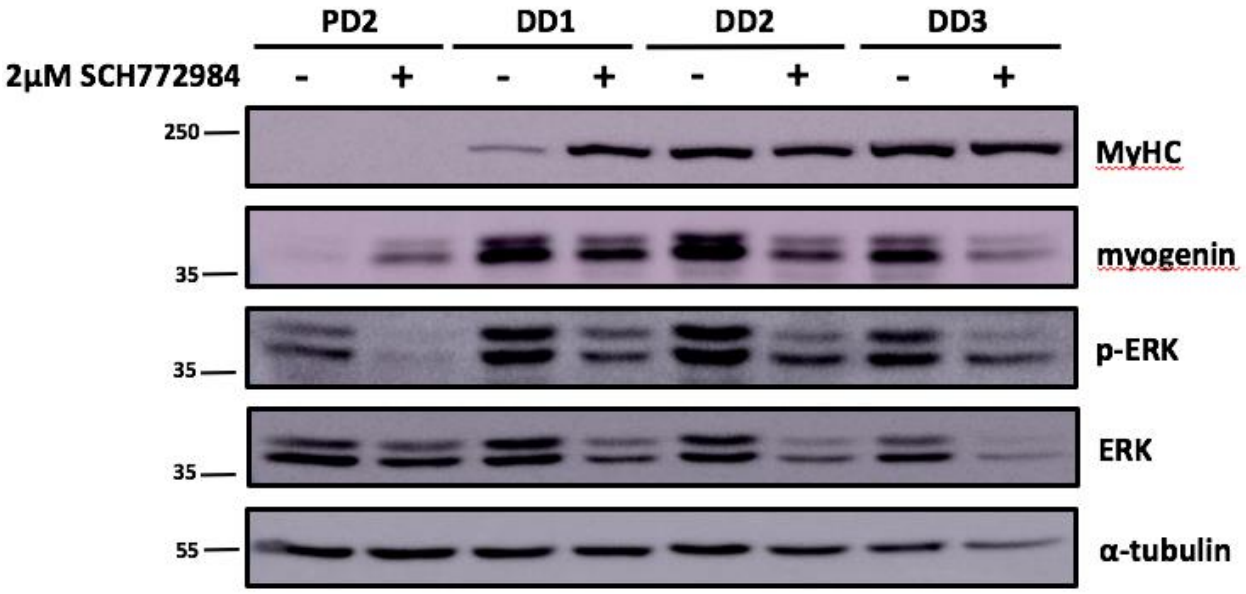

Figure 17. Inhibition of ERK1/2 using a pharmacologic inhibitor inhibits muscle cell differentiation and attenuates ERK-MAPK signaling. Pharmacologic inhibitor SCH772984 (2 μM) was applied to C_2C_{12} cells 24 hours post-plating or cells were mock-treated using DMSO. Cells were maintained in proliferation media (DMEM + 10% FBS) for 2 days followed by a switch to differentiation media (DMEM + 2% FBS) 2 days post-plating. Inhibitor treatments were applied every 24 hours until cells were harvested at 48 hours post-plating, as well as 1, 2, and 3 days after cells were switched to differentiation media. Western blot analysis of MyHC, myogenin, p-ERK, whole ERK comparing inhibitor treated C_2C_{12} cells and control cells.

Inhibition of ERK1/2 attenuates MAPK signaling in skeletal muscle.

C_2C_{12} cells were treated with either 2 μM ERK Inhibitor (SCH772984) or treated with the vehicle DMSO 24 hours post-plating and then harvested 24 hours post-treatment (PD2), while remaining cells were switched to differentiation media (2% serum) and treated every 24 hours

until being harvested at 24, 48, and 72 hours post-media switch. Western blots were then performed to evaluate markers of MAP kinase signaling pathway activity over the time course. A mouse monoclonal antibody against phosphorylated ERK (p-ERK) (1:1000 dilution) was used to analyze the level of p-ERK in muscle cells treated with SCH772984 compared to control cells. Inhibition of ERK1/2 resulted in significantly reduced levels of p-ERK in cells treated with SCH772984 throughout proliferation and differentiation (PD2-DD3) (Figure 17). Likewise, whole ERK levels were analyzed using a rabbit polyclonal antibody against whole ERK (1:1000 dilution) and were observed to be dramatically blunted in the inhibitor treated cells at all time points (PD2-DD3), suggesting that inhibition of ERK1/2 affects phosphorylation as well as whole protein levels of ERK (Figure 17).

Inhibition of MEK1/2 inhibits proper muscle cell differentiation.

C_2C_{12} cells were treated with either 5 μM MEK Inhibitor (GSK1120212) or treated with the vehicle DMSO 24 hours post-plating and then harvested 24 hours post-treatment (PD2), while remaining cells were switched to differentiation media (2% serum) and treated every 24 hours until being harvested at 24, 48, and 72 hours post-media switch. Western blots were conducted to analyze markers of skeletal muscle differentiation across this time course. Mouse monoclonal antibodies against MyHC and myogenin (1:1000) were used to analyze expression of markers of muscle cell differentiation in control muscle cells compared to cells that had been treated with GSK1120212. Inhibition of MEK results in a significant increase in MyHC expression observed throughout all days of differentiation (DD1-DD3) and an increase in myogenin observed in proliferation (PD2) that declined as cells began to differentiate (DD1-DD3) (Figure 18).

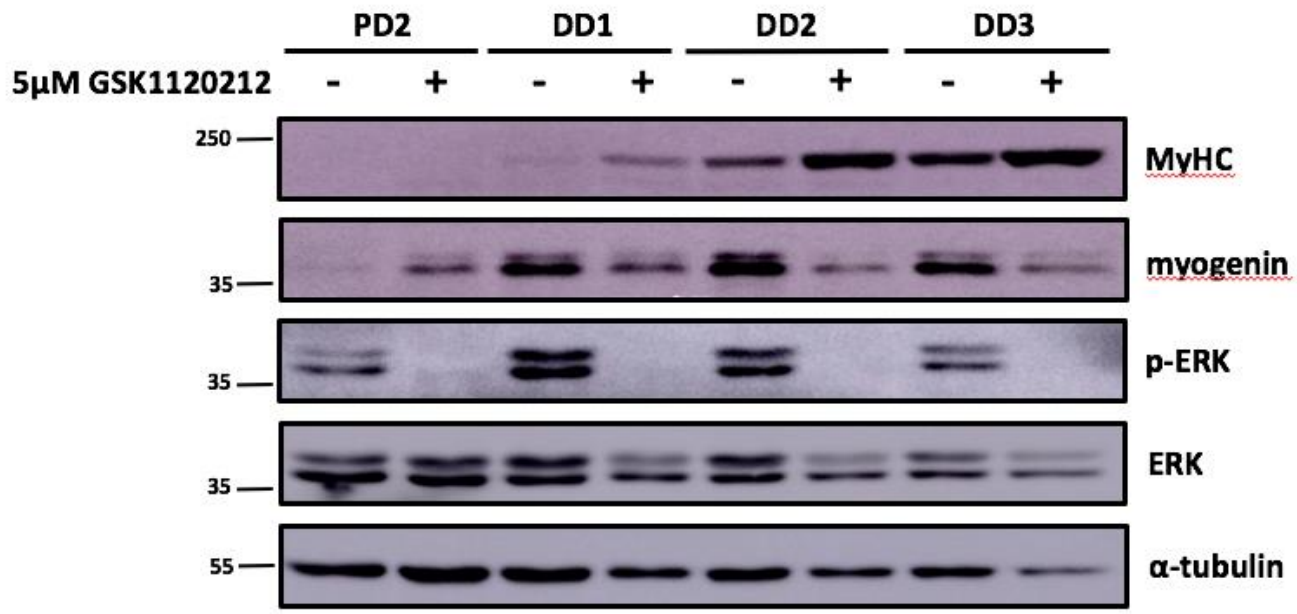

Figure 18. Inhibition of MEK1/2 using a pharmacologic inhibitor significantly inhibits myoblast differentiation and blocks ERK-MAPK signaling. Pharmacologic inhibitor GSK1120212 (5 μM) was applied to C_2C_{12} cells 24 hours post-plating or cells were mock-treated using DMSO. Cells were maintained in proliferation media (DMEM + 10% FBS) for 2 days followed by a switch to differentiation media (DMEM + 2% FBS) 2 days post-plating. Inhibitor treatments were applied every 24 hours until cells were harvested at 48 hours post-plating, or 1, 2, and 3 days after cells were switched to differentiation media. Western blot analysis of MyHC, myogenin, p-ERK, and whole ERK in cells treated with GSK1120212 compared to control cells.

Inhibition of MEK1/2 attenuates MAPK signaling in skeletal muscle.

C_2C_{12} cells were treated with either 5 μM MEK inhibitor (GSK1120212) or treated with the vehicle DMSO 24 hours post-plating and then harvested 24 hours post-treatment (PD2), while the remaining cells were switched to differentiation media (2% serum) and treated every 24 hours until being harvested at 24, 48, and 72 hours post-media switch. Western blots were then performed to evaluate markers of the MAP kinase signaling pathway over the time course. A mouse monoclonal antibody against phosphorylated ERK (p-ERK) was used to analyze the level of p-ERK in muscle cells treated with GSK1120212 compared to control cells. Inhibition of MEK1/2 resulted in dramatically reduced levels of p-ERK in cells treated with GSK1120212

throughout proliferation and differentiation (PD2-DD3) (Figure 18). Likewise, whole ERK levels were significantly blunted in the inhibitor treated cells at all time points (PD2-DD3), suggesting that inhibition of MEK1/2 affects phosphorylation of ERK as well as whole ERK protein levels (Figure 18).

Dusp4 Conclusions

Ectopic overexpression of Dusp4-WT and Dusp4-DN inhibits myoblast differentiation.

To observe if Dusp4 has any effect on myogenesis, Dusp4-WT and Dusp4-DN were ectopically expressed in C_2C_{12} myoblasts over a time course ranging from proliferation to late differentiation. Protein lysates isolated from these cells were analyzed via Western blot and probed for the myogenic differentiation markers MyHC and myogenin. Compared to control cells, cells overexpressing Dusp4-WT showed a reduction in MyHC and myogenin expression at the start of differentiation, but levels of MyHC and myogenin returned to control levels as differentiation proceeded (Figure 10). This suggests that overexpression of Dusp4-WT delays myoblast differentiation but does not prevent cell differentiation entirely. On the other hand, ectopic overexpression with the Dusp4-DN construct led to a significant reduction in MyHC and myogenin expression at every differentiation time point (DD1-DD4) suggesting that overexpression of Dusp4-DN entirely halts the differentiation process (Figure 12).

Ectopic overexpression of Dusp4-WT and Dusp4-DN attenuates MAPK signaling in myoblasts.

To observe effects on MAPK signaling when Dusp4-WT and Dusp4-DN are ectopically expressed, Western blots were probed for p-ERK and whole ERK. Compared to control cells, p-ERK levels were significantly lower in the Dusp4-WT overexpression cells but did not show a difference in whole ERK levels (Figure 11). Dusp4-DN overexpressing cells initially exhibit

higher levels of p-ERK and whole ERK that returned to control levels as cells began to differentiate (Figure 13). It is hypothesized that these increased levels of p-ERK and whole ERK in the DN overexpressing cells are likely due to Dusp4-DN binding specifically and irreversibly to ERK and thus preventing ERK protein turnover to occur as long as Dusp4-DN is being highly expressed and bound to ERK. Since p-ERK appears to be constitutively bound by the Dusp4-DN, this likely also inhibits its ability to activate its downstream targets, thus attenuating MAPK signaling downstream, as observed with the AP-1 reporter data (Figure 9B, 9D).

Dusp4-DN preferentially and irreversibly binds to ERK1/2 but not to p38.

Based upon the AP-1 reporter data and Western blot results, we hypothesized that the Dusp4-DN double mutant acts in a dominant negative fashion by preferentially and irreversibly binding to phosphorylated ERK1/2. To investigate this hypothesis further, we performed a co-immunoprecipitation analysis. Previous literature in cardiac muscle found that Dusp4 preferentially dephosphorylates p38 MAP kinase but not ERK1/2, contrary to our findings in this study, thus we wanted to confirm that Dusp4 does not interact with p38 in skeletal muscle (Auger-Messier et al., 2013). Our pulldown results show significant interaction between the Dusp4-DN and whole ERK1/2, confirming our hypothesis that the dominant negative construct constitutively binds to ERK1/2. This is especially accentuated by the Dusp4-WT pulldown results which show less Dusp4 overall, likely due to rapid protein turnover, as well as, no ERK1/2 binding, as this interaction between wild-type Dusp4 and ERK is likely a short and transient interaction in cells. Our results also showed that p38 is not bound by the Dusp4-DN construct, conveying selectivity of Dusp4 for ERK1/2 in skeletal muscle, and differentiating the function of Dusp4 from its role as a negative regulator of the p38 MAPK branch in cardiac muscle.

ERK1/2 and MEK1/2 inhibitors do not mimic Dusp4 overexpression in skeletal muscle cells.

To determine if Dusp4's mechanism of inhibiting MAPK signaling is similar to that of a small-molecule inhibitor, we treated C_2C_{12} cells across a time course from proliferation through differentiation with inhibitors specific to ERK1/2 (SCH772984) or MEK1/2 (GSK1120212). Protein lysates from control cells, as well as, the inhibitor treated cells were harvested and lysates were analyzed by Western blot for MyHC and myogenin to determine if inhibitors of MAPK signaling affect myogenesis. Inhibition of ERK1/2 results in a significant increase in MyHC expression at the start of differentiation (DD1) and an increase in myogenin was observed during proliferation (PD2). MyHC levels return to control levels as differentiation proceeds (DD2-DD3), while myogenin levels match controls as differentiation begins (DD1-DD3) (Figure 15). Inhibition of MEK1/2 using the GSK1120212 inhibitor resulted in a significant increase in MyHC expression throughout all days of differentiation (DD1-DD3) and an increase in myogenin was observed during proliferation (PD2) and then declined as cells differentiated (DD1-DD3) (Figure 16), suggesting that inhibition of MEK1/2 using a small molecule inhibitor prevents myoblasts from differentiating entirely.

As expected, the ERK1/2 and MEK1/2 inhibitors inhibit phosphorylation of ERK similar to the effects observed when Dusp4 was overexpressed; however, the GSK1120212 inhibitor also appears to inhibit whole ERK1/2 protein levels which was not observed in the Dusp4 overexpressing cells (Figure 15 and Figure 16). Furthermore, as expected, treatment with these inhibitors in combination with the AP-1 reporter showed dramatically inhibited downstream MAPK signaling similar to that observed when cells were overexpressing Dusp4-WT and Dusp4-DN (Figure 17 and Figure 18). Taken together, the AP-1 reporter clearly shows that

Dusp4 acts to repress MAPK signaling and phosphorylation of ERK similar to the repression observed when cells are treated with inhibitors of the ERK1/2 MAPK signaling pathway. However, MyHC and myogenin exhibited differential patterns of myogenesis progression, suggesting that Dusp4 does not act through the same mechanism as small-molecule inhibitors, but rather might be acting through a system of more complex protein-protein interactions.

.

Chapter 3: Protein Phosphatase Methylesterase 1 (Ppme1) is Upregulated During Skeletal Muscle Atrophy and Modulates MAP Kinase Signaling

Background: Ppme1

Based on our observations of the function that the protein phosphatase Dusp4 plays in on MAPK signaling and muscle differentiation, our lab also decided to investigate the function of a phosphatase-regulating gene induced during neurogenic atrophy called protein phosphatase methylesterase 1 (Ppme1). Ppme1 is an enzyme that negatively regulates the serine/threonine phosphatase protein phosphatase 2A (PP2A) by catalyzing the demethylation of the C-terminal Leu309 residue of the PP2A catalytic subunit (Kaur et al., 2016; Yabe et al., 2015). Structurally, PP2A is a heterotrimeric protein composed of a 36 kDa catalytic C subunit and a 65 kDa structural/scaffolding A subunit that makes up the core enzyme, which then associates with a regulatory B subunit (Orgad et al., 1990; Seshacharyulu et al., 2013; Yabe et al., 2018). The B subunit is the most diverse of these three units in that there are four different families, known as B (B55 or PR55), B' (B56 or PR61), B" (PR48, PR72, and PR130), as well as B"' (PR93/PR110) that work to control localization and substrate specificity of PP2A (Janssens and Goris, 2001; Yabe et al., 2018). The methylation of the C-terminal Leu309 residue of the catalytic subunit is an essential regulatory mechanism for proper interaction of thie PP2A holoenzyme. Methylation of PP2AC is believed to enhance the affinity of the PP2A core enzyme for a subset of B regulatory subunits (Yabe et al., 2018). Ppme1 is hypothesized to act not only in its role as a methyl-esterase, but also is believed to inhibit PP2A by binding directly to the active site of PP2AC through Ppme1's catalytic triad residues (Ser156, His349, and Asp181) which then displaces a manganese ion essential for proper formation of the functional holoenzyme (Xing et al., 2014; Yabe et al., 2018).

The PP2A phosphatase is believed to play diverse cellular roles and has been linked to various biological processes such as mediating cdc2 kinase activation during the cell cycle, DNA replication, transcription, translation, signal transduction, cell proliferation, cell mobility, dynamics of the cytoskeleton, and apoptosis (Alberts et al., 1993; Schonthal 2001; Seshacharyulu et al., 2013). As PP2A is a tumor suppressor, inactivation of PP2A by Ppme1 has been linked to a number of cancers through promotion of the oncogenic MAPK and Akt pathways (Xing et al., 2008; Yabe et al., 2015). For example, Ppme1 overexpression has been shown to correlate with increased cell proliferation and invasive phenotypes in endometrial adenocarcinoma where it sustains the ERK and Akt pathways by inhibiting PP2A (Kaur et al., 2016). Additionally, it has been observed that the Ppme1 methylesterase activity protects PP2AC from ubiquitin/proteasome degradation, thus Ppme1 activity is necessary to maintain protein stability of PP2AC (Lipina et al, 2014; Yabe et al., 2015). Furthermore, previous research indicates that loss of Ppme1 enhances the association of the B55 class of B regulatory subunits with the PP2A core enzyme (Wang et al., 2018). While this information is currently known in regards to Ppme1's involvement in various cancers, it has yet to be functionally characterized in skeletal muscle, which is why it is of particular interest for this study.

Materials and Methods

Cell culture, transfections, reporter gene assays, and statistics for these experiments conducted as described in chapter 2.

Promoter cloning of the Ppme1 gene

To amplify the proximal promoter region of *Ppme1*, first genomic DNA was isolated from C_2C_{12} cells using the DNeasy Blood and Tissue Kit (Qiagen, Valencia, CA) following manufacturer

protocol. Polymerase chain reaction (PCR) was conducted using 1 μg of isolated genomic DNA and Taq DNA Polymerase (Life Technologies, Grand Island, NY) following manufacturer protocol. The amplified PCR products were then cloned into the pGEM-T vector (Promega, Madison, WI) following manufacturer protocol. Next, the *Ppme1* promoter fragments were subcloned into the Mlu1 and XhoI sites of the pSEAP2 Basic plasmid (Clontech, Mountain View, CA) to create the pSEAP2-Ppme1-Pro500 and pSEAP2-Ppme1-Pro1000 reporter constructs and sequenced to confirm proper orientation of the promoter fragment within the plasmid and the absence of mutations.

Table 1. List of primers used in this study.

Primer Sequences (5' to 3')	
Ppme1-Pro500-F	GCACGCGTCTAAGCTGTACGCTCCCGCCATCCC
Ppme1-Pro1000-F	GCACGCGTCACGATGTCCTCTATCACACACCC
Ppme1-Pro-R	GCCTCGAGCTCTCTCCTCTAACGACGCCCAGTCGCC
Ppme1- Ebox Mut-F	GATTGGGCACTGCATGGGTGG
Ppme1- Ebox Mut-R	CCACCCATGCAGTGCCCAATC
Ppme1-qPCR-F	CTTCATGGAGGAGGCCATTCC
Ppme1-qPCR-R	GCAGATCCAGAGCCACAATCC

Site-directed Mutagenesis

The identified conserved E-box enhancer sequence within the 500bp *Ppme1* promoter region (Ebox3) was mutated using the primers listed in Table 1. The QuikChange II Site-Directed Mutagenesis protocol using PfuTurbo DNA Polymerase was conducted in accordance with manufacturer protocol (Agilent Technologies, Santa Clara, CA). Then the reaction was digested with DpnI (New England Biolabs, Ipswich, CA) and transformed into DH5α competent cells (Life Technologies, Grand Island, NY). Clones were grown up and the plasmid was purified and

sequenced to confirm mutagenesis of the E-box sequence was successful and without extraneous mutations.

Bioinformatic analysis

The nucleotide sequence corresponding to the regulatory regions of mouse, rat, and human *Ppme1* (Ensembl Transcript ID: ENSMUST00000032963.9, ENSRNOT00000023648.7, ENST00000328257.12) from -2000 through the first exon were downloaded from the Ensembl database (www.ensembl.org), aligned using the ClustalW2 alignment tool on the EMBL website (http://www.ebi.ac.uk/Tools/msa/clustalw2/), followed by Boxshade analysis of the ClustalW2 alignment output data (http://www.ch.embnet.org/software/BOX_form.html). The amino acid sequences for Ppme1 were downloaded from the Ensembl database and aligned and shaded as described for the nucleotide sequences.

Quantitative PCR (qPCR)

Total RNA was isolated from C_2C_{12} cells harvested during proliferation (PD2) as well as differentiation (DD2 and DD7) using the RNeasy Mini Kit (Qiagen, Valencia, CA) following manufacturer protocol. Then 1µg of total RNA was reverse-transcribed using the iScript cDNA Synthesis Kit in accordance with manufacturer protocol (Bio-Rad, Hercules, CA). qPCR was performed utilizing the iTaq Universal SYBR Green Reaction Supermix following manufacturer protocol (Bio-Rad, Hercules, CA) and the quantitative analysis of *Ppme1* expression was determined for PD2, DD2, and DD7 using the CFX Connect Real Time PCR System (Bio-Rad, Hercules, CA). Each RNA timepoint was conducted in biological triplicates, each biological replicate was used for performing RT reactions in duplicate, and each cDNA reaction was used for qPCR in technical triplicates, which results in 18 individual reads per biological sample. The

experiment was repeated at least once, and the relative *Ppme1* expression levels were calculated using the $2^{-\Delta\Delta C_T}$ Livak method with GAPDH as the internal control.

Western blotting

C_2C_{12} cells were differentiated over a 10 day time course by plating cells into 10cm culture dishes and maintaining them in proliferation media (DMEM + 10% serum) for 2 days followed by a switch to differentiation media (DMEM + 2% serum) at 2 days post-plating. The time course consisted of harvesting cells grown in proliferation media for 1 and 2 days, as well as, cells grown for 2 days in proliferation media followed by continued culturing for 1, 3, 5, 7, 9, and 10 days in differentiation media. Harvested cells were spun down and stored at -80℃ until cell lysis and protein purification was performed. Protein purification and running of the SDS-PAGE gel were conducted as described in chapter 2.

Blots were probed with anti-Pme1 (B-12, Santa Cruz Biotechnology, Dallas, TX), anti-Myosin Heavy Chain (MYH1/2/4/6) (F59, Santa Cruz Biotechnology, Dallas, TX), anti- myogenin (F5D, Santa Cruz Biotechnology, Dallas, TX), anti-p-ERK (E-4, Santa Cruz Biotechnology, Dallas, TX), anti-ERK (K-23, Santa Cruz Biotechnology, Dallas, TX), anti-AKT1-phospho-S473 (66444-I-Ig, Proteintech, Rosemont, IL), anti-AKT (60203-2-Ig, Proteintech, Rosemont, IL), anti-p-cJun (KM-1, Santa Cruz Biotechnology, Dallas, TX), anti-Jun (66313-I-Ig, Proteintech, Rosemont, IL), anti-PP2A-Cα/β (1D6, Santa Cruz Biotechnology, Dallas, TX), or anti-α-tubulin (DM1A, Santa Cruz Biotechnology, Dallas, TX) primary antibodies followed by incubation with either Mouse anti-Rabbit IgG-HRP (Santa Cruz Biotechnology, Dallas, TX) or Rabbit anti-Mouse IgG (H+L) (Thermo Scientific, Rockford, IL) HRP-conjugated secondary as appropriate for the primary antibody species. Blots were imaged and stripped as described in chapter 2.

AMZ-30 Inhibitor Treatment

Pharmacologic inhibitor AMZ-30 (20 μM) (EMD Millipore Corp., Billerica, MA) was applied to C_2C_{12} cells 24 hours post-plating. Cells were maintained in proliferation media (DMEM + 10% FBS) for 2 days followed by a switch to differentiation media (DMEM + 2% FBS) 2 days post-plating. Inhibitor treatments were applied every 24 hours until cells were harvested at 48 hours post-plating (PD2), as well as 24, 48, and 72 hours after those cells were switched to differentiation media (DD1, DD2, and DD3). Harvested cells were spun down and stored at -80℃ until the cells were lysed and the protein was isolated and purified.

Results

Ppme1 is induced during skeletal muscle atrophy but is not differentially expressed in MuRF1-null mice.

An Illumina mouse-6 v1.1 expression beadchip array was performed on RNA isolated from triceps surae (TS) muscle from mice subjected to denervation inducing neurogenic atrophy as previously described (Furlow et al., 2013). Further analysis of the data SubSeries (GEO: GSE44205) deposited as part of a SuperSeries (GEO: GSE44259) submitted to the NCBI Gene Expression Omnibus (GEO) identified numerous genes previously undescribed in skeletal muscle and exhibited differential expression patterns in response to denervation-induced muscle atrophy. *Ppme1*, originally identified as a Riken gene (2700017M01RIK) in the Illumina beadchip array, showed *Ppme1* is expressed in control muscle tissue, and is significantly induced in response to neurogenic atrophy at both 3 days and 14 days post-denervation (Figure 19A and 19B). The MuRF1-null mice at both 3 days and 14 days post-denervation show a slightly blunted effect on activity compared to the wild-type mice, but this difference is not significant (Figure 19A and 19B).

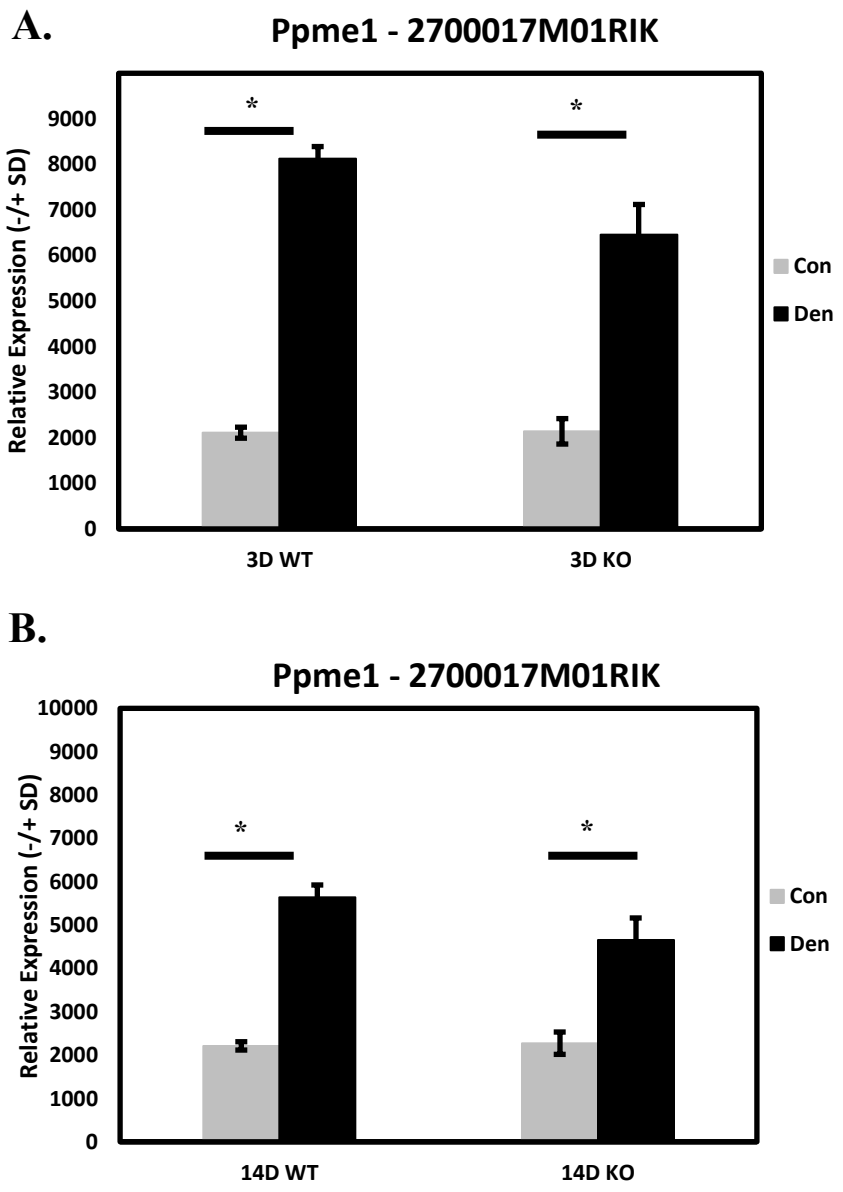

Figure 19. Ppme1 is expressed in muscle tissue and is induced during neurogenic skeletal muscle atrophy. Whole genome expression analysis was conducted on triceps surae muscle from wild-type (WT) and MuRF1-null (KO) control mice after (A) 3 days (3D) and (B) 14 days (14D) of denervation (DEN). *Ppme1* expression increased significantly at 3 days and 14 days of denervation in the wild-type and MuRF1-null animals. Each condition represents the average expression from three animals and error bars represent ± SD. White bars, controls; black bars, DEN. Significant difference between denervated mice and control mice in the same group. (**:$P < 0.01$) (Furlow et al., 2013).

Ppme1 is expressed during muscle cell proliferation and differentiation.

Ppme1 is located on chromosome 7 in *M. musculus* (Figure 20A) and has one validated transcript consisting of 14 coding exons (Figure 20B).

A.

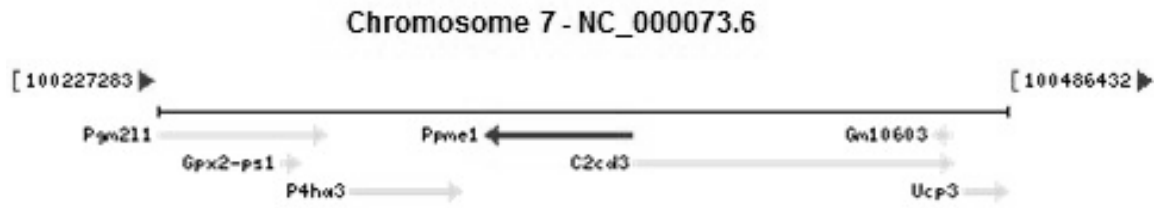

B.

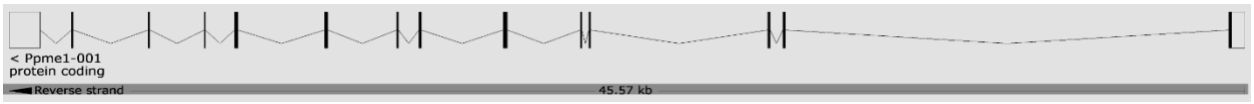

Figure 20. Schematics for the Ppme1 gene locus and transcript. (A) Location of Ppme1 on Chromosome 7 and relative locations of adjacent genes. **(B)** Schematic of the Ppme1 transcript of the Ppme1 gene in mouse. Darkened rectangles represent the exons containing the translated region, open rectangles represent exons containing the untranslated regions and the lines connecting these rectangles represent introns.

To confirm that *Ppme1* is expressed endogenously at the mRNA level in skeletal muscle cells, qPCR was performed using RNA isolated from proliferating myoblasts (PD2), as well as, from myotubes at early (DD2) and late (DD7) stages of differentiation. The qPCR results show that Ppme1 RNA levels steadily decrease as muscle cells enter into late differentiation (Figure 21A). To determine the expression pattern of Ppme1 at the protein level, C_2C_{12} cells were differentiated and harvested over a 10 day time course and lysates were analyzed by Western blot for endogenous Ppme1 (Figure 21B). Ppme1 protein levels exhibit uniform expression throughout proliferation and differentiation. To determine that cells were properly differentiating throughout this time course, the blot was also probed for myosin heavy chain using a mouse monoclonal

antibody. Myosin heavy chain increases as C_2C_{12} cells exit the cell cycle and enter into the differentiation process from myoblasts to myotubes (Figure 21B). To confirm protein was equally loaded, the blot was also probed for α-tubulin using a mouse monoclonal antibody (Figure 21B).

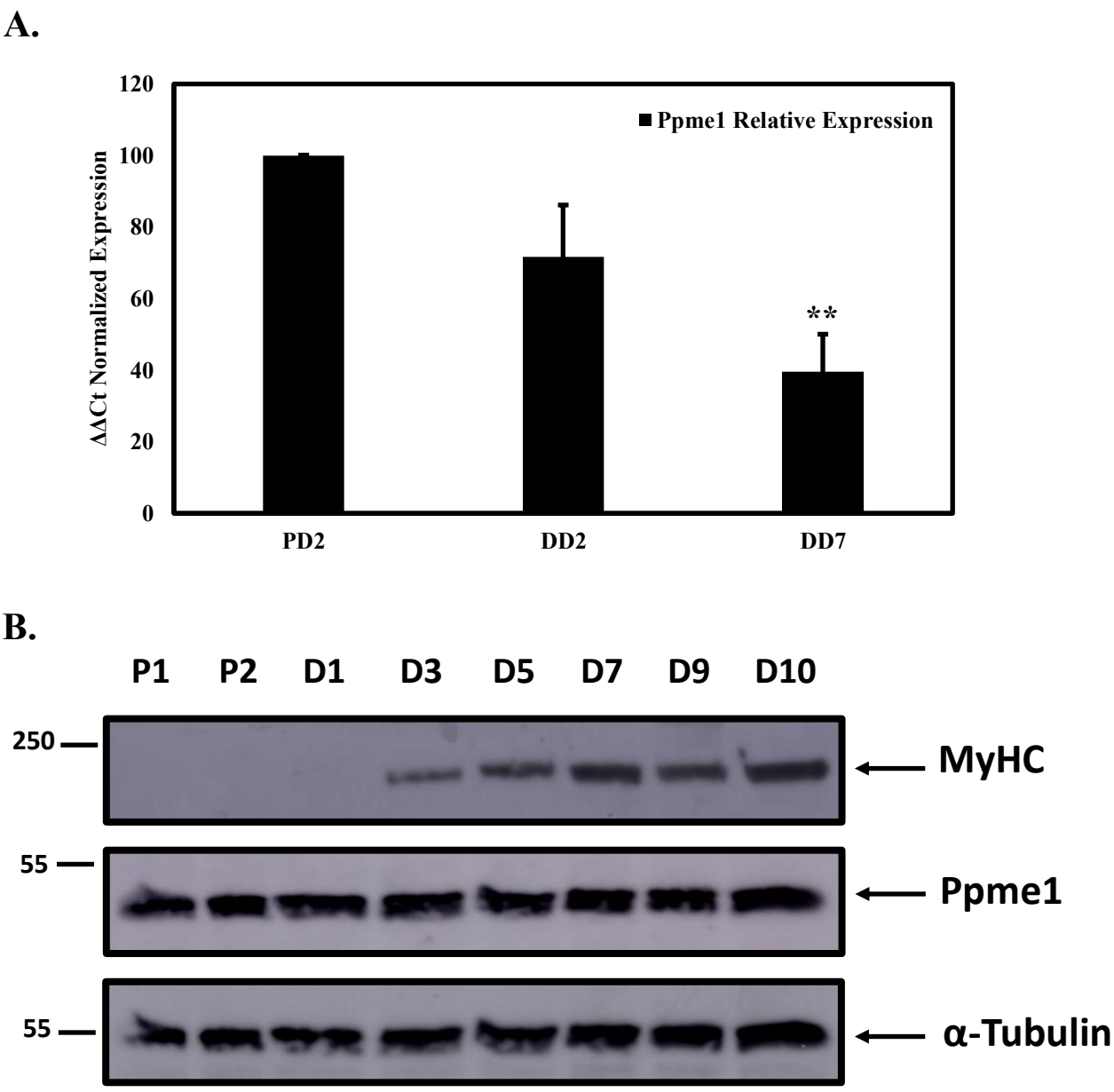

Figure 21. Ppme1 mRNA levels decrease as C_2C_{12} cells differentiate while protein levels show uniform expression throughout proliferation and differentiation. (A) Ppme1 mRNA is expressed throughout proliferation and differentiation. Quantitative polymerase chain reaction (qPCR) was utilizing cDNA from proliferating (P) and differentiated (D) C_2C_{12} cells harvested at proliferation day 2 (PD2), differentiation day 2 (DD2) and differentiation day 7 (DD7). Cells were maintained in proliferation media (10% FBS) and harvested at 2 days post-plating and the remaining cells were then switched to differentiation media (2% FBS) and harvested at 2 and 7 days post-media change. **(B)** Western blot analysis was performed using a mouse monoclonal antibody against Ppme1 on protein homogenates from proliferating (P) and differentiating (D) C_2C_{12} cells harvested over a 10 day differentiation time course. Cells were maintained in proliferation media (10% FBS) and harvested at 1 and 2 days post-plating, and remaining cells were switched to differentiation media (2% FBS) and harvested at 1, 3, 5, 7, 9, and 10 days post-media change. Myosin Heavy Chain (MyHC) was used as a marker of proper myoblast differentiation and α-tubulin was analyzed to confirm equal protein loading. (**:$P < 0.01$).

Putative functional domains of Ppme1 facilitate demethylation of target proteins.

Mouse Ppme1 has one characterized protein isoform that is 386 amino acids in length and has a predicted molecular weight of ~44kDa. The Ppme1 amino acid sequence is highly conserved between rodents and humans as visualized in the schematic shown in Figure 22. Using the SMART database and the NCBI Conserved Domain Database (CDD), the Ppme1 protein is predicted to have a large Pimeloyl-ACP methyl ester carboxylesterase Domain highlighted in green (Figure 22). This domain is essential for the capability of Ppme1 to bind to the PP2AC subunit through the Ppme1 catalytic triad, as well as catalyze the demethylation and subsequent inactivation of the PP2A protein (Xing et al., 2008).

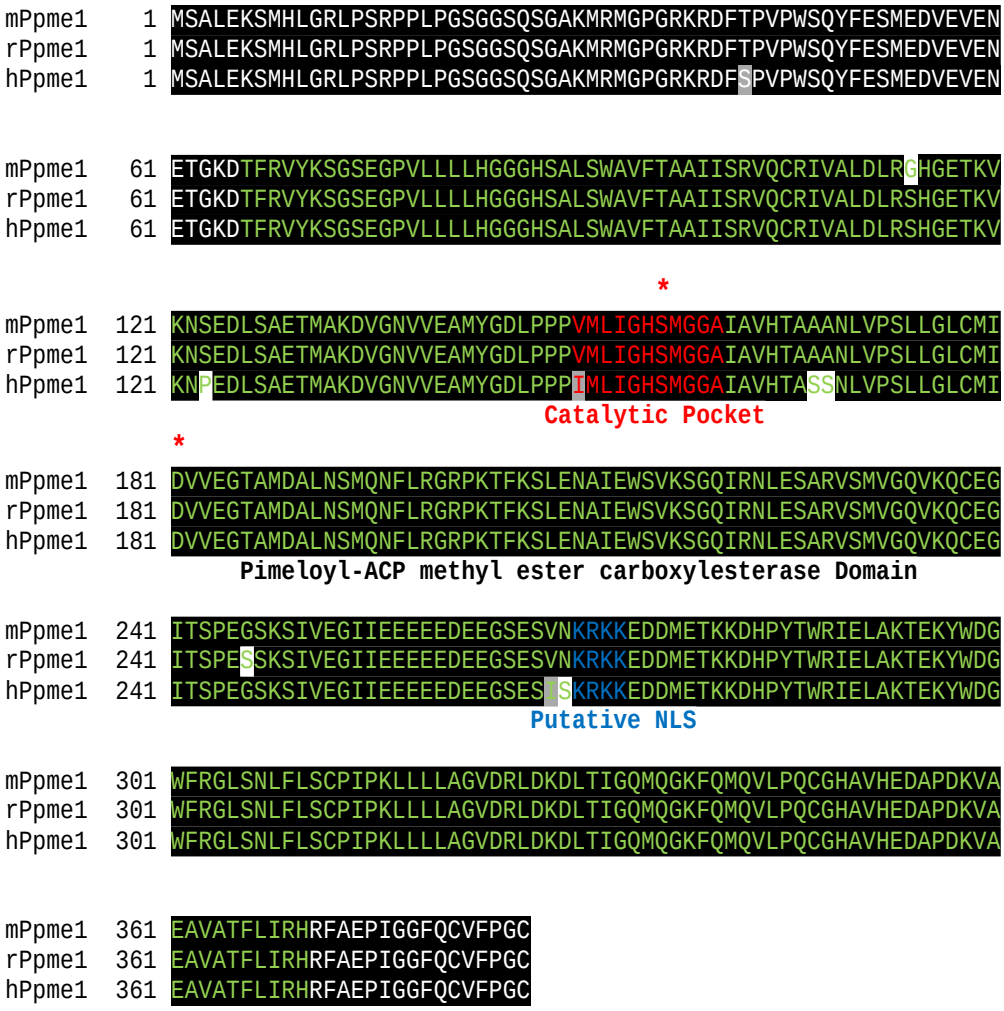

Figure 22. Protein sequence alignment of Ppme1 from mouse, rat, and human. Sequences of the mouse, rat, and human Ppme1 protein were downloaded from the Ensembl database and aligned using the ClustalW2 algorithm. Approximate positions of the pimeloyl-ACP methyl ester carboxylesterase domain are highlighted in green, the catalytic pocket is highlighted in red, and a putative nuclear localization signal is highlighted in blue in the alignment. The gene structure schematic images were downloaded from the Ensembl database (www.ensembl.org).

Cloning and analysis of the proximal regulatory region of Ppme1.

To assess the level of conservation between organisms for the proximal promoter regions of mouse, human, and rat Ppme1 and to identify putative regulatory elements within this promoter region, genomic sequences for the regulatory region of this gene for all three species were aligned (Figure 23A). Several enhancer elements were identified, including a conserved E-box

sequence highlighted in in the promoter alignment schematic (Figure 23A). In addition to the conserved E-box, there are also 2 non-conserved E-box elements, highlighted in yellow, shared between mouse and rat but not human, as well as, 3 conserved TFIIB Recognition Elements (BRE) highlighted in green (Figure 23A).

To confirm that the regulatory region of Ppme1 is transcriptionally active in muscle cells, 500 and 1000 bp fragments of the proximal promoter region of the Ppme1 gene were cloned using the primer pairs listed in Table 1. The promoter fragments were ligated into the secreted alkaline phosphatase (SEAP) reporter plasmid to create the pSEAP-Ppme1-Pro500 and pSEAP-Ppme1-Pro1000 reporter constructs. C_2C_{12} cells were transfected with the Ppme1-Pro500 and Ppme1-Pro1000 reporter plasmids and SEAP activity levels were analyzed 48 hours following a switch to differentiation media. These activity levels were compared to cells transfected with an empty pSEAP2-Basic plasmid, which acts as a negative control . The Ppme1-Pro500 and Ppme1-Pro1000 reporter plasmids exhibit dramatic transcriptional activity compared to the empty SEAP reporter plasmid transfected alone (Figure 23B and 23C).

A.

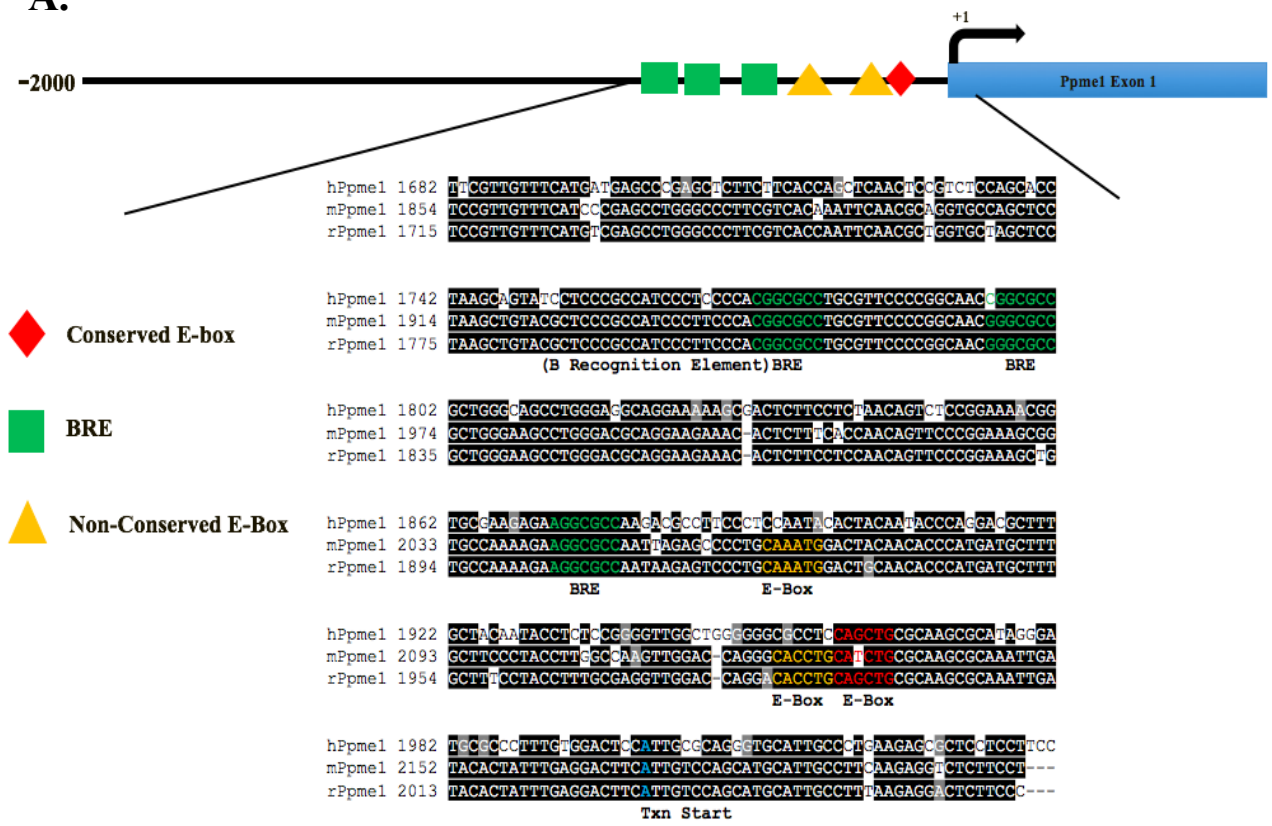
+1
-2000
Ppme1 Exon 1
Conserved E-box
BRE
Non-Conserved E-Box
(B Recognition Element) BRE
BRE
E-Box
E-Box E-Box
Txn Start

B.

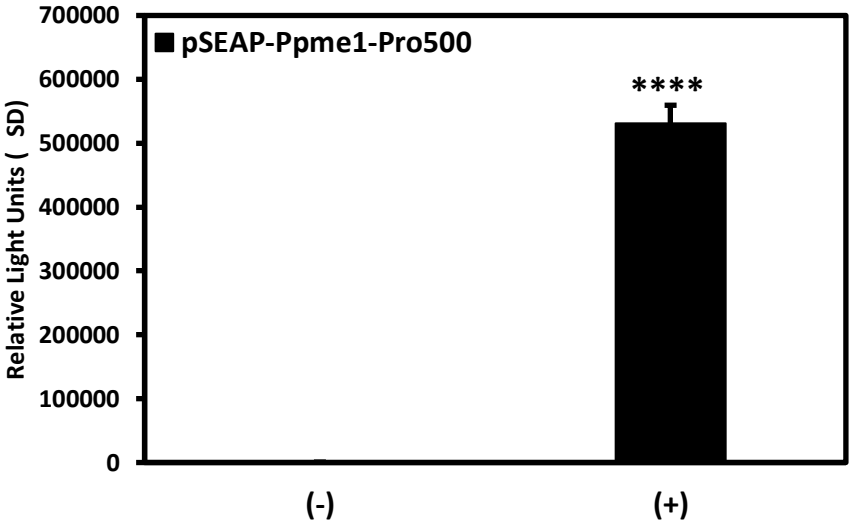
pSEAP-Ppme1-Pro500
****
Relative Light Units (SD)
700000
600000
500000
400000
300000
200000
100000
0
(-)
(+)

C.

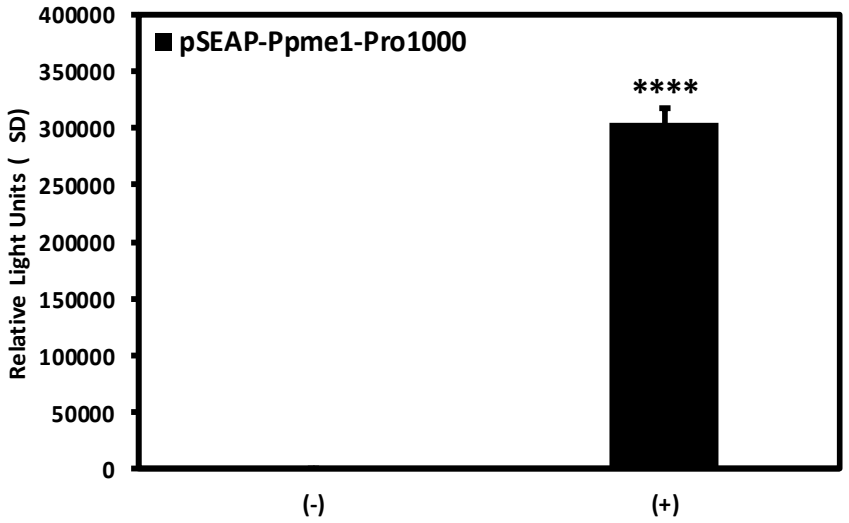

Figure 23. Schematic, sequence alignment, and analysis of the *Ppme1* promoter region. (A) Promoter sequences from mouse, rat, and human *Ppme1* (2000 base pairs upstream of the start of the transcription start site (+1) through the first exon) were downloaded from the Ensembl database (www.ensembl.org) and aligned using the ClustalW algorithm. Approximate positions of putative transcription factor binding sites are indicated in the schematic of the *Ppme1* regulatory region at the top. Putative TFIIB Response Element (BRE) 5'-(G/C)(G/C(G/A)CGCC-3' (highlighted in green) and putative consensus E-box elements 5'-CANNTG-3' (highlighted in yellow and red) are indicated. N represents any nucleotide. Conserved nucleotides are highlighted in black, transitions are highlighted in gray and transversions are highlighted in white. The transcription initiation start site is highlighted in blue. Cloning and analysis of the proximal regulatory region of *Ppme1* was conducted by transfecting C_2C_{12} myoblasts with either an empty reporter plasmid or a reporter plasmid containing **(B)** ~500 bp or **(C)** ~1000 bp of the *Ppme1* promoter fused to the Secreted Alkaline Phosphatase (SEAP) reporter gene. Each condition was performed in triplicate and each experiment was repeated at least once. The graphs are of a representative experiment and values correspond to the mean relative light unit (RLU) values ± SD. Significant difference between the control empty reporter plasmid (pSEAP2-Basic) and either the pSEAP-Ppme1-Pro500 or pSEAP-Ppme1-Pro1000 reporter constructs (****: $P < 0.0001$).

Ppme1 reporter gene activity is modestly repressed in response to ectopic MRF expression

Myogenic regulatory factors (MRFs) are basic helix-loop-helix (bHLH) transcription factors that are specifically present in muscle tissue and regulate myogenesis. The members of the MRF family include MyoD, Myf5, myogenin, and MRF4, which all contain a conserved DNA binding domain that binds to enhancer boxes (E-boxes) (Dilworth and Singh, 2013; Londhe and Davie, 2011). E-boxes are DNA response elements that regulate gene expression in muscle, and thus are

found in the promoter regions of most muscle-specific genes, such as MuRF1 and MAFbx. The consensus E-box sequence, 5'-CANNTG-3' in which N can represent any nucleotide, is bound by MRFs to regulate gene transcription. The expression of MRFs is skeletal muscle-specific; however, their function also requires heterodimerization with a ubiquitously expressed E-protein family of bHLH transcription factors, Tcf3 and Tcf12, to bind the E-box sequences and modulate transcriptional activity (Dilworth and Singh, 2013; Londhe and Davie, 2011). MRFs act to regulate gene activity through their interactions with co-activators or co-repressors at the promoters of muscle-specific genes, and are often found to be upregulated during muscle atrophy conditions.

Of the genes that comprise the MRF family, the two key MRFs that have been identified as important in skeletal muscle are MyoD and myogenin. MyoD is believed to establish an open chromatin structure at muscle-specific genes, while myogenin drives the transcription of genes within this accessible chromatin state (Dilworth and Singh, 2013). Thus, MyoD plays an important role in regulating the effects of myogenin in muscle cells. MyoD also has been observed to directly activate genes involved in cell cycle progression, which leads to active myoblast proliferation (Dilworth and Singh, 2013). Myogenin on the other hand, activates genes that shut down cell proliferation, leading to cell cycle exit and differentiation of myoblasts and is also required for cell viability (Dilworth and Singh, 2013). Furthermore, previous research has indicated that myogenin is required for full induction of MuRF1 and MAFbx under neurogenic atrophy conditions (Moresi et al, 2010). Additionally, it has been shown that deletion of myogenin results in lower levels of MuRF1 in skeletal muscle and resistance to muscle wasting in mice in which atrophy has been induced via denervation (Moresi et al, 2010). Previously

unpublished data from our lab also suggests that MuRF1 may work in tandem with MRFs to transcriptionally regulate atrogenes (Olson, 2013).

Neurogenic atrophy has previously shown massive upregulation of MRF expression (Cohen et al., 2007; Williams et al., 2009; Furlow et al., 2013). Due to the identification of a conserved E-box within the Ppme1 promoter region, we evaluated potential regulation by MRFs on the 500bp and 1000bp promoter region of Ppme1. C_2C_{12} cells were transfected with the pSEAP-Ppme1-Pro500 or pSEAP-Ppme1-Pro1000 reporter constructs alone or in combination with ectopic expression of MyoD1 or myogenin. The Ppme1 500bp reporter shows modest repression of promoter activity by MyoD ectopic expression but is unaffected by myogenin compared to cells not treated with MRFs (Figure 24A). Whereas the Ppme1 1000bp promoter activity is repressed, albeit modestly, by ectopic expression of both MyoD and myogenin compared to the cells not ectopically expressing MRFs (Figure 24B).

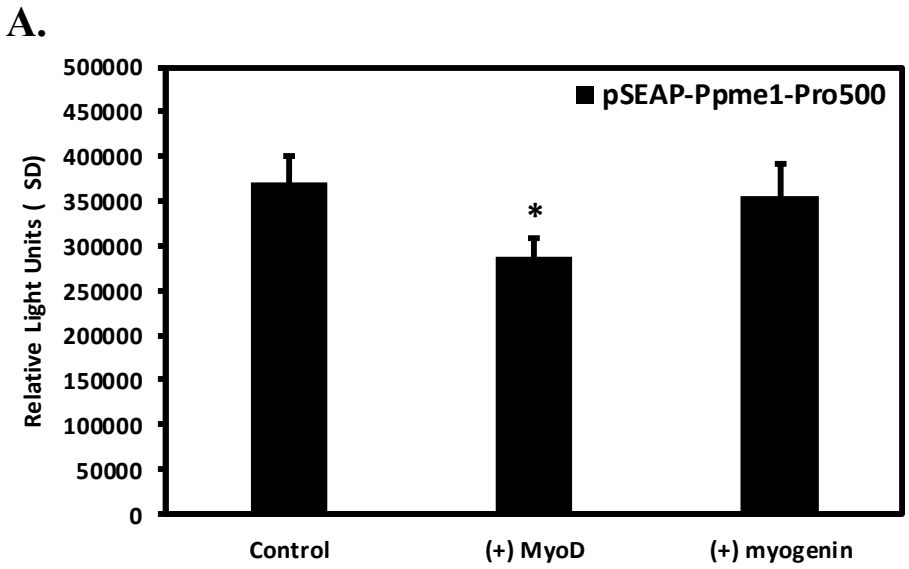

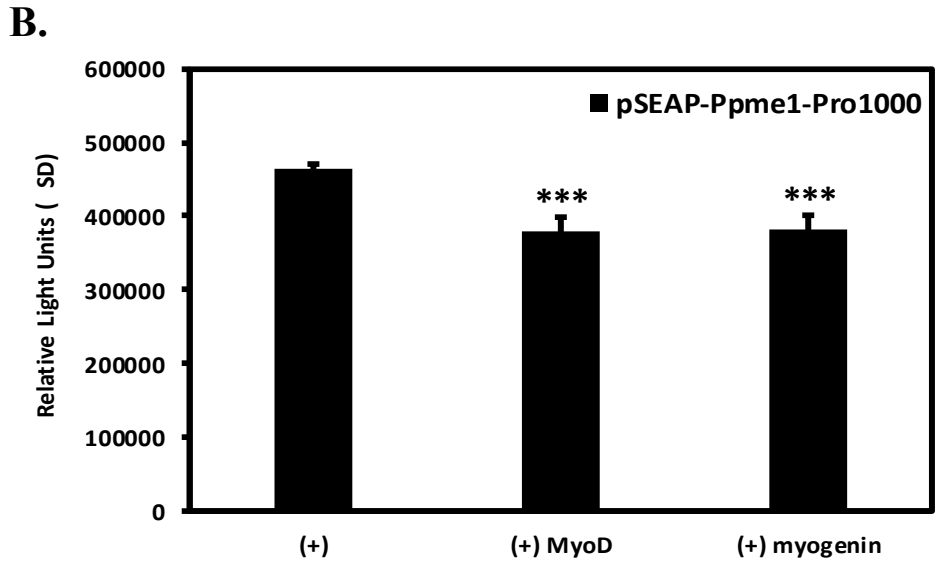

Figure 24. MRF Overexpression modestly inhibits Ppme1 reporter gene activity. C_2C_{12} myoblasts were transfected with the pSEAP-Ppme1-Pro500 reporter construct, in combination with expression plasmids for MyoD and myogenin. The myoblasts were transfected while being maintained in standard culture media to promote cell proliferation, then 24 hours post-transfection were switched to culture media promoting cell differentiation. The media was then sampled 72 hours post-transfection to measure SEAP activity. SEAP activity was normalized to β-galactosidase activity to correct for variations in transfection efficiency. Conditions were performed in triplicate and error bars reflect ±SD (*: $P \leq 0.05$; ***: $P < 0.001$).

Characterization of the conserved E-box element in the regulatory region of Ppme1.

A sequence matching the canonical E-box element sequence (5'-CANNTG-3') was identified in the proximal promoter region of Ppme1 and found to be conserved between mouse, rat, and human (Figure 25A). To determine if this putative E-box element is necessary for proper promoter activation, site-directed mutagenesis was conducted utilizing the 500 base pair promoter fragment of Ppme1, resulting in generation of the pSEAP-Ppme1-Pro500 Ebox3 mutant construct. Mutation of this conserved E-box in the 500 base pair promoter region resulted in significantly lower reporter gene activity compared to the wild-type reporter activity in transfected C_2C_{12} cells. Looking at comparative reporter activity across a time course from proliferation day 2 (PD2) to differentiation day 4 (DD4) showed the most significant repression

at PD2 of the E-box mutant compared to wild-type, but by DD4 the activity of the mutant appears to be trending towards wild-type reporter activity (Figure 25B-D).

A.

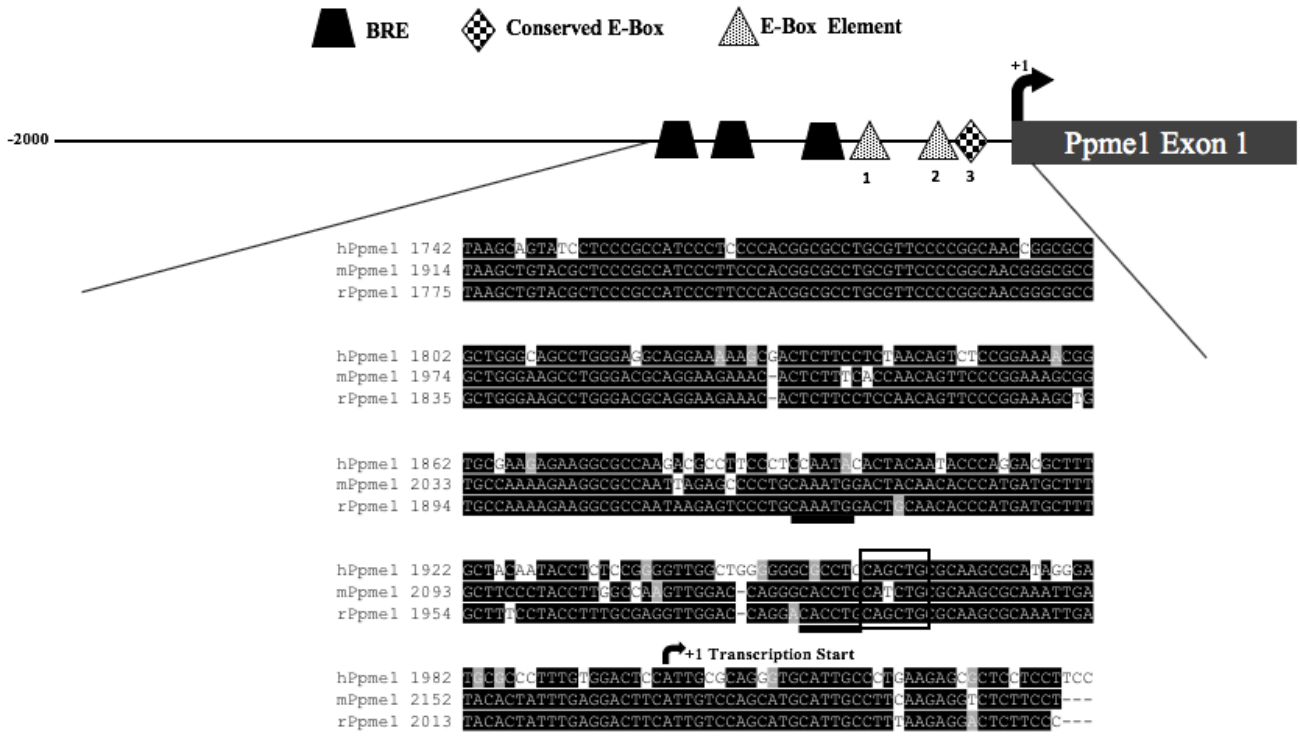

B.

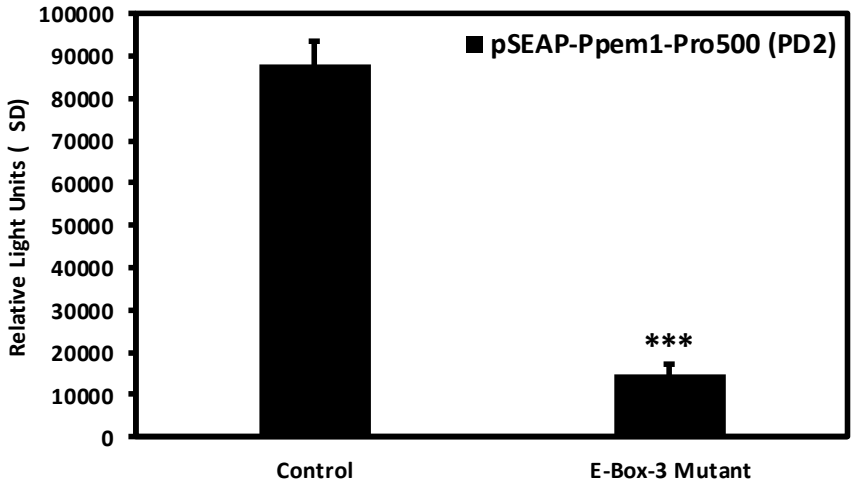

C.

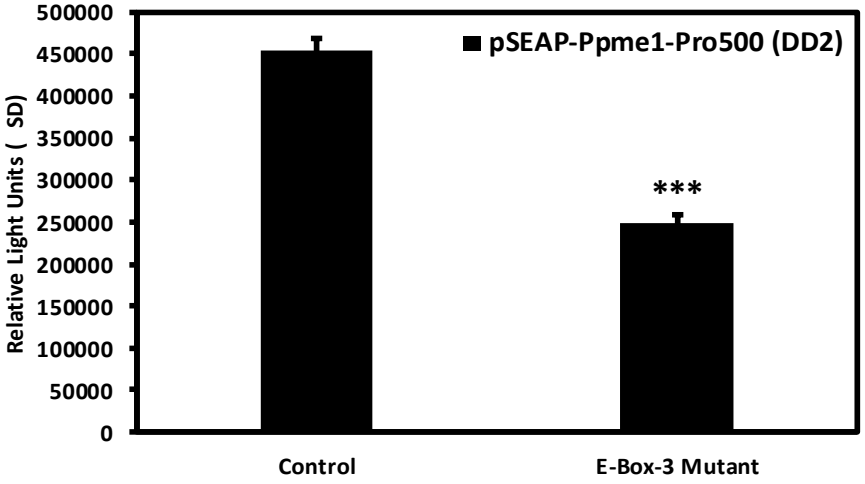

D.

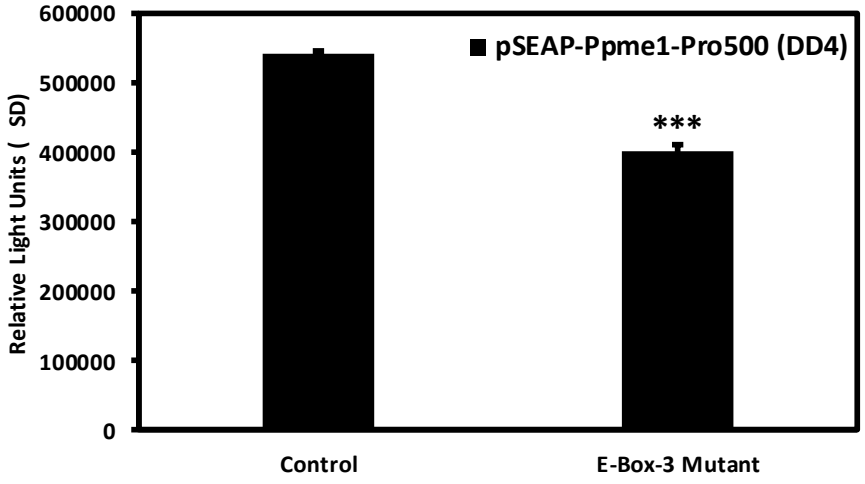

Figure 25. The conserved E-box in the proximal promoter region of Ppme1 is necessary for full reporter gene activity. (A) Schematic sequence alignment and analysis of the Ppme1 promoter region contains multiple putative consensus E-box elements 5'-CAANNTG-3'. The promoter region contains 2 non-conserved E-box elements (underlined in sequence) and 1 conserved E-box (boxed in sequence) between human, mouse, and rat (grey triangle and checkered diamond in schematic). C_2C_{12} myoblasts were transfected with the pSEAP-Ppme1-Pro500 wild-type or pSEAP-Ppme1-Pro500-Ebox3 mutant reporter plasmid, a β-galactosidase reporter plasmid and filler DNA to 1μg/well of total DNA. **(B)** The media was assayed for SEAP activity 24 hours post transfection. Then the cells were switched to differentiation media (2% FBS) and media was assayed at **(C)** 48 hours post-media switch and **(D)** 96 hours post-media switch. All SEAP values were normalized to β-galactosidase to correct for variations in transfection efficiency. All conditions were performed in triplicate and each experiment was repeated at least once. The graphs are of a representative experiment and values correspond to the mean relative light unit (RLU) values ± SD. (***: $P < 0.001$).

Inhibition of Ppme1 attenuates AP-1 reporter activity in a dose dependent manner.

To determine whether inhibiting Ppme1 results in decreased MAP kinase signaling, we transfected the AP-1 reporter into C_2C_{12} cells and treated the cells 24 hours post-transfection with either DMSO or with increasing concentrations of AMZ-30 (specific inhibitor of Ppme1). The media was changed to differentiation media (2% FBS) 24 hours post-treatment and the cells were treated again. Reporter gene activity was measured 24 hours later by sampling the growth media and analyzing the level of secreted alkaline phosphatase (SEAP) activity. Muscle cells treated with the Ppme1 inhibitor exhibited significantly reduced AP-1 reporter gene activity when compared to the cells that were only transfected with the AP-1 reporter treated with DMSO only (Figure 26).

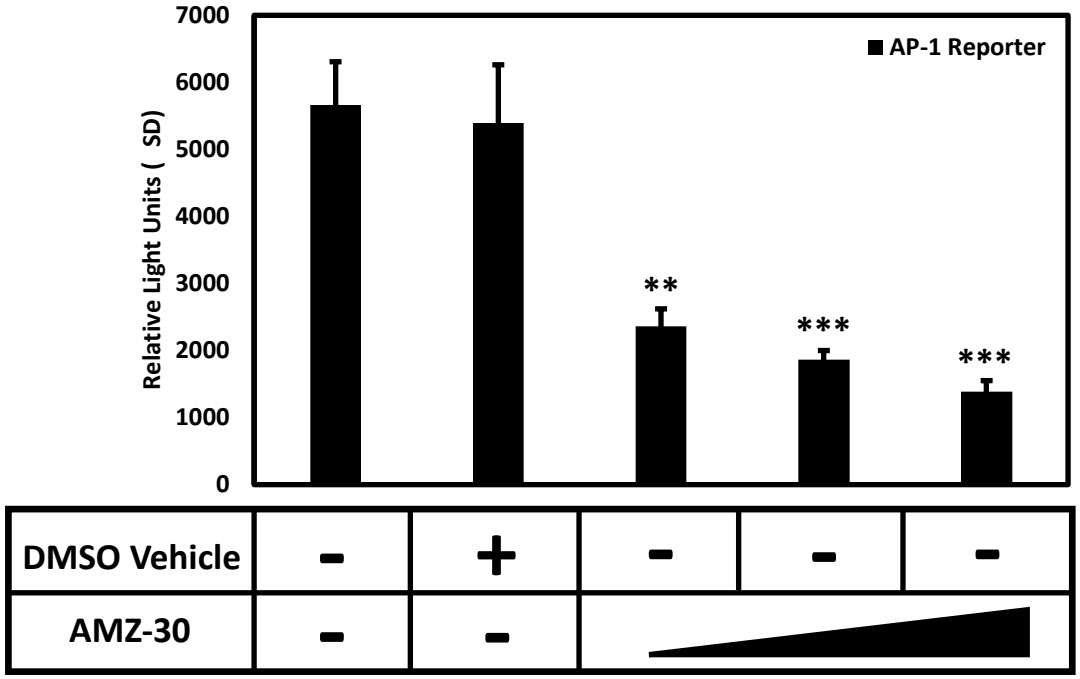

Figure 26. Treatment with a Ppme1 inhibitor attenuates AP-1 gene reporter activity in C_2C_{12} myoblasts in a dose-dependent manner. C_2C_{12} cells were transfected with an AP-1 reporter plasmid approximately 24 hours post-plating, the media was refreshed (DMEM + 10% FBS) 24 hours post-transfection and the inhibitor AMZ-30 (10μM, 20μM, or 40μM) was applied or cells were treated with DMSO. Cells were then switched to differentiation media (DMEM + 2% FBS) approximately 24-hours later, treated again with inhibitor or DMSO, and incubated for an additional 24 hours until a SEAP reporter assay was performed (**:$P < 0.01$;***: $P < 0.001$).

Inhibition of Ppme1 results in elevated PP2AC subunit levels.

C_2C_{12} cells were treated with 20 μM AMZ-30, of a Ppme1-specific inhibitor, DMSO vehicle 24 hours post-plating and then harvested 24 hours post-treatment (PD2), while the remaining cells were switched to differentiation media (2% serum) and treated every 24 hours until being harvested at 24, 48, and 72 hours post-media switch. Ppme1 protein levels, analyzed using a mouse monoclonal antibody against Ppme1 showed no difference between the control and inhibitor treated muscle cells at any time point, suggesting the inhibitor acts through preventing Ppme1 methylesterase activity but does not affect whole Ppme1 protein levels (Figure 27). Since

previous literature has characterized Ppme1 as a negative regulator of PP2A through its C subunit, a mouse monoclonal antibody against whole PP2ACα/β was used to analyze the expression level of PP2ACα/β in response to treatment with an inhibitor for Ppme1. Treatment with the AMZ-30 inhibitor resulted in a modest increase in PP2AC levels during differentiation (DD2-DD3) (Figure 27). α-tubulin levels were analyzed to confirm equal protein loading and remained constant across proliferation and differentiation.

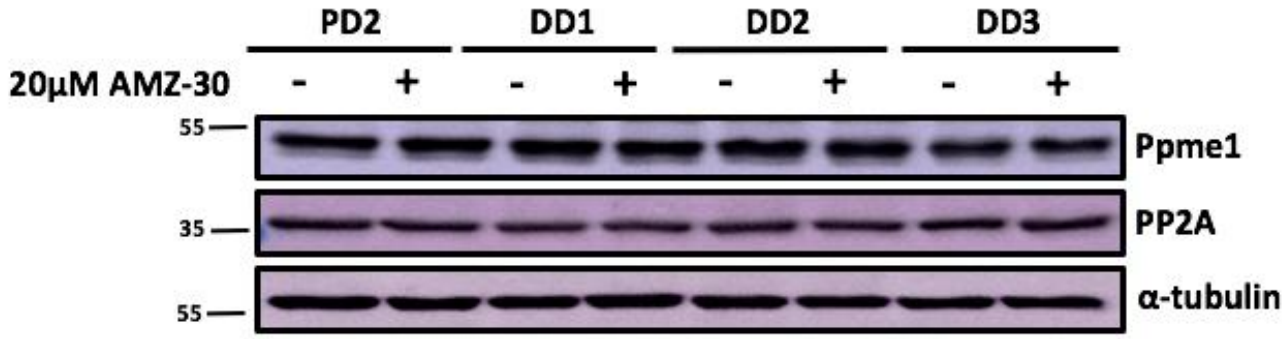

Figure 27. Inhibition of Ppme1 in C_2C_{12} muscle cells does not affect Ppme1 protein levels but does increase PP2A levels during muscle cell differentiation. Pharmacologic inhibitor AMZ-30 (20 μM) was applied to C_2C_{12} cells 24 hours post-plating or cells were mock-treated using DMSO. Cells were maintained in proliferation media (DMEM + 10% FBS) for 2 days followed by a switch to differentiation media (DMEM + 2% FBS) 2 days post-plating. Inhibitor treatments were applied every 24 hours until cells were harvested at 48 hours post-plating, as well as, 1, 2, and 3 days after cells were switched to differentiation media. Western blot analysis of Ppme1 and whole PP2A using protein lysates from proliferating (PD) and differentiating (DD) C_2C_{12} treated with Ppme1 inhibitor and harvested over a 3 day differentiation time course.

AMZ-30 (20 μM) was applied to C_2C_{12} cells 24 hours post-plating or cells were mock-treated using DMSO in biological quadruplicates. Cells were maintained in proliferation media (DMEM + 10% FBS) for 2 days followed by a switch to differentiation media (DMEM + 2% FBS) 2 days post-plating. Cells were treated with inhibitor every 24 hours until control and Ppme1 inhibitor treated cells were harvested at differentiation day 2 (DD2). At DD2, the quadruplicates show no significant change in Ppme1 expression levels by Western blot (Figure 28A and 28B). However,

a significant increase in PP2A protein levels is observed in the inhibitor treated cells, providing evidence for the hypothesis that PP2A protein levels accumulate as cells begin to enter into later differentiation (Figure 28A and 28C).

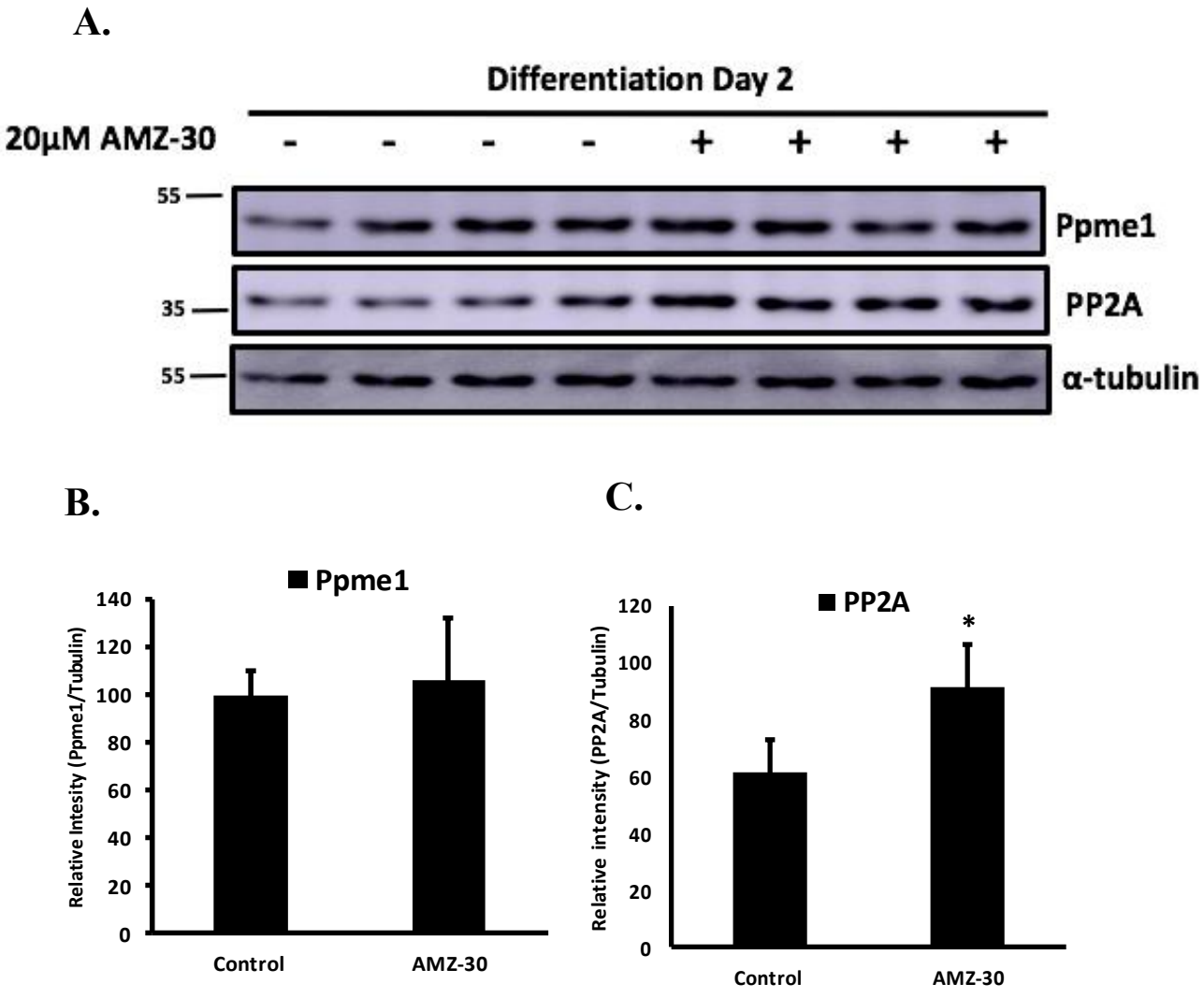

Figure 28. AMZ-30 inhibition of Ppme1 resulted in elevated protein expression of PP2A. Ppme1 inhibitor AMZ-30 (20 μM) was applied to C_2C_{12} cells 24 hours post-plating or cells were mock-treated using DMSO in quadruplicate. Cells were maintained in proliferation media (DMEM + 10% FBS) for 2 days followed by a switch to differentiation media (DMEM + 2% FBS) 2 days post-plating. Cells were treated with inhibitor every 24 hours until control and inhibitor treated cells were harvested at differentiation day 2 (DD2). (A) Western blot analysis of Ppme1 and PP2A. Quantification of (B) Ppme1 and (C) PP2A from blots after normalization to α-tubulin. Significant difference between control cells and cells treated with AMZ-30 (*: $P \leq 0.05$).

Inhibition of Ppme1 delays muscle cell differentiation.

C_2C_{12} cells were treated with 20 μM of a Ppme1-specific inhibitor (AMZ-30) or mock-treated with DMSO across a time course. Western blots were conducted and mouse monoclonal antibodies against Myosin Heavy Chain (MyHC) and myogenin were used to analyze expression of these markers of muscle cell differentiation in control C_2C_{12} cells compared to those treated with AMZ-30. Inhibition of Ppme1 results in decreased expression of MyHC (DD1 and DD2) but did not inhibit cells from eventually differentiating (DD3) (Figure 29). Myogenin is only slightly affected in early differentiation (DD1 and DD2); however, myogenin expression levels are essentially the same as cells further differentiate (DD3) (Figure 29). α-tubulin levels were analyzed to confirm equal protein loading and remain constant across proliferation and differentiation. At DD2 we confirmed a significant inhibition of MyHC and myogenin through Western blot analysis and subsequent quantification (Figure 30A-C).

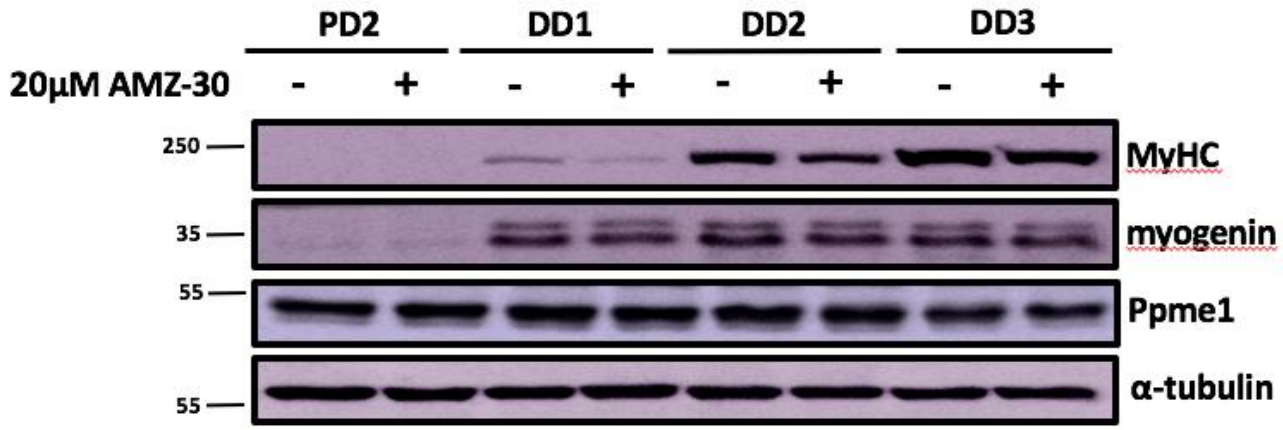

Figure 29. Inhibition of Ppme1 in C_2C_{12} muscle cells delays myogenesis. Ppme1 inhibitor AMZ-30 (20 μM) was applied to C_2C_{12} cells 24 hours post-plating or cells were mock-treated using DMSO. Cells were maintained in proliferation media (DMEM + 10% FBS) for 2 days followed by a switch to differentiation media (DMEM + 2% FBS) 2 days post-plating. Inhibitor treatments were applied every 24 hours until cells were harvested at 48 hours post-plating, as well as, 1, 2, and 3 days after those cells were switched to differentiation media. Western blot analysis of Ppme1, Myosin Heavy Chain (MyHC) and myogenin using protein lysates from proliferating (PD) and differentiating (DD) C_2C_{12} treated with Ppme1 inhibitor and harvested over a 3 day differentiation time course.

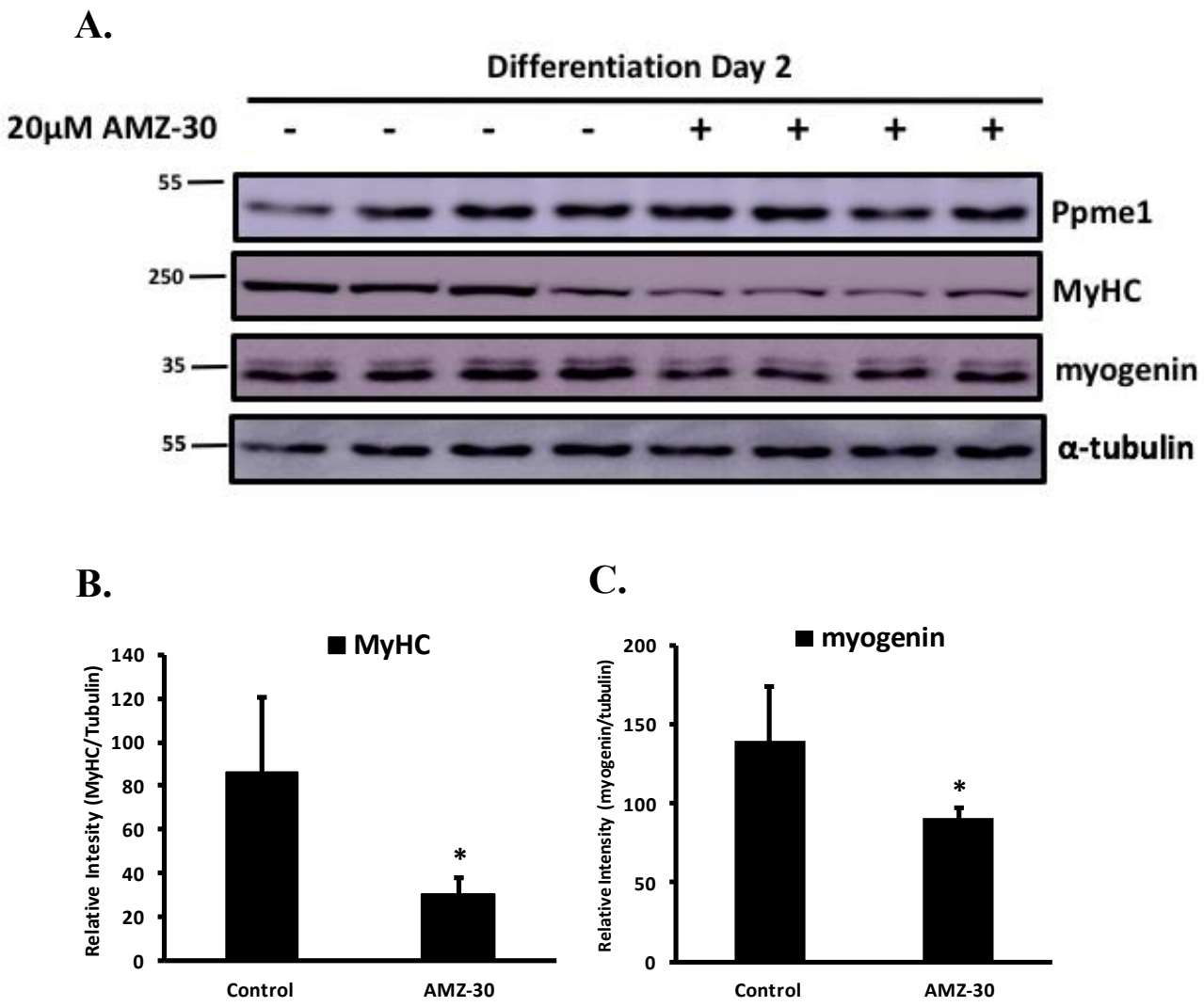

Figure 30. Inhibition of Ppme1 attenuates myogenesis in C2C12 cells. Ppme1 inhibitor AMZ-30 (20 μM) was applied to C_2C_{12} cells 24 hours post-plating or cells were mock-treated using DMSO in quadruplicate. Cells were maintained in proliferation media (DMEM + 10% FBS) for 2 days followed by a switch to differentiation media (DMEM + 2% FBS) 2 days post-plating. Cells were treated with inhibitors every 24 hours until control and inhibitor treated cells were harvested at differentiation day 2 (DD2). (A) Western blot analysis of Ppme1, Myosin Heavy Chain (MyHC), and myogenin. Quantification of (B) MyHC and (C) myogenin from blots after normalization to α-tubulin. Significant difference between control cells and cells treated with AMZ-30 (*: $P \leq 0.05$).

Inhibition of Ppme1 does not change levels of p-ERK and ERK.

C_2C_{12} cells were treated with 20 μM of a Ppme1-specific inhibitor (AMZ-30) or mock-treated with DMSO and Western blots were then performed to evaluate markers of MAP kinase

signaling activity. Phosphorylated ERK (p-ERK) was probed using a mouse monoclonal antibody to analyze the level of p-ERK in muscle cells treated with an inhibitor for Ppme1 compared to control cells. Treatment with AMZ-30 results in no change in p-ERK or whole ERK levels at any day (Figure 31). α-tubulin levels were analyzed to confirm equal protein loading and remain constant across proliferation and differentiation.

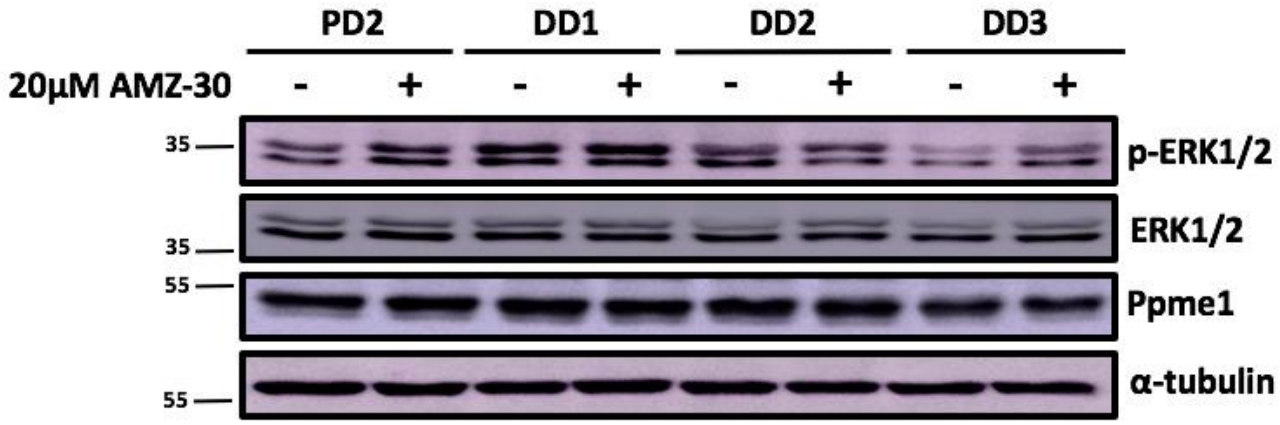

Figure 31. Inhibition of Ppme1 in C_2C_{12} cells does not affect phosphorylation of ERK1/2. Ppme1 inhibitor AMZ-30 (20 μM) was applied to C_2C_{12} cells 24 hours post-plating or cells were mock-treated using DMSO. Cells were maintained in proliferation media (DMEM + 10% FBS) for 2 days followed by a switch to differentiation media (DMEM + 2% FBS) 2 days post-plating. Inhibitor treatments were applied every 24 hours until cells were harvested at 48 hours post-plating, as well as 1, 2, and 3 days after cells were switched to differentiation media. Western blot analysis of Ppme1, phosphorylated ERK (p-ERK) and whole ERK using protein lysates from proliferating (PD) and differentiating (DD) C_2C_{12} treated with Ppme1 inhibitor and harvested over a 3 day differentiation time course.

To quantify the ratio of change between p-ERK and whole ERK levels at DD2, cells were treated with inhibitor every 24 hours until control and Ppme1 inhibitor treated cells were harvested at differentiation day 2 (DD2). Western blots were performed for p-ERK and whole ERK levels (Figure 32A), and quantification of the ratio of p-ERK to whole ERK was conducted to determine if there is a change between the inhibitor treated and control cells. Quantification of the ratio between these levels of p-ERK to whole ERK showed no significant change in the amount of phosphorylation relative to whole protein expression (Figure 32B).

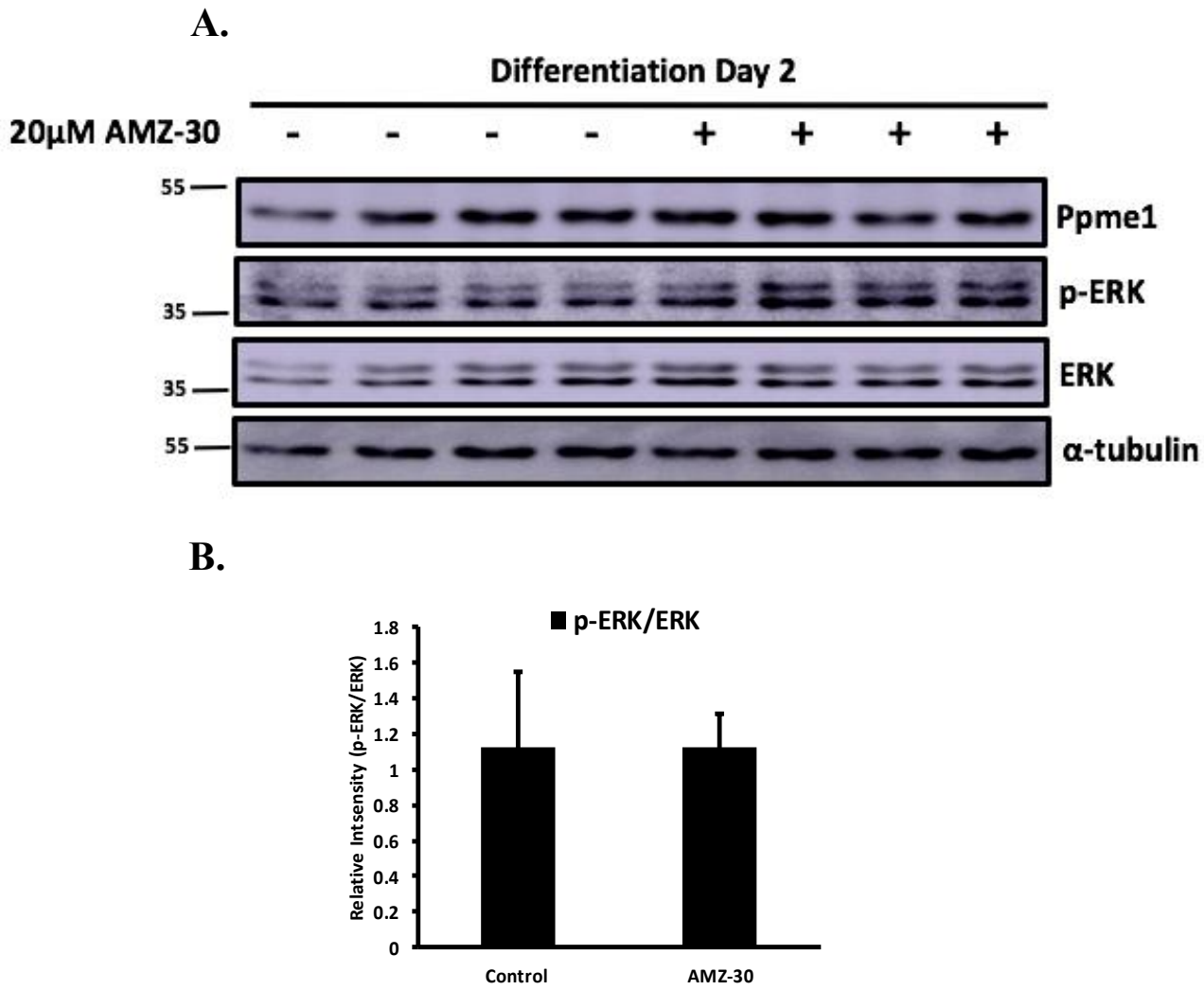

Figure 32. Ppme1 inhibition does not cause a change in phosphorylated ERK level in C2C12 cells. Ppme1 inhibitor AMZ-30 (20 μM) was applied to C_2C_{12} cells 24 hours post-plating or cells were mock-treated using DMSO in quadruplicate. Cells were maintained in proliferation media (DMEM + 10% FBS) for 2 days followed by a switch to differentiation media (DMEM + 2% FBS) 2 days post-plating. Cells were treated with inhibitors every 24 hours until control and inhibitor treated cells were harvested at differentiation day 2 (DD2). (A) Western blot analysis of Ppme1, phosphorylated ERK (p-ERK) and whole ERK. (B) Quantification of the ratio of p-ERK/ERK from quadruplicates after normalization to α-tubulin. Western blots were repeated in quadruplicate as shown.

Inhibition of Ppme1 does not affect phosphorylation of c-Jun.

Since the AP-1 reporter is composed of consensus elements for c-Jun and c-Fos, c-Jun was of interest as a potential target of downregulation due to Ppme1 inhibition. Phosphorylated c-Jun (p-c-Jun) levels were analyzed using a mouse monoclonal antibody for cells treated with the

Ppme1 inhibitor and control cells. Inhibition of Ppme1 results in no observable change in phosphorylation status of p-c-Jun over time (Figure 33). When whole c-Jun expression levels were assessed using a mouse monoclonal antibody, cells treated with the Ppme1 inhibitor also show equal expression of c-Jun compared to control cells (Figure 33). α-tubulin levels were analyzed to confirm equal protein loading and remain consistent across proliferation and differentiation.

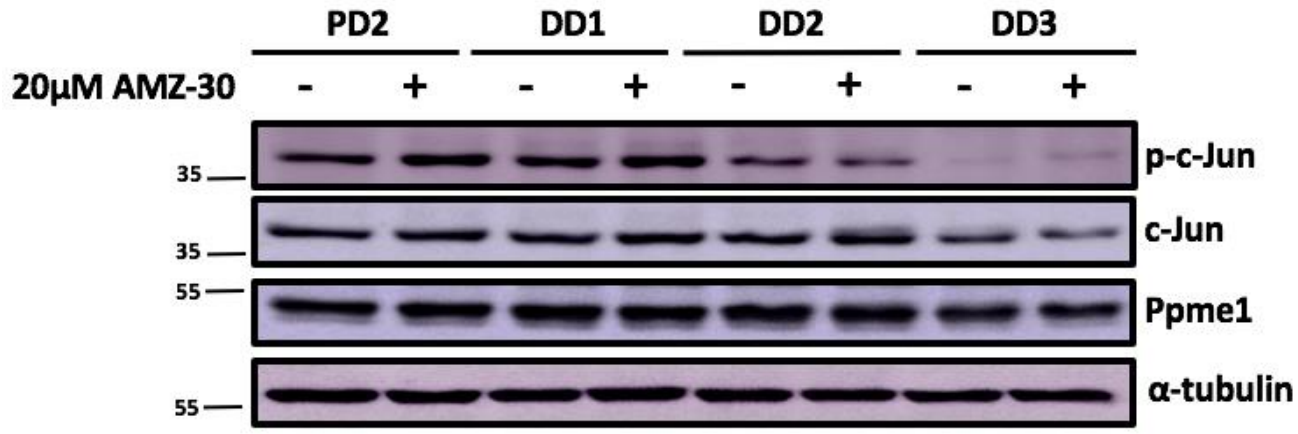

Figure 33. Inhibition of Ppme1 in C_2C_{12} cells does not affect phosphorylation of c-Jun. Pharmacologic inhibitor AMZ-30 (20 μM) was applied to C_2C_{12} cells 24 hours post-plating or cells were mock-treated using DMSO. Cells were maintained in proliferation media (DMEM + 10% FBS) for 2 days followed by a switch to differentiation media (DMEM + 2% FBS) 2 days post-plating. Inhibitor treatments were applied every 24 hours until cells were harvested at 48 hours post-plating, as well as 1, 2, and 3 days after those cells were switched to differentiation media. Western blot analysis of Ppme1, phosphorylated c-Jun (p-c-Jun) and whole c-Jun using protein lysates from proliferating (PD) and differentiating (DD) C_2C_{12} treated with Ppme1 inhibitor and harvested over a 3 day differentiation time course.

To confirm there is no significant difference in the ratio of p-c-Jun to whole c-Jun levels at DD2 between control and inhibitor treated cells, Western blots for p-c-Jun and c-Jun were conducted. The Western blots for p-c-Jun and c-Jun at DD2 exhibit no change in expression levels when cells are treated with Ppme1 inhibitor (Figure 34A). These findings were confirmed through quantification of the ratio of p-c-Jun to whole c-Jun levels (Figure 34B).

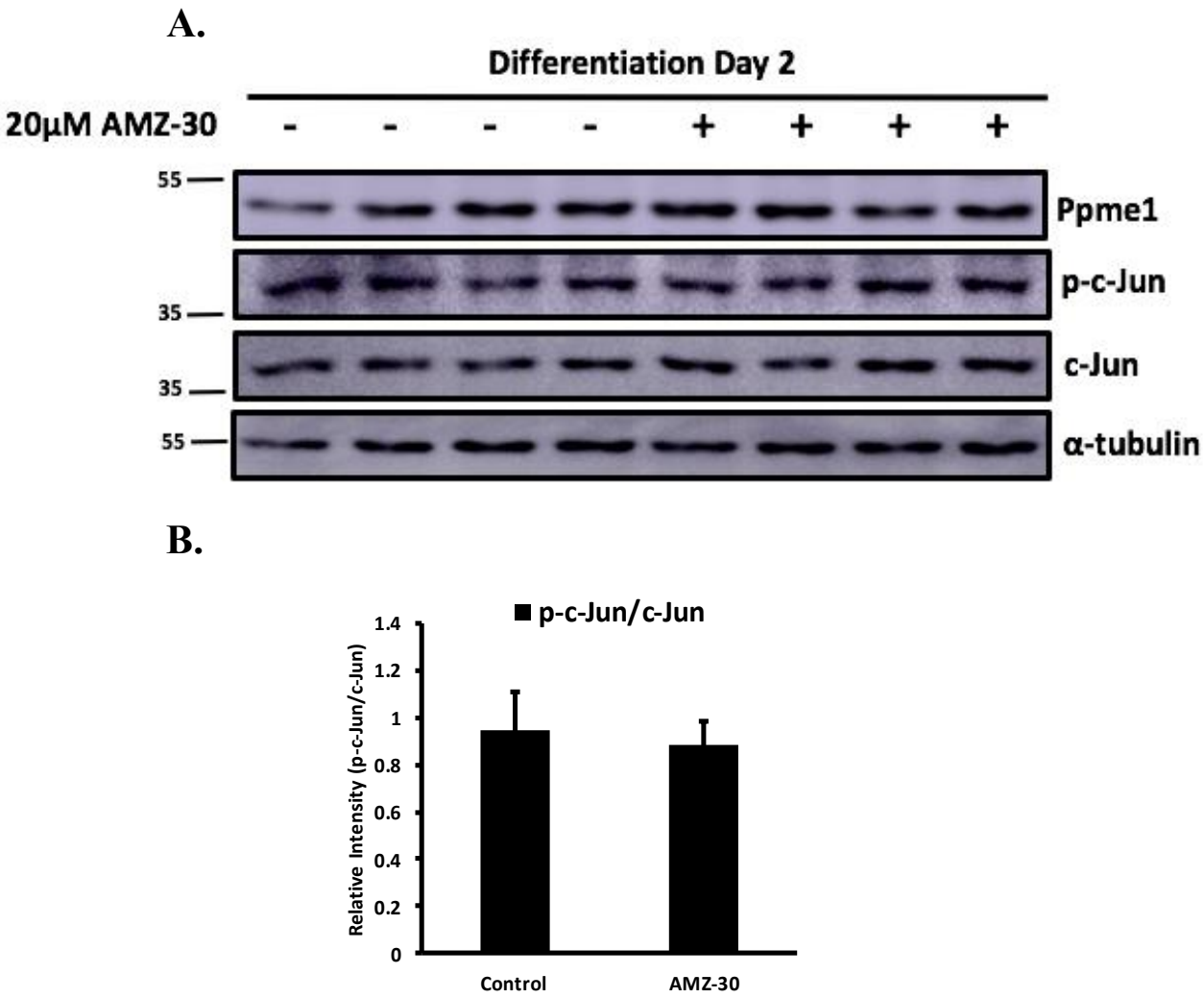

Figure 34. Ppme1 inhibition does not cause a change in phosphorylated c-Jun level in C_2C_{12} cells. Pharmacologic inhibitor AMZ-30 (20 μM) was applied to C_2C_{12} cells 24 hours post-plating or cells were mock-treated using DMSO in quadruplicate. Cells were maintained in proliferation media (DMEM + 10% FBS) for 2 days followed by a switch to differentiation media (DMEM + 2% FBS) 2 days post-plating. Cells were treated with inhibitors every 24 hours until control and inhibitor treated cells were harvested at differentiation day 2 (DD2). A) Western blot analysis of Ppme1, phosphorylated c-Jun (p-c-Jun) and whole c-Jun. Quantification of (B) the ratio of p-c-Jun/c-Jun from quadruplicates after normalization to α-tubulin. Western blots were repeated in quadruplicate as shown.

Inhibition of Ppme1 does not affect phosphorylation status of p-AKT.

Previous literature has indicated that PP2A negatively regulates AKT signaling through dephosphorylation of AKT in gastric and lung cancer, which made it a desired target for study in skeletal muscle (Li et al., 2014). A mouse monoclonal antibody for phosphorylated AKT (p-

AKT) was used to assess if inhibition of Ppme1 activity has an effect on phosphorylation of AKT. Cells treated with an inhibitor for Ppme1 show no change in phosphorylation of AKT when compared to the control cells (Figure 35). Whole AKT levels were also assessed by Western blot utilizing a mouse monoclonal antibody and the results show no change in levels of whole AKT expression between the inhibitor treated and control cells (Figure 35). α-tubulin levels were analyzed to confirm equal protein loading and remain consistent across proliferation and differentiation. The Western blots conducted for p-AKT and whole AKT at DD2 exhibit no change in expression levels when cells are treated with Ppme1 inhibitor (Figure 36A), confirmed through quantification of the ratio of p-AKT to whole AKT levels (Figure 36B).

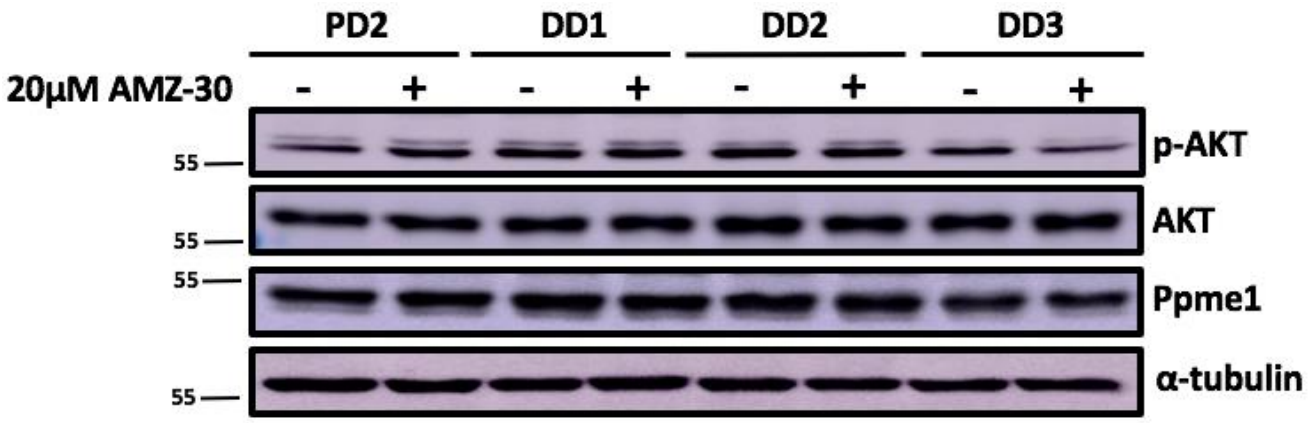

Figure 35. Inhibition of Ppme1 in C_2C_{12} cells does not affect phosphorylation of AKT. Pharmacologic inhibitor AMZ-30 (20 μM) was applied to C_2C_{12} cells 24 hours post-plating or cells were mock-treated using DMSO. Cells were maintained in proliferation media (DMEM + 10% FBS) for 2 days followed by a switch to differentiation media (DMEM + 2% FBS) 2 days post-plating. Inhibitor treatments were applied every 24 hours until cells were harvested at 48 hours post-plating, as well as 1, 2, and 3 days after those cells were switched to differentiation media. Western blot analysis of Ppme1, phosphorylated AKT (p-AKT), and whole AKT using protein lysates from proliferating (PD) and differentiating (DD) C_2C_{12} treated with Ppme1 inhibitor and harvested over a 3 day differentiation time course.

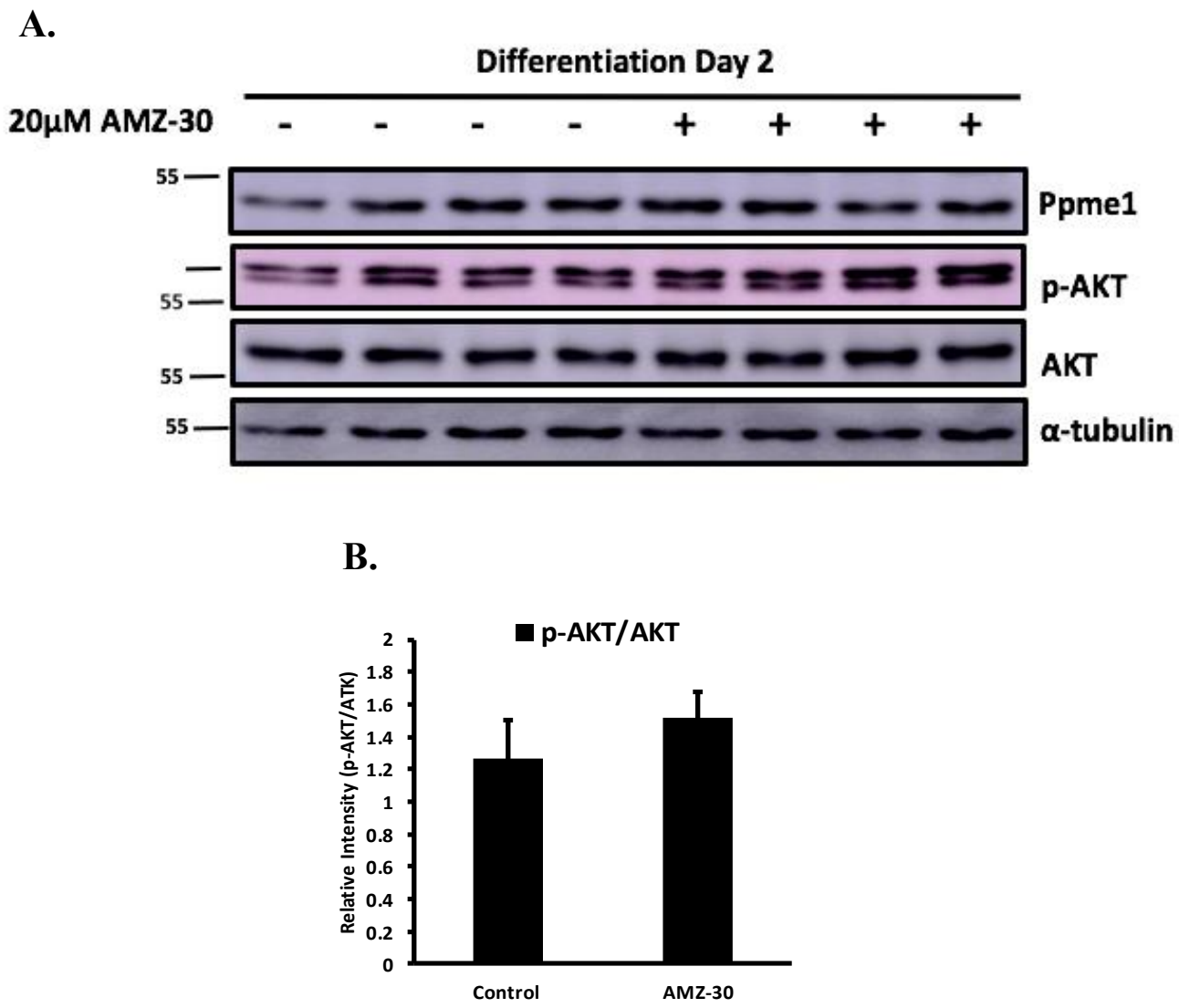

Figure 36. Ppme1 inhibition does not cause a change in phosphorylated AKT level in C_2C_{12} cells
Pharmacologic inhibitor AMZ-30 (20 μM) was applied to C_2C_{12} cells 24 hours post-plating or cells were mock-treated using DMSO in quadruplicate. Cells were maintained in proliferation media (DMEM + 10% FBS) for 2 days followed by a switch to differentiation media (DMEM + 2% FBS) 2 days post-plating. Cells were treated with inhibitors every 24 hours until control and inhibitor treated cells were harvested at differentiation day 2 (DD2). A) Western blot analysis of Ppme1, phosphorylated AKT (p-AKT) and whole AKT. Quantification of (B) the ratio of p-AKT/AKT from quadruplicates after normalization to α-tubulin. Western blots were repeated in quadruplicate as shown.

Inhibition of ERK1/2 and MEK1/2 impact myogenesis and MAPK signaling but does not affect PP2A or Ppme1 protein levels.

To quantify changes in markers of myogenesis as well as MAP kinase signaling in response to treatment with inhibitors for ERK1/2 and MEK1/2, treatments in biological triplicates were

performed. Pharmacologic inhibitors SCH772984 (2 μM) (ERK1/2 inhibitor) or GSK1120212 (5 μM) (MEK1/2 inhibitor) were applied to C_2C_{12} cells 24 hours post-plating or cells were mock-treated using DMSO in biological triplicates. Cells were treated with inhibitors every 24 hours until control and inhibitor treated cells were harvested at differentiation day 1 (DD1). Mouse monoclonal antibodies were used for Western blotting for MyHC and myogenin to quantify effects on myogenesis. The inhibitor for ERK1/2 results in significant upregulation of MyHC at DD1 (Figure 37A and 37B), but does not affect myogenin levels significantly (Figure 37A and 37C). Whereas, the MEK1/2 inhibitor only slightly increases the expression level of MyHC at DD1 (Figure 37A and 37B), but significantly inhibits myogenin expression (Figure 37A and 37C).

To quantify the difference in phosphorylation of ERK and c-Jun between inhibitor treated cells and control cells, Western blots were conducted and probed for p-ERK, ERK, p-c-Jun, and c-Jun. Mouse monoclonal antibodies were used to assess p-ERK, p-c-Jun, and c-Jun expression levels and a rabbit polyclonal antibody was used to examine the expression levels of whole ERK. Interestingly, whole ERK levels are significantly reduced in both sets of inhibitor treated cells, however, the ratio of p-ERK to whole ERK is significantly elevated in the ERK1/2 inhibitor treated cells (Figure 37A). By comparison to control cells, the ratio of p-ERK to whole ERK is significantly diminished in the MEK1/2 treated cells (Figure 37D). Further, the ratio of p-c-Jun to whole c-Jun is relatively unchanged between the control triplicates and the inhibitor treated triplicates (Figure 37E), with a modest reduction in whole c-Jun in the inhibitor treated cells (Figure 37F).

To determine if there was an effect on whole Ppme1 and PP2AC protein levels, Western blots were performed and probed using mouse monoclonal antibodies for Ppme1 and PP2AC. Ppme1 and PP2AC levels remain consistent throughout the control and inhibitor treated triplicates at DD1 (Figure 37A, 37H, and 37I).

A.

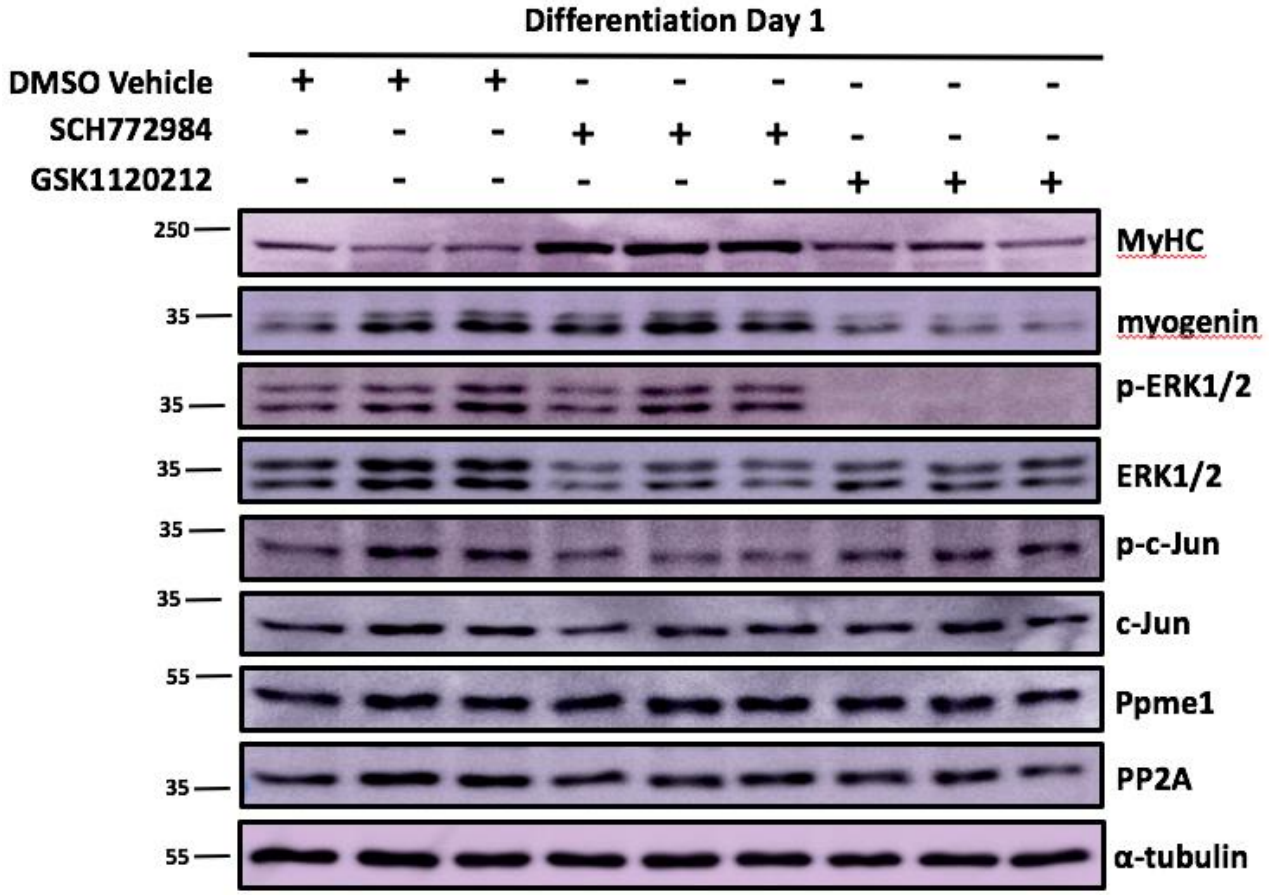

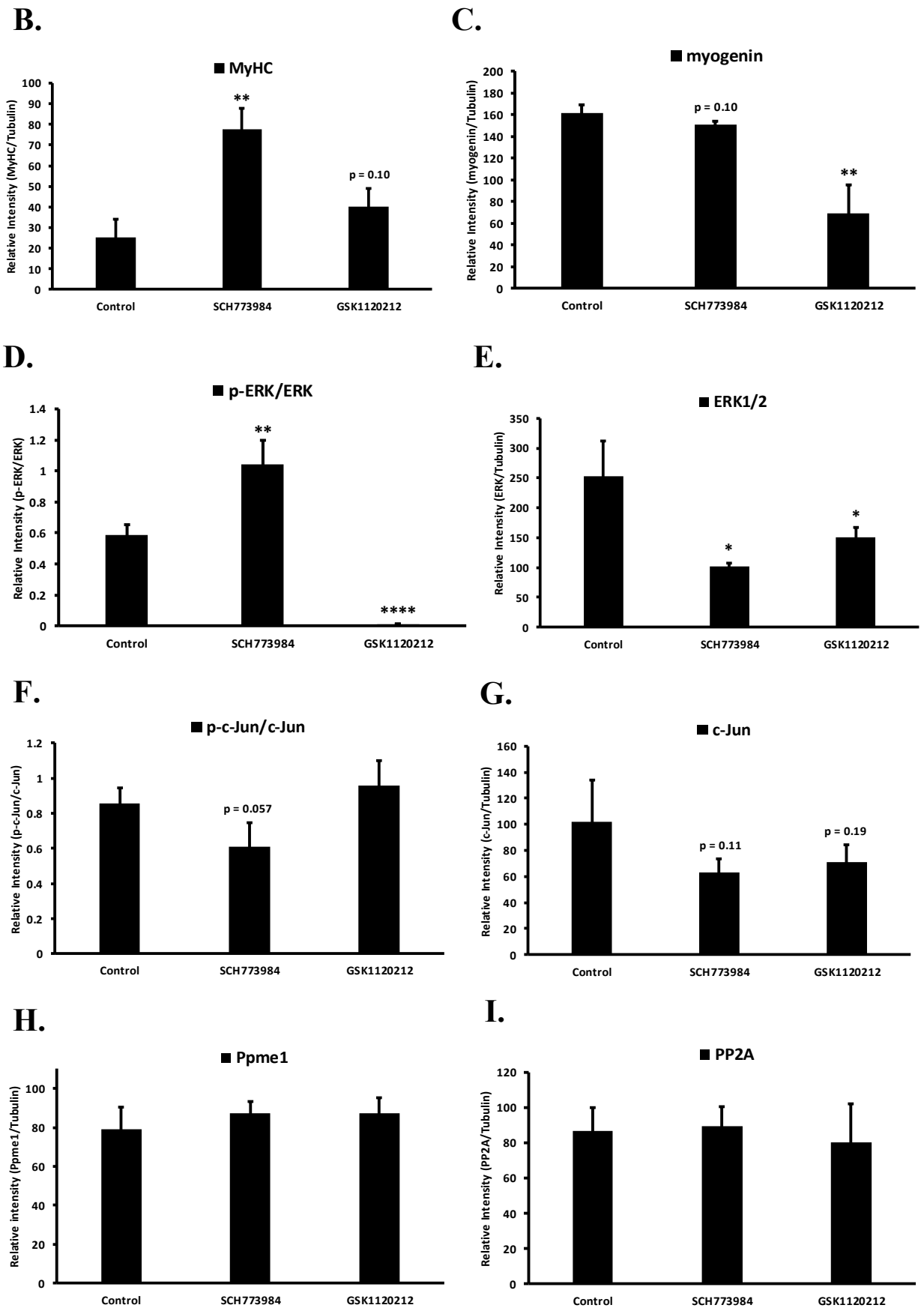
B.
MyHC
Relative Intensity (MyHC/Tubulin)
**
p = 0.10
Control
SCH773984
GSK1120212
C.
myogenin
Relative Intensity (myogenin/Tubulin)
p = 0.10
**
Control
SCH773984
GSK1120212
D.
p-ERK/ERK
Relative Intensity (p-ERK/ERK)
**
****
Control
SCH773984
GSK1120212
E.
ERK1/2
Relative Intensity (ERK/Tubulin)
*
*
Control
SCH773984
GSK1120212
F.
p-c-Jun/c-Jun
Relative Intensity (p-c-Jun/c-Jun)
p = 0.057
Control
SCH773984
GSK1120212
G.
c-Jun
Relative Intensity (c-Jun/Tubulin)
p = 0.11
p = 0.19
Control
SCH773984
GSK1120212
H.
Ppme1
Relative intensity (Ppme1/Tubulin)
Control
SCH773984
GSK1120212
I.
PP2A
Relative Intensity (PP2A/Tubulin)
Control
SCH773984
GSK1120212

Figure 37. Inhibition of ERK1/2 and MEK1/2 in C_2C_{12} cells inhibits myogenesis and MAP kinase signaling but not Ppme1 and PP2A levels. Pharmacologic inhibitors SCH772984 (2 μM) or GSK1120212 (5 μM) were applied to C_2C_{12} cells 24 hours post-plating or cells were mock-treated using DMSO in triplicate. Cells were maintained in proliferation media (DMEM + 10% FBS) for 2 days followed by a switch to differentiation media (DMEM + 2% FBS) 2 days post-plating. Cells were treated with inhibitors every 24 hours until control and inhibitor treated cells were harvested at differentiation day 1 (DD1). **(A)** Western blot analysis was conducted of MyHC, myogenin, p-ERK, whole ERK, p-c-Jun, c-Jun, whole PP2AC, and Ppme1 comparing inhibitor treated C_2C_{12} cells and control cells. Quantification of (B) MyHC (C) myogenin (D) p-ERK levels relative to whole-ERK levels (E) ERK1/2 (F) p-c-Jun levels relative to whole-c-Jun levels (G) whole c-Jun (H) Ppme1 and (I) whole PP2AC from blots after normalization to α-tubulin. Western blots were repeated in triplicate as shown. Significant difference between control cells and cells treated with SCH772984 or GSK1120212 (*: $P \leq 0.05$; **:$P < 0.01$;****: $P < 0.0001$).

Ppme1 Conclusions

Ppme1 is upregulated in neurogenic skeletal muscle atrophy.

Microarray data first identified Ppme1 as a gene of interest within skeletal muscle atrophy as it is upregulated in expression both 3 and 14 days post-denervation in wild-type (WT) as well as MuRF1 null mice (Figure 19A and 19B). There is observed to be a slightly blunted effect on induction of Ppme1 during atrophy in MuRF1-null mice compared to the MuRF1 WT mice at 3 and 14 days post-denervation (Figure 19A and 19B). These data suggest that full induction of Ppme1 during atrophy may require functional MuRF1 and that Ppme1 is involved in the atrophy pathway.

Ppme1 is expressed at the mRNA and protein level in skeletal muscle.

Data shown in this study determines the expression profile for Ppme1 *in vitro*, as the qPCR data from C_2C_{12} myoblasts show reduced Ppme1 mRNA expression in late differentiation (DD7) compared to proliferation (PD2) and early differentiation (DD2) (Figure 21A). Western blot analysis shows a differential pattern than the qPCR data in that protein expression levels remain constant across proliferation and differentiation (Figure 21B). Through a reporter gene system,

this study confirmed that Ppme1 is highly transcriptionally active in skeletal muscle cells, as the Ppme1 promoter contains several putative regulatory elements (Figure 23A-C). This data shows Ppme1 expression is induced via its proximal promoter region.

Ppme1 promoter activity is repressed by myogenic regulatory factors and its conserved Ebox is necessary for full induction of its promoter activity.

The Ppme1 transcript contains a conserved E-box sequence in its 500bp proximal promoter region, so reporter assays were done to test what the effects of ectopically expressing these MRFs would have on promoter activity for the 500bp and the 1000bp promoter fragment. For the Ppme1 Pro500 promoter, repression was observed with the addition of MyoD, however no change was observed when myogenin was ectopically expressed (Figure 24A). For the Ppme1 Pro1000 promoter, modest repression was observed with the addition of both MyoD as well as myogenin (Figure 24B). This data suggests that Ppme1 is regulated at the transcriptional level in differentiating muscle cells.

To determine whether the conserved E-box element within the Ppme1 500bp proximal promoter region is essential for transcriptional activity of Ppme1, this E-box was mutagenized to inhibit the binding of MRFs. Media was sampled across a time course to observe the promoter activity with this mutagenized E-box compared to the Ppme1 wild-type (WT) promoter over time. The results suggest that the most dramatic repression of promoter activity is observed at proliferation day 2 (PD2) when MyoD is highly active. MyoD acts to directly transcriptionally regulate target gene expression throughout the myogenic program (Tapscott, 2005). Thus, the presence of MyoD acting upon this E-box is potentially necessary for full induction of the Ppme1 promoter (Figure 25B). This is further confirmed as cells begin to enter differentiation (DD2-DD4) when

MyoD expression decreases that the E-box mutant begins to trend towards the activity level of the WT promoter (Figure 24C-D).

The Methylester Carboxylesterase Domain of Ppme1 may facilitate its regulation of PP2A and other target proteins.

Since the function of Ppme1 in skeletal muscle has yet to be fully elucidated, this study wanted to identify putative functional domains of Ppme1. An analysis of the functional domains within Ppme1's 386 amino acids identified a large Pimeloyl-ACP methyl ester carboxylesterase domain (Figure 22). The presence of this methyl ester carboxylesterase domain allows Ppme1 to demethylate its specific target substrates. Ppme1 also contains a putative nuclear localization signal (Figure 22) that would mean it localizes and functions within the nucleus. This suggests that Ppme1 may act in regulation of transcription factors that modulate myogenesis, however confocal microscopy would need to be conducted to confirm Ppme1 localization in skeletal muscle cells.

Inhibition of Ppme1 inhibits myoblast differentiation.

To observe effects on myogenesis, Ppme1 was inhibited through the use of a pharmacological inhibitor (AMZ-30) across a time course ranging from proliferation to late differentiation. Protein lysates from inhibitor treated and control C_2C_{12} muscle cells were then harvested and analyzed by Western blotting and probed for MyHC and myogein as markers of muscle cell differentiation. Compared to the control cells, cells treated with AMZ-30 show reductions in MyHC and myogenin at early differentiation, however the control and inhibitor treated cells appear to have similar levels of these markers by late differentiation. This suggests inhibiting Ppme1 inhibits differentiation by reducing muscle-specific gene expression required for myogenesis as muscle cells initiate differentiation (Figure 29 and Figure 30).

Inhibition of Ppme1 significantly attenuates AP-1 reporter activity.

To observe the downstream effects of Ppme1 inhibition on MAPK signaling, an AP-1 reporter gene assay was performed. An AP-1 reporter construct was transfected into C_2C_{12} myoblasts with and without treatments of a Ppme1 inhibitor (AMZ-30) and reporter expression levels were analyzed at differentiation day 1 (DD1). C_2C_{12} cells transfected with the AP1 reporter and then treated with AMZ-30 exhibit significant repression of the AP1 reporter, showing that MAPK signaling is significantly attenuated (Figure 26). The inhibition of MAP kinase signaling in early differentiation corroborates the Western blot results indicating that initiation of myogenesis is delayed when Ppme1 is inhibited.

Inhibition of Ppme1 does not affect phosphorylation of ERK, c-Jun, or AKT in mouse myoblasts.

To observe effects on the phosphorylation status of MAPK members ERK1/2 and c-Jun, Western blots were performed and probed for p-ERK1/2, ERK1/2, p-c-Jun, and c-Jun. Compared to control cells there were no observable changes in the ratio of p-ERK or ERK or p-c-Jun to c-Jun in the Ppme1 inhibitor treated cells (Figure 32, Figure 34, and Figure 36).

We also wanted to determine if inhibition of Ppme1 results in changes in levels of the whole PP2AC subunit. Interestingly, we observed modestly elevated amounts of whole PP2AC protein, suggesting that Ppme1 methylesterase function may be required for proper regulation of PP2AC protein stability (Figure 27 and Figure 31). While it is evident that Ppme1 inhibition has an effect on PP2AC levels and AP-1 reporter activity, it does not appear to affect upstream members of MAP kinase signaling. Previous literature has also linked PP2A to regulation of the AKT signaling pathway by acting to dephosphorylate AKT. To determine if inhibition of Ppme1 influences AKT signaling, Western blots were conducted and probed for phosphorylated AKT

(p-AKT) and AKT. The results show that there is no difference in the level of phosphorylation of AKT when C_2C_{12} cells are treated with the Ppme1 inhibitor.

ERK1/2 and MEK1/2 inhibits do not mimic Ppme1 inhibition in skeletal muscle cells.

In order to quantify the effects of inhibitors for ERK1/2 and MEK1/2 on myogenesis and MAP kinase signaling, we conducted Western blots in biological triplicates for treated and untreated C_2C_{12} cells at differentiation day 1 (DD1). Western blot analysis was conducted to probe for MyHC and myogenin, as well as p-ERK1/2, ERK1/2, p-c-Jun, and c-Jun. As observed in the time course for the ERK1/2 and MEK1/2 inhibitors, the treated triplicates show MyHC upregulated in early differentiation (significantly for ERK1/2 and very modestly for MEK1/2 inhibited cells) (Figure 37). The Ppme1 inhibitor treated cells exhibited inhibition of MyHC and myogenin in early differentiation (Figure 29), thus indicating that Ppme1's role in myogenesis might be different from that of ERK1/2.

Interestingly, whole ERK levels are significantly reduced in the inhibitor treated cells in addition to whole c-Jun expression being slightly blunted at DD1 (Figure 37A, 37E, and 37G). The ratio of p-ERK to whole ERK is significantly elevated in the ERK1/2 inhibitor treated cells, whereas the ratio is significantly diminished in the MEK1/2 treated cells (Figure 37D). This suggests that even though the ERK1/2 inhibitor is inhibiting ERK's kinase function, there is a significant amount of ERK that was or continues to be phosphorylated by MEK1/2. When MEK1/2 is inhibited, as expected, we observe a significant reduction of ERK1/2 phosphorylation and activation (Figure 37D). Further, the ratio of p-c-Jun to whole c-Jun is relatively unchanged between the control triplicates and the inhibitor treated triplicates (Figure 37F), suggesting that

even though ERK and MEK function are being inhibited there are additional pathways still phosphorylating c-Jun.

Additionally, we wanted to determine if the effects observed by inhibition of ERK1/2 or MEK1/2 are potentially mediated through changes in whole protein levels of Ppme1 or PP2AC. Western blot results indicate that inhibiting the function of ERK1/2 or MEK1/2 does not alter the levels of Ppme1 or PP2AC (Figure 37A, 37H, and 37I). Overall, these results show that inhibition of Ppme1 does not affect MAP kinase signaling in the same way that inhibition of ERK1/2 and MEK1/2 does.

Chapter 4: Discussion and Future Directions

Dusp4 and Ppme1 are upregulated during neurogenic atrophy.

Skeletal muscle is a dynamic tissue that has the ability to regulate its size in response to a variety of external cues. A balance between protein synthesis and protein degradation is maintained in order to regulate muscle mass, and when protein degradation outpaces the rate of protein synthesis this leads to muscle atrophy (McKinnell and Rudnicki, 2004; Bodine and Baehr, 2014). Despite these protein degradation pathways being well characterized (i.e. the ubiquitin proteasome system), the molecular mechanisms of muscle atrophy still have yet to be fully elucidated. Dual specificity phosphatase 4 (Dusp4) and Protein phosphatase methylesterase 1 (Ppme1) are two genes identified in skeletal muscle as being upregulated in response to denervation, indicating that these two genes may play roles within the neurogenic atrophy cascade.

Dusp4 has been previously characterized as a type 1 nuclear localized dual specificity phosphatase that negatively regulates mitogen-activated protein (MAP) kinase signaling (Auger-Messier et al., 2013; Huang and Tan, 2012; Peng et al., 2010). Ppme1 itself is not a phosphatase, however protein phosphatase 2A (PP2A) has been identified as a direct target of Ppme1 demethylation and inactivation. (Kaur et al., 2016; Xing et al., 2008; Yabe et al., 2015; Yabe et al., 2018). Through their roles as phosphatases both Dusp4 and PP2A have been linked to a number of cell signaling pathways, such as MAP kinase and AKT signaling. These genes have yet to be investigated in skeletal muscle, thus the identification and characterization of them in this context provides novel data regarding what roles these genes may play in the larger atrophy picture.

Dusp4 and Ppme1 are expressed in skeletal muscle.

Previous data obtained from our lab determined that Dusp4 is highly expressed during proliferation, but decreases in expression significantly as muscle cells enter into differentiation (Haddock, 2016). Since Ppme1 was observed to be upregulated under neurogenic atrophy, this study wanted to validate that Ppme1 was expressed in skeletal muscle as well as determine its expression profile throughout proliferation and differentiation. Ppme1's mRNA expression appears to decrease as C_2C_{12} cells differentiate, while its protein level remains constant. This suggests that although Ppme1 may be negatively regulated at the transcriptional level, Ppme1 expression is constant at the protein level. It also possesses significant transcriptional activity through analysis of its proximal promoter at the 500 and 1000 base pair (bp) levels. Ppme1 demethylates and inactivates PP2A in a coordinated interplay with leucine carboxyl methyltransferase (LCMT), which methylates and thus activates PP2A (Kaur et al., 2016; Yabe et al., 2015). It is thought that the coordinated activation and inactivation of PP2A serves to regulate these cell signaling pathways as cells continue through the cell cycle (Alberts et al., 1993; Schonthal 2001; Seshacharyulu et al., 2013). Thus, constant Ppme1 expression could be integral in inactivating PP2A phosphatase activity to allow for activation of cell signaling pathways that are essential in the transition from proliferating myoblasts into specialized myotubes.

Ppme1 promoter activity is repressed by myogenic regulatory factors and its conserved Ebox is necessary for full induction of its promoter activity.

As previously described, MRFs are muscle specific transcription factors that regulate gene expression during myogenesis through binding canonical E-box sequences in the promoters of these genes (Singh and Dilworth, 2013; Londhe and Davie, 2011). MRFs can function by

forming homodimers or heterodimers with ubiquitously expressed E-proteins such as TCF3 and TCF12 (Singh and Dilworth, 2013; Londhe and Davie, 2011). The Ppme1 transcript contains one conserved and two non-conserved E-boxes in its 500 bp proximal promoter, so reporter assays were conducted to test effects of MRFs on the Ppme1 promoter. A 500 bp promoter fragment was found to have modest repression of reporter activity by MyoD, while a 1000 bp fragment was found to have modest repression of reporter activity by both MyoD and myogenin. These results indicate that Ppme1 may be regulated transcriptionally by muscle specific transcription factors.

We also wanted to determine if MRF regulation is necessary for activation of the Ppme1 promoter, thus we mutagenized the conserved E-box within the Ppme1 promoter to inhibit the binding of MRFs. We observed a significant attenuation of activity in the mutagenized E-box promoter compared to the WT promoter during muscle cell proliferation. This data suggests that the expression of Ppme1 in skeletal muscle is regulated by MRFs and this binding of MRFs to the conserved E-box sequence facilitates this transcriptional regulation. Interestingly, we observed that, as muscle cells proceeded through differentiation, the mutagenized promoter appeared to catch up to the WT promoter activity. MyoD's expression has been previously characterized as being highest during proliferation and early differentiation, with activity decreasing as cells proceed through differentiation in corroboration with myogenin upregulation (Singh and Dilworth, 2013; Londhe and Davie, 2011). Because we observed the greatest repression of promoter activity when the E-box is mutagenized during proliferation, we hypothesize Ppme1 could be significantly regulated by the MRF MyoD. This suggests Ppme1 regulation by MRFs may be integral during the period of muscle cell growth, division, and myogenic commitment to differentiation.

Inhibition of Ppme1 destabilizes the PP2AC subunit.

Previous literature has indicated that functional Ppme1 is necessary for protection of the PP2AC subunit from ubiquitin proteasome degradation (Yabe et al., 2015). Since this stabilization of PP2AC by Ppme1 has been observed, we wanted to determine if Ppme1 plays a role in PP2AC stabilization in skeletal muscle. We performed Western blots for whole PP2AC with control cells and cells that had been treated with a Ppme1 inhibitor. The Western blots revealed a destabilization of the level of PP2AC as C_2C_{12} cells differentiate when in the presence of an inhibitor for Ppme1. This suggests that part of Ppme1's role in skeletal muscle may be stabilizing the activity of PP2AC. To further understand how Ppme1 inhibition affects PP2A activity, a co-IP could be performed to determine how the PP2AB regulatory subunit and PP2AC catalytic subunit interact in the presence of the Ppme1 inhibitor. A previous study has also suggested that in the absence of Ppme1 function, the PP2A core enzyme may have a higher affinity for interaction with the B55 regulatory subtype (Yabe et al., 2018). In order to function properly, the heterotrimeric components of PP2A must be directly interacting, thus if we do not observe this interaction, this could indicate that active Ppme1 is required for stabilization of this interaction. The B regulatory subunit also provides specificity for PP2A target substrates, thus determining any differential B subunit interaction in the absence of Ppme1 could help elucidate PP2A-Ppme1 function in skeletal muscle (Yabe et al., 2018).

Ectopic expression of Dusp4 and inhibition of Ppme1 attenuates myoblast differentiation.

Protein lysates from cells overexpressing Dusp4-wild type or Dusp4-dominant negative were analyzed via Western blot and probing for MyHC and myogenin as markers of muscle cell differentiation. Compared to control cells, cells overexpressing Dusp4-wild type exhibited delayed differentiation, however MyHC and myogenin levels appeared to be similar to control

cells by late differentiation. This suggests ectopic Dusp4 overexpression inhibits myoblast differentiation but does not prevent myoblasts from terminally differentiating. Ectopic expression of Dusp4-dominant negative, however, significantly attenuated levels of MyHC and myogenin at all differentiation time points. This suggests that overexpression of Dusp4-dominant negative may prevent myoblasts from differentiating entirely. Protein lysates from cells treated with an inhibitor for Ppme1 were also analyzed via Western blot by probing for MyHC and myogenin and, similar to cells ectopically expressing Dusp4, the Ppme1 inhibitor treated cells showed delayed differentiation compared to control cells. Expression levels of the differentiation markers are equivalent to control levels in late differentiation, suggesting Ppme1 inhibition delays differentiation but does not entirely prevent myoblast differentiation.

Dusp4 overexpression and Ppme1 inhibition lead to attenuation of MAP kinase signaling. Several signaling pathways are required for proper myogenesis, with one such pathway being the ERK1/2 branch of the MAP kinase signaling cascade. The MAP kinase signaling pathway is a well described pathway that modulates gene expression and impacts cell proliferation and differentiation. If this pathway is impaired, proper myogenesis is prevented (Knight and Kothary, 2011). Activation of the ERK1/2 pathway leads to phosphorylation and activation of ERK which then acts downstream to control processes such as proliferation, cell migration, and differentiation (Raman et al., 2007; Morrison 2012). At different steps along the MAP kinase cascade, phosphatases can act by removing phosphate groups from these protein kinases resulting in a deactivation of the MAP kinase pathway (Raman et al., 2007; Kondoh and Nishida, 2006). Dusp4 and PP2A are phosphatases that have been previously identified as dephosphorylating MAP kinase members, thus playing putative roles in skeletal muscle as negative regulators of this pathway.

One of the downstream transcription factors activated by the ERK1/2 pathway is the AP-1 protein, which binds to AP-1 consensus elements within the promoters of target genes to modulate their activity. Thus, the use of an AP-1 reporter gene allowed us to quantify the activity of downstream MAP kinase signaling. Overexpression of Dusp4-wild type and Dusp4-dominant negative in C_2C_{12} cells exhibits attenuation of AP-1 reporter gene activity. Furthermore, through Western blot analysis across a differentiation time course we determined that Dusp4-WT overexpression attenuates phosphorylated ERK1/2 levels. Additionally, we also did not observe a change in whole ERK levels, suggesting that Dusp4 affects the activation of the MAP kinase pathway through dephosphorylation and not simply promoting a decrease in the amount of ERK available to be phosphorylated. We also determined through co-immunoprecipitation analysis that the Dusp4-DN construct acts by binding constitutively and irreversibly to ERK1/2 but not p38, denoting that in skeletal muscle Dusp4 has specificity for ERK1/2. This differentiates Dusp4's function in skeletal muscle from its function in cardiac muscle, where a previous study found that Dusp4 preferentially dephosphorylates p38 but not ERK1/2 (Auger-Messier, 2013). Taking the reporter and Western blot data together, it is apparent that Dusp4 overexpression inhibits myogenesis by attenuating the ERK1/2 MAP kinase signaling pathway required for proper muscle cell differentiation. Since Dusp4 is highly expressed during proliferation it is possible that Dusp4 may act to negatively regulate ERK1/2 activity allowing myoblasts to exit the cell cycle and trigger myotube differentiation.

Interestingly, inhibition of Ppme1 also resulted in attenuation of AP-1 reporter activity. Thus, we wanted to determine where along the ERK1/2 pathway PP2A may attenuate MAP kinase signaling in the absence of Ppme1 activity. However, unlike Dusp4 overexpression, Western blots showed no differential expression of phosphorylated ERK when C_2C_{12} cells were treated

with an inhibitor for Ppme1. We also did not observe any change in whole ERK levels in cells treated with the inhibitor, suggesting that inhibiting Ppme1 is not destabilizing the level of ERK available for phosphorylation. The AP-1 protein is most commonly composed of a heterodimer between the proteins c-Jun and c-Fos, both of which can be phosphorylated and activated by ERK1/2 when it translocates into the nucleus. Thus, we hypothesized that PP2A might be negatively regulating this pathway through dephosphorylating c-Jun directly. Western blots revealed no change in the phosphorylation status of c-Jun in the Ppme1 inhibitor treated cells. This suggests that PP2A may be targeting c-Fos for dephosphorylation, thus Western blots could be performed to determine if we observe greater dephosphorylation of c-Fos in cells treated with an inhibitor for Ppme1. Despite the lack of identification of a distinct target of inactivation along this pathway, the reporter data indicates that the inhibition of myogenesis observed is likely due to the downstream attenuation of MAP kinase signaling required for cell differentiation.

We could study this idea further by performing a co-IP to determine how c-Jun and c-Fos are interacting together to affect the AP-1 reporter. The c-Jun and c-Fos proteins form a complex that regulates transcription by acting on promoters that contain AP-1 elements. c-Jun has specific DNA binding activity, while c-Fos possesses homology to the putative DNA binding domain of c-Jun (Halazonetis et al., 1988). Dimerization between the two proteins occurs via interaction between leucine zipper domains and serves to bring into proper juxtaposition regions rich in amino acids that form a DNA-binding domain (Gentz et al, 1989; Glover and Harrison, 1995; Turner and Tijan, 1989). A previous study found that while c-Jun can bind as a homodimer to AP-1 elements, c-Fos fails to dimerize and displays seemingly no affinity for the AP-1 element (Halazonetis et al., 1988). However, the ability of c-Fos to homodimerize is contested within the literature as other studies have found that it is able to function in a homodimerized state (Turner

and Tijan, 1989). The heterodimer formed between c-Jun and c-Fos reportedly binds more efficiently to the AP-1 elements than the c-Jun homodimer does on its own (Halazonetis et al., 1988; Ryseck and Bravo, 1991). Also, it has been observed that in the absence of c-Fos, the c-Jun protein may result in aberrant homodimeric transcription complexes, which can affect normal gene expression (Halazonetis et al., 1988). Thus, if c-Jun or c-Fos are complexing in a manner that has less DNA binding affinity in the presence of a Ppme1 inhibitor this may explain why we observe attenuation of AP-1 reporter gene activity.

ERK1/2 and MEK1/2 inhibitors do not mimic Dusp4 overexpression or Ppme1 inhibition in skeletal muscle cells.

Because inhibition of Ppme1 and overexpression of Dusp4 hinder MAP kinase signaling, we wanted to determine if these genes mimic pharmacological inhibition of MAP kinase signaling. Dusp4 is capable of dephosphorylating ERK1/2, thus we utilized an inhibitor specific for ERK1/2 as well as an inhibitor for its upstream kinase, MEK1/2. The first peak in ERK1/2 activity during myogenesis prevents premature cell cycle exit and differentiation (Knight and Kothary, 2011). Thus, when we inhibit ERK1/2 or MEK1/2 with a small molecule we observe a greater increase in MyHC at the start of differentiation and myogenin appears prematurely during proliferation, suggesting that the inhibitor treated cells have exited the cell cycle and are beginning to differentiate prematurely. (Knight and Kothary, 2011; Adi et al, 2002; Sarbassov et al., 1997). Similarly, ectopic expression of Dusp4-wild type or inhibition of Ppme1 attenuates proper myoblast differentiation, but we did not observe the same increases in MyHC during early differentiation or the presence of myogenin duringproliferation, suggesting that ERK1/2 is still functioning in its prevention of premature cell cycle exit. This disparity is likely due to the nuclear localization and function of Dusp4 and Ppme1. Dusp4 is only able to act on ERK1/2 that

has already translocated into the nucleus, but not cytoplasmic ERK1/2; whereas the small molecule inhibitors for ERK1/2 and MEK1/2 are able to act upon both nuclear and cytoplasmic pools of ERK and MEK. In the case of Ppme1, we do not observe Ppme1 acting on ERK through PP2A-mediated dephosphorylation, thus if Ppme1 is acting on ERK it might be through a demethylation event on nuclear localized ERK.

As expected, inhibition of ERK1/2 or MEK1/2 results in significant attenuation of the AP-1 reporter gene activity, similar to what is observed when Ppme1 is inhibited or Dusp4 is overexpressed. However, inhibition of ERK1/2 or MEK1/2 with inhibitors leads to both inhibition of phosphorylated ERK as well as a destabilization of whole ERK. This differs from Dusp4-wild type overexpression or Ppme1 inhibition in which we do not observe changes in whole ERK protein levels. From the disparities observed in these markers we determined that Dusp4 and Ppme1 do not function by simply dephosphorylating and inactivating the ERK1/2 pathway in the same way a small molecular inhibitor does. It is possible that Dusp4 and Ppme1 may act through a series of more complex protein-protein interactions that modulate MAP kinase signaling.

Ppme1 does not modulate protein synthesis or degradation through regulation of the AKT signaling pathway in skeletal muscle.

The IGF1-AKT/PKB pathway is a highly conserved signaling pathway that plays an important role in the regulation of skeletal muscle growth (Otto and Patel, 2010; Egerman and Glass, 2014). AKT phosphorylates mTOR and GSK3β which leads to downstream stimulation of protein synthesis, as well as, has been shown to induce hypertrophy (Schiaffino and Mammucari, 2011; Stitt et al., 2004). On the other hand, AKT has also been shown to prevent activation of the previously described atrophy mediators MuRF1 and MAFbx through phosphorylation and

inhibition of the FoxO family of transcription factors (Schiaffino and Mammucari, 2011; Stitt et al., 2004). Specifically, AKT phosphorylates FoxO transcription factors on multiple sites, which leads to the sequestering of these phosphorylated FoxO proteins from the nucleus and preventing their transcriptional activity. Therefore, AKT is able to suppress catabolic pathways that are participatory in denervation-induced muscle atrophy. Previous literature has found that PP2A negatively regulates phosphorylation of AKT, thus potentially modulating the pathways of both protein synthesis/hypertrophy, as well as, protein degradation/atrophy. We found that in the presence of a Ppme1 inhibitor there was no observable change in the level of phosphorylation of AKT. Thus, in skeletal muscle, it does not appear that PP2A has specificity for regulating the AKT kinase through dephosphorylation.

Ppme1 may demethylate substrates other than PP2A in skeletal muscle signaling pathways.
The potential role of protein methylation as a post-translational modification in signal transduction has not been investigated to the same depth as protein phosphorylation. In the last decade, many important observations have identified protein methylation as subject to dynamic regulatory events involved in ligand-stimulated signal transduction (Lee et al., 2005). To date, Ppme1 has only been identified as a methylesterase specific for demethylating the PP2A catalytic subunit, however, it is possible that Ppme1 could also potentially have additional targets that affect various signaling pathways. Post-translational methylation has recently been found to be involved in transcriptional repression through modification of coactivators, such as CREB-binding protein (CBP), p300, and steroid receptor coactivators (SRCs) by the methyltransferase coactivator-associated arginine methyltransferase (CARM1) (Feng et al, 2006; Lee et al., 1998; Lee et al., 2005). Transcription coactivators frequently function by bridging transcription factors to the components of the basal transcriptional apparatus. In particular, the CBP and p300

coactivators have been shown to be essential for transcriptional activation by transcription factors including nuclear receptors, CREB, NF-κB, basic helix-loop-helix factors, STATs, and AP-1 (Li et al., 2007). Additionally, the conserved coactivator protein members of the SRC family have been shown to interact with other proteins such as myogenin, MEF-2, NF-κB, AP-1, STAT, p53, and E2F1, suggesting that these coactivators are important in various cellular processes (Lee et al., 1998).

Differentiation of skeletal muscle cells is regulated by basic helix-loop-helix (bHLH) proteins, which include MRFs such as MyoD and myogenin. Previous literature indicates that p300/CBP can interact with bHLH proteins in activating gene expression by stimulating E-box directed transcription (Eckner et al., 1996). They found that microinjection of p300/CBP antibodies into myoblasts blocked terminal differentiation, the ability of cells to fuse, and the transcriptional activity of myogenic bHLH proteins (Eckner et al., 1996). Thus, these coactivators could be essential in the execution of myoblast differentiation. Further, it has been observed that SRC-1 is capable of forming a complex with CBP and p300, which in turn acts to coactivate AP-1 (Lee et al., 1998). SRC-1 synergistically works with p300 to specifically bind to c-Jun and c-Fos in order to regulate AP-1 dependent transactivation and mediate the transcriptional activity of the AP-1 transcription factor (Bannister and Kouzarides, 1995; Lee et al., 1998). Thus, Ppme1 could be functioning within these pathways in demethylation of co-activators that aid in the transcriptional regulation of genes in skeletal muscle by MRFs and the AP-1 protein.

Interestingly, FOXO1 is methylated at Arg248 and Arg250 by protein arginine methyltransferase 1 (PRMT1) which inhibits phosphorylation of FOXO1 at Ser253 by AKT, in turn blocking exclusion of FOXO1 from the nucleus (Wang et al., 2016). This methylated FOXO1 then

remains nuclear and activates expression of downstream target genes (Wang et al., 2016). Other studies have indicated that FOXO3 is methylated at Lys270 and Lys271 by SET domain containing lysine methyltransferase 7 (Set9), and as a result has lower DNA binding activity and transactivation (Wang et al., 2016). These results have found that there appears to be specificity of different methyltransferases for various FOXO transcription factors, and that these methylation events serve to modulate AKT signaling. To date, Ppme1 has only been identified as a negative regulator of PP2A, but not by acting to demethylate other target substrates. Further research will need to be conducted in looking at methylation status of co-activators and other proteins along both the MAP kinase and AKT signaling pathways to understand how specific demethylation events carried out by Ppme1 may be critical for proper cell signaling.

References

Alberts AS, Thorburn AM, Shenolikar S, Mumby MC, Feramisco JR. Regulation of cell cycle progression and nuclear affinity of the retinoblastoma protein by protein phosphatases. Proc. Natl. Acad. Sci. U. S. A. 1993;90:388–392.

Ardley HC, Robinson PA. 2005. E3 ubiquitin ligases. *Essays In Biochemistry*. 41:15-30.

Auger- Messier M, Accornero F, Goonasekera SA, Bueno OF, Lorenz JN, van Berlo JH, Willette RN, and Molkentin JD. Unrestrained p38 MAPK activation in Dusp1/4 double-null mice induces cardiomyopathy. Circ Res 112: 48-56, 2013.

Bannister, A. J. and Kouzarides, T. (1995), CBP-induced stimulation of c-Fos activity is abrogated by E1A.. The EMBO Journal, 14: 4758-4762.

Bodine SC, Latres E, Baumhueter S, et al. 2001. Identification of ubiquitin ligases required for skeletal muscle atrophy. *Science Signaling*. 294(5547):1704.

Bodine SC, Baehr LM. 2014. Skeletal muscle atrophy and the E3 ubiquitin ligases MuRF1 and MAFbx/atrogin-1. *American Journal of Physiology - Endocrinology and Metabolism*. 307: LE469-E484.

Carrió, E., and Suelves, M. (2015). DNA methylation dynamics in muscle development and disease. Front. Aging Neurosci. *7*, 19.

Cohen TJ, Waddell DS, Barrientos T, et al. 2007. The Histone Deacetylase HDAC4 Connects Neural Activity to Muscle Transcriptional Reprogramming. *The Journal of Biological Chemistry*. 282: 33752-33759.

Dilworth FJ, Singh K. 2013. Differential modulation of cell cycle progression distinguishes members of the myogenic regulatory family of transcription factors. *FEBS Journal*. 280: 3991-4003.

Dodd, R. 2011. Ubiquitylation [open access image]. Attribution: By Rogerdodd at the English language Wikipedia, CC BY-SA 3.0, https://commons.wikimedia.org/w/index.php?curid=7677277

Eckner, R., Yao, T.P., Oldread, E., and Livingston, D.M. (1996). Interaction and functional collaboration of p300/CBP and bHLH proteins in muscle and B-cell differentiation. Genes Dev. *10*, 2478–2490.

Egerman, M.A., and Glass, D.J. (2014). Signaling pathways controlling skeletal muscle mass. Crit. Rev. Biochem. Mol. Biol. *49*, 59–68.

Farooq A, and Zhou MM. Structure and regulation of MAPK phosphatases. *Cell Signal* 16: 769-779, 2004.

Feng, Q., Yi, P., Wong, J., and Malley, B.W. (2006). Signaling within a Coactivator Complex: Methylation of SRC-3/AIB1 Is a Molecular Switch for Complex Disassembly. Mol. Cell. Biol. *26*, 7846 LP-7857.

Furlow JD, Watson ML, Waddell DS, et al. 2013. Altered gene expression patterns in muscle ring finger 1 null mice during denervation and dexamethasone induced muscle atrophy. *Physiological genomics*. 45:1168-1185.

Gentz, R., Rauscher, F.J., Abate, C., and Curran, T. (1989). Parallel association of Fos and Jun leucine zippers juxtaposes DNA binding domains. Science (80-.). *243*, 1695 LP-1699.

Glover, J.N.M., and Harrison, S.C. (1995). Crystal structure of the heterodimeric bZIP transcription factor c-Fos–c-Jun bound to DNA. Nature *373*, 257–261.

Haddock, Ashley Noel, "Transcriptional Regulation of Dual-Specificity Phosphatase 4 (Dusp4) by Muscle RING Finger 1 (MuRF1) and Myogenic Regulatory Factors" (2016). UNF Theses and Dissertations. 618.

Halazonetis, T.D., Georgopoulos, K., Greenberg, M.E., and Leder, P. (1988). c-Jun dimerizes with itself and with c-Fos, forming complexes of different DNA binding affinities. Cell *55*, 917–924.

Huang CY, and Tan TH. DUSPs, to MAP kinases and beyond. *Cell Biosci* 2: 24, 2012.

Janssens V & Goris J (2001) Protein phosphatase 2A: a highly regulated family of serine/threonine phosphatases implicated in cell growth and signaling. *Biochem J*. 353, 417-439.

Kaur A, Westermarck J. 2016. Regulation of protein phosphatase 2A (PP2A) tumor suppressor function by PME-1. *Biochem Soc Trans*. 44(6): 1683-1693.

Kaur, A., Elzagheid, A., Birkman, E.-M., Avoranta, T., Kytölä, V., Korkeila, E., Syrjänen, K., Westermarck, J., and Sundström, J. (2015). Protein phosphatase methylesterase-1 (PME-1) expression predicts a favorable clinical outcome in colorectal cancer. Cancer Med. *4*, 1798–1808.

Lai, K.M., Gonzalez, M., Poueymirou, W.T., Kline, W.O., Na, E., Zlotchenko, E., Trevor, N., Economides, A.N., Yancopoulos, G.D., and Glass, D.J. (2004). Conditional activation of Akt in adult skeletal muscle induces rapid hypertrophy. Mol. Cell. Biol. *24*, 9295–9304.

Lawan A, Torrance E, Al-Harthi S, Shweash M, Alnassar S, Neamatallah T, Schroeder J, and Plevin R. MKP-2: out of the DUSP-bin and back into the limelight. *Biochem Soc Trans* 40: 235-239, 2012.

Lee, D.Y., Stallcup, M.R., Strahl, B.D., and Teyssier, C. (2005). Role of Protein Methylation in Regulation of Transcription. Endocr. Rev. *26*, 147–170.

Lee, S., Heinrich, E.L., Lu, J., Lee, W., Choi, A.H., Luu, C., Chung, V., Fakih, M., and Kim, J. (2016). Epidermal Growth Factor Receptor Signaling to the Mitogen Activated Protein Kinase Pathway Bypasses Ras in Pancreatic Cancer Cells. Pancreas *45*, 286–292.

Lee, Y.-H., Coonrod, S.A., Kraus, W.L., Jelinek, M.A., and Stallcup, M.R. (2005). Regulation of coactivator complex assembly and function by protein arginine methylation and demethylimination. Proc. Natl. Acad. Sci. U. S. A. *102*, 3611 LP-3616.

Li J., Han S., Qian Z., et al. 2014. Genetic amplification of PPME1 in gastric and lung cancer and its potential as a novel therapeutic target. *Cancer Biology and Therapy*. 15:1: 128-134.

Li, S., and Shang, Y. (2007). Regulation of SRC family coactivators by post-translational modifications. Cell. Signal. *19*, 1101–1112.

Lipina C, Hundal HS. 2014. Carnosic acid stimulates glucose uptake in skeletal muscle cells via a PME-1/PP2A/PKB signaling axis. *Cell Signal.* 26(11): 2343-9.

Londhe, P., Davie, J. 2011. Sequential association of myogenic regulatory factors and E proteins at muscle-specific genes. *Skeletal Muscle*. 1:14.

McKinnell IW, Rudnicki MA. 2004. Molecular mechanisms of muscle atrophy. *Cell.* 119(7): 907-910.

Montesano A, Luzi L, Senesi P, Teruzzi I. Modulation of Cell Cycle Progression by 5-Azacytidine Is Associated with Early Myogenesis Induction in Murine Myoblasts. *Int J Biol Sci* 2013; 9(4):391-402.

Moresi V, Williams AH, Meadows E, et al. 2010. Myogenin and Class II HDACs control neurogenic muscle atrophy by inducing E3 ubiquitin ligases. *Cell*. 143(1): 35-45.

Oda, K., Matsuoka, Y., Funahashi, A., and Kitano, H. (2005). A comprehensive pathway map of epidermal growth factor receptor signaling. Mol. Syst. Biol. *1*, 2005.0010-2005.0010.

Olson T. 2013. Transcriptional Regulation of Neurogenic Atrophy-Induced Gene Expression by Muscle RING Finger-1 and Myogenic Regulatory Factors. (Thesis). University of North Florida, Jacksonville, Florida.

Orgad S, Brewis ND, Alphey L, Axton JM, Dudai Y, Cohen PT. The structure of protein phosphatase 2A is as highly conserved as that of protein phosphatase 1. FEBS Lett. 1990;275:44–48.

Peng DJ, Zhou JY, and Wu GS. Post-translational regulation of mitogen-activated protein kinase phosphatase -2 (MKP-2) by ERK. *Cell Cycle* 9: 4650-4655, 2010.

Ryseck, R.P., and Bravo, R. (1991). c-JUN, JUN B, and JUN D differ in their binding affinities to AP-1 and CRE consensus sequences: effect of FOS proteins. Oncogene *6*, 533–542.

Schiaffino, S., and Mammucari, C. (2011). Regulation of skeletal muscle growth by the IGF1-Akt/PKB pathway: Insights from genetic models. Skelet. Muscle *1*, 4.

Schonthal AH. Role of serine/threonine protein phosphatase 2A in cancer. Cancer Lett. 2001;170:1–13.

Seshacharyulu, P., Pandey, P., Datta, K., and Batra, S.K. (2013). Phosphatase: PP2A structural importance, regulation and its aberrant expression in cancer. Cancer Lett. *335*, 9–18.

Singh K, Dilworth FJ. 2013. Differential modulation of cell cycle progression distinguishes members of the myogenic regulatory factor family of transcription factors. *The FEBS Journal*. 280: 3991-4003.

Stitt, T.N., Drujan, D., Clarke, B.A., Panaro, F., Timofeyva, Y., Kline, W.O., Gonzalez, M., Yancopoulos, G.D., and Glass, D.J. (2004). The IGF-1/PI3K/Akt pathway prevents expression of muscle atrophy-induced ubiquitin ligases by inhibiting FOXO transcription factors. Mol. Cell *14*, 395–403.

Tapscott, S.J. (2005). The circuitry of a master switch: Myod and the regulation of skeletal muscle gene transcription. Development *132*, 2685 LP-2695.

Turner, R., and Tjian, R. (1989). Leucine repeats and an adjacent DNA binding domain mediate the formation of functional cFos-cJun heterodimers. Science (80-.). *243*, 1689 LP-1694.

Waddell DS, Baehr LM, van den Brant J, et al. 2008. The glucocorticoid receptor and FOXO1 synergistically activate the skeletal muscle atrophy-associated MuRF1 gene. *American Journal of Physiology - Endocrinology and Metabolism*. 295: 785-797.

Wang, F., Zhu, S., Fisher, L.A., Wang, W., Oakley, G.G., Li, C., and Peng, A. (2018). Protein interactomes of protein phosphatase 2A B55 regulatory subunits reveal B55-mediated regulation of replication protein A under replication stress. *Sci. Rep. 8*, 2683.

Wang, Z., Yu, T., & Huang, P. (2016). Post-translational modifications of FOXO family proteins (Review). Molecular Medicine Reports, 14, 4931-4941.

William AH, Valdez G, Moresi V, et al. 2009. MicroRNA-206 Delays ALS Progression and Promotes Regeneration of Neuromuscular Synapses in Mice. *Science*. 326: 1549- 1554.

Xing Y., Li Zhu, Chen Y., et al. 2008. Structural Mechanism of Demethylation and Inactivation of Protein Phosphatase 2A. *Cell.* 133: 154-163.
Yabe R, Miura A, Usui T, Mudrak I, Ogris E, Ohama T, et al. (2015) Protein Phosphatase Methyl-Esterase PME-1 Protects Protein Phosphatase 2A from Ubiquitin/Proteasome Degradation. *PLoS ONE* 10(12)

Yabe, R., Tsuji, S., Mochida, S., Ikehara, T., Usui, T., Ohama, T., and Sato, K. (2018). A stable association with PME-1 may be dispensable for PP2A demethylation: Implications for the detection of PP2A methylation and immunoprecipitation.

Sydney Ann Labuzan

Education

M.S. Biology Candidate Spring 2019
University of North Florida, Jacksonville, Florida
Characterizing the Role of Neurogenic Atrophy-Induced Protein Phosphatases in Skeletal Muscle

B.S. Biology 2016
Rollins College, Winter Park, Florida

Professional Experience

Graduate Teaching Assistant, Principles of Biology Fall 2016- April 2019
University of North Florida. Jacksonville, Florida

Biology Intensive Orientation- Freshman Learning Improvement and Transition Enhancement (BIO-FLITE) Lab Instructor August 2017, August 2018
University of North Florida, Jacksonville, Florida

Research Experience

University of North Florida
Molecular Genetics Lab (PI: Dr. David Waddell) August 2016- April 2019

Publications

Haddock A*, **Labuzan S*,** Hayes C, Haynes A, Kakareka K, and Waddell DS. (2019). Dual-Specificity Phosphatase 4 (Dusp4) is Upregulated During Skeletal Muscle Atrophy and Modulates Extracellular Signal-Regulated Kinase (ERK) Activity. American Journal of Physiology—Cell Physiology. (* denotes equal contribution)

Research Presentations

Labuzan, S. Waddell, D. 2019. Isolation and functional characterization of protein phosphatase methylesterase (ppme1) in skeletal muscle atrophy. Experimental Biology. Oral Poster Presentation. Orlando, FL.

Labuzan, S. Cooper, L. Lynch, S. Waddell, D. 2018. MuRF1-/+ mice response to denervation connected to ERK signaling. Indy Atrophy Collaborative Meeting. Oral Presentation. Indianapolis, IN.

Labuzan, S. Waddell, D. 2018. Isolation and functional characterization of protein phosphatase methylesterase (ppme1) in skeletal muscle atrophy. Experimental Biology. Oral Poster Presentation. San Diego, CA.

Labuzan, S. Waddell, D. 2018. Isolation and functional characterization of protein phosphatase methylesterase (ppme1) in skeletal muscle atrophy. Showcase of Osprey Advancements in Research and Scholarship. Oral Poster Presentation. Jacksonville, FL.

Labuzan, S. Waddell, D. 2017. Isolation and functional characterization of protein phosphatase methylesterase (ppme1) in skeletal muscle atrophy. Showcase of Osprey Advancements in Research and Scholarship. Oral Poster Presentation. Jacksonville, FL.

Labuzan, S. Waddell, D. 2017. Isolation and functional characterization of protein phosphatase methylesterase (ppme1) in skeletal muscle atrophy. 2017 Natural Sciences Poster Presentation. Oral Poster Presentation. Jacksonville, FL.